

# **IMPLEMENTATION AND TUNING OF PID, FRACTIONAL PID AND LA CONTROLLERS FOR pH CONTROL**



uOttawa

L'Université canadienne  
Canada's university

**By:**

**Servatius Bismanditio Ardinugroho**

---

This thesis is submitted to the Faculty of Graduate and Postdoctoral  
Studies as one of the requirements to obtain Master of Applied  
Science degree

**Department of Chemical and Biological Engineering  
Faculty of Engineering  
University of Ottawa**

## Abstract

Maintaining the pH of a fluid or a solution at a specific value is a concern in many industrial processes, wastewater management, and food and pharmaceutical production. Given the importance of controlling pH in many processes, the objective of this thesis is to study and compare the effectiveness of some controller algorithms to control the pH of a process. In this study, the performance of three controller algorithms, namely PID, fractional PID and LA controllers, is evaluated for the control of a simple neutralization process using conventional controller performance metrics. Performance metrics used are the response time, the Integral of the Time weighted Absolute Error (ITAE), the Integral of the Squared Error (ISE), and the Integral of the Squares of the changes ( $\Delta U$ ) in the manipulated variable (ISDU). The three controllers were therefore tuned to minimize one or a combination of the controller performance metrics. Results show that PID, fractional PID and LA controllers implemented and tested in this research are all worthy controllers for maintaining pH of the neutralization process. Simulation results show that the three controllers can be used with confidence to cope with the high nonlinearity of a pH neutralization process provided that the process is properly designed. The relative small gain in performance obtained with the fractional PID controller, compared to a linear PID controller, suggests that it is not worth resorting to a fractional PID controller given its complexity and higher computation effort. Results show that PID and LA controllers are easy to implement with short response time and low ITAE and ISDU performance metrics.

Keywords: pH control, PID controller, fractional PID controller, LA controller, controller tuning, controller performance metrics.

## Résumé

Le maintien du pH d'un fluide ou d'une solution à une valeur spécifique est une préoccupation dans de nombreux procédés industriels ainsi que dans la gestion des eaux usées et la production alimentaire et pharmaceutique. Étant donné l'importance du contrôle du pH dans de nombreux procédés, l'objectif de cette thèse est d'étudier et de comparer l'efficacité de certains algorithmes de régulation servant au contrôle du pH d'un procédé de neutralisation. Dans cette étude, les performances de trois types de contrôleurs, à savoir les contrôleurs PID,  $PI^{\lambda}D^{\mu}$  à dérivation et intégration partielles et LA, sont évaluées pour le contrôle d'un procédé de neutralisation simple à l'aide de mesures conventionnelles des performances des contrôleurs. Les mesures de performance utilisées sont le temps de réponse, l'intégrale de l'erreur absolue pondérée dans le temps (ITAE), l'intégrale de l'erreur au carré (ISE) et l'intégrale des carrés des changements ( $\Delta U$ ) de la variable manipulée (ISDU). Les trois contrôleurs ont donc été réglés pour minimiser une ou plusieurs mesures de performance. Les résultats montrent que les contrôleurs PID,  $PI^{\lambda}D^{\mu}$  à dérivation et intégration partielles et LA mise en œuvre et testés dans le cadre de cette recherche sont tous de bons contrôleurs permettant de maintenir adéquatement le pH du processus de neutralisation. Les résultats de la simulation montrent que les trois contrôleurs peuvent être utilisés en toute confiance pour faire face à la non-linéarité élevée d'un procédé de neutralisation, à condition que le procédé soit correctement conçu. Le faible gain relatif de performance obtenu avec le contrôleur  $PI^{\lambda}D^{\mu}$  à dérivation et intégration partielles, comparé à un contrôleur PID linéaire, suggère qu'il ne vaut pas la peine de recourir à ce type de contrôleur étant donné sa complexité et les efforts de calcul plus importants. Les résultats montrent que les contrôleurs PID et LA sont faciles à mettre en œuvre et offrent de très bonnes performances avec des temps de réponse très faibles.

Mots clés: contrôle du pH, contrôleur PID, contrôleur  $PI^{\lambda}D^{\mu}$  à dérivation et intégration partielles, contrôleur LA, réglage des contrôleurs, mesures de performance.

## **Acknowledgement**

In the beginning of this study, I was quite pessimistic on my ability to complete this research project, mainly because I was not confident enough in my programming skills and my knowledge of process control was quite limited as these subjects were not taught adequately in my undergraduate program. I then mentioned my hesitations to my supervisor Professor Jules Thibault that I would prefer to get involved in another research topic. However, Professor Thibault encouraged me to face my fears. At the same time, I had the strong desire to gain the necessary knowledge in both process control and programming that could better prepare me for a future employment. My supervisor was sure that I could learn these skills doing this project. He has always been there to help and support me throughout this project. I am glad that I persevered, as I was able to gain valuable knowledge in VBA programming and in process control. I would therefore like to thank Professor Thibault for the faith he had in me.

Many people have contributed to make this journey a more pleasant one. I would like to particularly thank my friends for their support throughout my time at the University of Ottawa, especially Nneka Usifoh, Janani Mahendran and Xuewei Meng. Because of their continuous support and valuable cooperation, I was able to perform very well in my courses. In addition, I would also like to thank my department colleagues for their generous help and friendship: Sean Wilson, Fahad Chowdhury, Dennis Vierra, Xin Shen, Haoyu Wu, Shazadi Rana, Khoi Phan, Yasmine Hajar, and Charbel Atallah. I am appreciative of the help received by Fahad Chowdhury and Shazadi Rana for their teaching in the fundamentals of VBA. A special thank goes to Xin Shen and Haoyu Wu for their help in the development of the controller simulation program.

I would also like to thank my family for their love, support and prayers: my dad, my mom who is now resting in peace, my brother, my sister, my auntie. Even though my family lives thousands of kilometers away, I always felt their presence and encouragement to keep a positive attitude.

The last two years allowed me to experience life in a diverse and rich culture. I feel grateful to have pursued my master's degree at the University of Ottawa that has offered this environment. It has prepared me very well for my future.

It is not the end of my journey, but it is the beginning of a next phase of my life. I am looking forward to applying the acquired knowledge and solve real engineering problems.

# Table of Contents

<b>Abstract</b> -----	ii
<b>Résumé</b> -----	iii
<b>Acknowledgement</b> -----	iv
<b>Table of Contents</b> -----	vi
<b>Table of Figures and Tables</b> -----	viii
<b>List of Symbols, Notations, Abbreviations and Units</b> -----	xiii
<b>Chapter 1</b> -----	1
<b>Introduction</b> -----	1
1.1. Research Background-----	1
1.2. Research Objectives-----	3
1.3. Structure of the Thesis-----	3
<b>Chapter 2</b> -----	5
<b>pH Control System</b> -----	5
2.1. Description of the pH Control System-----	5
2.2. pH Measurement Device and Actuator-----	6
2.3. Simulation of the Neutralization Tank-----	8
<b>Chapter 3</b> -----	10
<b>PID, PI<sup>λ</sup>D<sup>μ</sup> and LA Controllers and Tuning Methods</b> -----	10
3.1. Proportional, Integral and Derivative (PID) Controller-----	10
3.2. Fractional PID (PI <sup>λ</sup> D <sup>μ</sup> ) Controller-----	11
3.3. LA Controller-----	15
3.4. Simulation Program of PID, PI <sup>λ</sup> D <sup>μ</sup> and LA Controllers-----	18
3.5. Controller Tuning-----	21
3.6. Simulation Program of Grid and Gradient Search-----	23
<b>Chapter 4</b> -----	24
<b>Results and Discussion</b> -----	24
4.1. Simulation Results-----	25
4.1.1. Desired pH of 5.0-----	25
4.1.2. Desired pH of 6.0-----	35
4.1.3. Desired pH of 7.0-----	43

4.1.4.	Desired pH of 8.0-----	50
4.1.5.	Desired pH of 9.0-----	57
4.1.6.	Desired pH of 10.0-----	64
4.2.	Discussion on PID, PI <sup>λ</sup> D <sup>μ</sup> and LA Controllers for Controlling pH-----	71
<b>Chapter 5</b>	-----	<b>77</b>
<b>Conclusion, Recommendations and Future Work</b>	-----	<b>77</b>
<b>References</b>	-----	<b>79</b>

## Table of Figures and Tables

<b>Figure 1</b> Schematic diagram of a typical pH control system -----	5
<b>Figure 2</b> Block diagram of the control loop of a pH control system -----	6
<b>Figure 3</b> Structure of a glass electrode pH meter (Source: <a href="http://www.ph-meter.info/pH-electrode-construction">http://www.ph-meter.info/pH-electrode-construction</a> ) -----	7
<b>Figure 4</b> Typical range of fractional orders $\lambda$ and $\mu$ values of the fractional $PI^\lambda D^\mu$ controller -----	12
<b>Figure 5</b> Block diagram of LA controller [37] -----	16
<b>Figure 6</b> pH as a function of time for a desired pH of 5.0 with $Q_{\max} = 0.5$ L/s for the three controllers tuned to minimize the sum of ITAE and ISDU-----	26
<b>Figure 7</b> pH as a function of time for a desired pH of 5.0 with $Q_{\max} = 1.0$ L/s for the three controllers tuned to minimize the sum of ITAE and ISDU-----	27
<b>Figure 8</b> pH as a function of time for a desired pH of 5.0 with $Q_{\max} = 5.0$ L/s for the three controllers tuned to minimize the sum of ITAE and ISDU-----	27
<b>Figure 9</b> pH as a function of time for a desired pH of 5.0 with $Q_{\max} = 100$ L/s for the three controllers tuned to minimize the sum of ITAE and ISDU-----	28
<b>Figure 10</b> pH as a function of time for a desired pH of 5.0 with a PID controller for the four different maximum reagent flow rates-----	29
<b>Figure 11</b> pH as a function of time for a desired pH of 5.0 with a fractional $PI^\lambda D^\mu$ controller for the four different maximum reagent flow rates -----	30
<b>Figure 12</b> pH as a function of time for a desired pH of 5.0 with a LA controller for the four different maximum reagent flow rates-----	30
<b>Figure 13</b> Response of the effluent pH as a function of time for a series of disturbances in the influent pH for a desired pH of 5.0 for the three controllers. -----	34
<b>Figure 14</b> Variation of the reagent flow rate as a function of time for a series of disturbances in the influent pH for a desired pH of 5.0 for the three controllers. -----	34
<b>Figure 15</b> pH as a function of time for a desired pH of 6.0 with $Q_{\max} = 0.5$ L/s for the three controllers tuned to minimize the sum of ITAE and ISDU. -----	36
<b>Figure 16</b> pH as a function of time for a desired pH of 6.0 with $Q_{\max} = 1.0$ L/s for the three controllers tuned to minimize the sum of ITAE and ISDU. -----	36

<b>Figure 17</b> pH as a function of time for a desired pH of 6.0 with $Q_{\max} = 5.0$ L/s for the three controllers tuned to minimize the sum of ITAE and ISDU.-----	37
<b>Figure 18</b> pH as a function of time for a desired pH of 6.0 with $Q_{\max} = 100$ L/s for the three controllers tuned to minimize the sum of ITAE and ISDU.-----	37
<b>Figure 19</b> pH as a function of time for a desired pH of 6.0 with a PID controller for the four different maximum reagent flow rates. -----	38
<b>Figure 20</b> pH as a function of time for a desired pH of 6.0 with a fractional $PI^{\lambda}D^{\mu}$ controller for the four different maximum reagent flow rates.-----	38
<b>Figure 21</b> pH as a function of time for a desired pH of 6.0 with a LA controller for the four different maximum reagent flow rates.-----	39
<b>Figure 22</b> Response of the effluent pH as a function of time for a series of disturbances in the influent pH for a desired pH of 6.0 for the three controllers.-----	42
<b>Figure 23</b> Variation of the reagent flow rate as a function of time for a series of disturbances in the influent pH for a desired pH of 6.0 for the three controllers. -----	42
<b>Figure 24</b> pH as a function of time for a desired pH of 7.0 with $Q_{\max} = 0.5$ L/s for the three controllers tuned to minimize the sum of ITAE and ISDU.-----	44
<b>Figure 25</b> pH as a function of time for a desired pH of 7.0 with $Q_{\max} = 1.0$ L/s for the three controllers tuned to minimize the sum of ITAE and ISDU-----	44
<b>Figure 26</b> pH as a function of time for a desired pH of 7.0 with $Q_{\max} = 5.0$ L/s for the three controllers tuned to minimize the sum of ITAE and ISDU-----	45
<b>Figure 27</b> pH as a function of time for a desired pH of 7.0 with $Q_{\max} = 100$ L/s for the three controllers tuned to minimize the sum of ITAE and ISDU-----	45
<b>Figure 28</b> pH as a function of time for a desired pH of 7.0 with a PID controller for the four different maximum reagent flow rates-----	46
<b>Figure 29</b> pH as a function of time for a desired pH of 7.0 with a fractional $PI^{\lambda}D^{\mu}$ controller for the four different maximum reagent flow rates -----	46
<b>Figure 30</b> pH as a function of time for a desired pH of 7.0 with a LA controller for the four different maximum reagent flow rates-----	47
<b>Figure 31</b> Response of the effluent pH as a function of time for a series of disturbances in the influent pH for a desired pH of 7.0 for the three controllers.-----	49

<b>Figure 32</b> Variation of the reagent flow rate as a function of time for a series of disturbances in the influent pH for a desired pH of 7.0 for the three controllers. -----	50
<b>Figure 33</b> pH as a function of time for a desired pH of 8.0 with $Q_{\max} = 0.5$ L/s for the three controllers tuned to minimize the sum of ITAE and ISDU.-----	51
<b>Figure 34</b> pH as a function of time for a desired pH of 8.0 with $Q_{\max} = 1.0$ L/s for the three controllers tuned to minimize the sum of ITAE and ISDU-----	52
<b>Figure 35</b> pH as a function of time for a desired pH of 8.0 with $Q_{\max} = 5.0$ L/s for the three controllers tuned to minimize the sum of ITAE and ISDU-----	52
<b>Figure 36</b> pH as a function of time for a desired pH of 8.0 with $Q_{\max} = 100$ L/s for the three controllers tuned to minimize the sum of ITAE and ISDU.-----	53
<b>Figure 37</b> pH as a function of time for a desired pH of 8.0 with a PID controller for the four different maximum reagent flow rates. -----	53
<b>Figure 38</b> pH as a function of time for a desired pH of 8.0 with a fractional $PI^{\lambda}D^{\mu}$ controller for the four different maximum reagent flow rates -----	54
<b>Figure 39</b> pH as a function of time for a desired pH of 8.0 with a LA controller for the four different maximum reagent flow rates-----	54
<b>Figure 40</b> Response of the effluent pH as a function of time for a series of disturbances in the influent pH for a desired pH of 8.0 for the three controllers. -----	56
<b>Figure 41</b> Variation of the reagent flow rate as a function of time for a series of disturbances in the influent pH for a desired pH of 8.0 for the three controllers. -----	57
<b>Figure 42</b> pH as a function of time for a desired pH of 9.0 with $Q_{\max} = 0.5$ L/s for the three controllers tuned to minimize the sum of ITAE and ISDU.-----	58
<b>Figure 43</b> pH as a function of time for a desired pH of 9.0 with $Q_{\max} = 1.0$ L/s for the three controllers tuned to minimize the sum of ITAE and ISDU.-----	59
<b>Figure 44</b> pH as a function of time for a desired pH of 9.0 with $Q_{\max} = 5.0$ L/s for the three controllers tuned to minimize the sum of ITAE and ISDU.-----	59
<b>Figure 45</b> pH as a function of time for a desired pH of 9.0 with $Q_{\max} = 100$ L/s for the three controllers tuned to minimize the sum of ITAE and ISDU.-----	60
<b>Figure 46</b> pH as a function of time for a desired pH of 9.0 with a PID controller for the four different maximum reagent flow rates. -----	60

**Figure 47** pH as a function of time for a desired pH of 9.0 with a fractional  $PI^\lambda D^\mu$  controller for the four different maximum reagent flow rates.-----61

**Figure 48** pH as a function of time for a desired pH of 9.0 with a LA controller for the four different maximum reagent flow rates.-----61

**Figure 49** Response of the effluent pH as a function of time for a series of disturbances in the influent pH for a desired pH of 9.0 for the three controllers.-----63

**Figure 50** Variation of the reagent flow rate as a function of time for a series of disturbances in the influent pH for a desired pH of 9.0 for the three controllers.-----64

**Figure 51** pH as a function of time for a desired pH of 10.0 with  $Q_{max} = 0.5$  L/s for the three controllers tuned to minimize the sum of ITAE and ISDU.-----65

**Figure 52** pH as a function of time for a desired pH of 10.0 with  $Q_{max} = 1.0$  L/s for the three controllers tuned to minimize the sum of ITAE and ISDU.-----66

**Figure 53** pH as a function of time for a desired pH of 10.0 with  $Q_{max} = 5.0$  L/s for the three controllers tuned to minimize the sum of ITAE and ISDU.-----66

**Figure 54** pH as a function of time for a desired pH of 10.0 with  $Q_{max} = 100$  L/s for the three controllers tuned to minimize the sum of ITAE and ISDU.-----67

**Figure 55** pH as a function of time for a desired pH of 10.0 with a PID controller for the four different maximum reagent flow rates.-----67

**Figure 56** pH as a function of time for a desired pH of 10.0 with a fractional  $PI^\lambda D^\mu$  controller for the four different maximum reagent flow rates.-----68

**Figure 57** pH as a function of time for a desired pH of 10.0 with a LA controller for the four different maximum reagent flow rates.-----68

**Figure 58** Response of the effluent pH as a function of time for a series of disturbances in the influent pH for a desired pH of 10.0 for the three controllers.-----70

**Figure 59** Variation of the reagent flow rate as a function of time for a series of disturbances in the influent pH for a desired pH of 10.0 for the three controllers.-----71

**Figure 60** Trends of the parameters of the PID controller versus the desired pH.-----73

**Figure 61** Trends of the parameters of the fractional  $PI^\lambda D^\mu$  controller versus the desired pH (1).-----74

**Figure 62** Trends of the parameters of the fractional  $PI^\lambda D^\mu$  controller versus the desired pH (2).-----75

**Figure 63** Trends of the parameters of the LA controller versus the desired pH. -----76

**Table 1** Summary of simulation results of desired pH of 5 system .....31

**Table 2** Summary of simulation results for desired pH of 6 system .....40

**Table 3** Summary of simulation results of desired pH of 7 system .....48

**Table 4** Summary of simulation results for desired pH of 8 system .....55

**Table 5** Summary of simulation results for desired pH of 9 system .....62

**Table 6** Summary of simulation results for desired pH of 10 system .....69

**Table 7** Simulation results of the PID controller for all desired pH .....72

**Table 8** Simulation results of the fractional PID controller for all desired pH .....74

**Table 9** Simulation results of the LA controller for all desired pH .....76

## List of Symbols, Notations, Abbreviations and Units

$C_{in}$	Inlet concentration	mol/L
$Conc_{(1)}$	Inlet $[H^+]$ concentration	mol/L
$Conc_{(2)}$	Reagent $[H^+]$ concentration	mol/L
$Conc_{(3)}$	Initial $[H^+]$ concentration	mol/L
$Conc_{(4)}$	Initial $[OH^-]$ concentration	mol/L
$C_{out}$	Output concentration	mol/L
$C_{OUT A}$	Exit $[H^+]$ concentration	mol/L
$C_{OUT B}$	Exit $[OH^-]$ concentration	mol/L
$C_{reagent}$	Reagent concentration	mol/L
${}_0D_t^{-\lambda}$	$\lambda$ -order fractional integral	-
${}_0D_t^{\mu}$	$\mu$ -order fractional derivative	-
$Flow_{(1)}$	Inlet flow rate	L/s
$Flow_{(2)}$	Reagent flow rate	L/s
ISDU	Integral of the Squares of the changes in the manipulated variable ( $\Delta U$ )	-
ITAE	Integral Time Absolute Error	-
$K_C$	Gain of a controller	-
LA	Leand et Artan controller	-
p	Controller output signal	-
$p_0$	Initial output signal	-
$pH^*$	Set/desired pH	-
Q	Reagent flow rate	L/s
R	Reaction rate	mol/(L.s)
U	Control signal from the controller that is an input to	-

	a controlled system	
$v_n$	Manipulated variable at time n in LA controller	-
$v(t)$	Control signal from the controller that is an input to a controlled system in LA controller	-
$X$	the amount of reactant converted into product	mol
$X_{\max}$	Upper grid plane limit	-
$X_{\min}$	Lower grid plane limit	-
$z(t)$	Process output of LA controller in fictitious domain	-
$z^*$	Set point in LA controller	-
$z_n$	Measured/controlled variable at the current time in LA controller	-
$\varepsilon$	Error	-
$\lambda$	Order of integration	-
$\theta$	LA sensitivity parameter	-
$\tau_D$	Derivative time constant	s
$\tau_I$	Integral time constant	s
$\mu$	Order of differentiation	-
$\omega_m^{(\alpha)}$ or $\omega_n^{(\alpha)}$	Fractional weights. $\alpha$ is either $\lambda$ or $\mu$	-
$\left\lfloor \frac{t-a}{h} \right\rfloor$	Number of step sizes in the integration of the Grünwald-Letnikov equation	-

# Chapter 1

## Introduction

### 1.1. Research Background

Maintaining the pH of a solution at a specific value is of paramount importance in many industrial processes. In the food industry as an example, the pH needs to be well regulated to lead to products with consistent and well-defined properties in addition to often have to meet strict regulatory requirements. For instance, in the butter manufacturing process, the pasteurization of butter is performed at a very narrow range of pH from 6.7 to 6.85 if sweet butter is desired whereas it is performed in the range of pH of 4.6 to 5.0, using citric acid, to obtain sour butter [1]. The pH of solution in cheese manufacturing has an impact on the hardness (soft or hard) of final products. The importance of pH also prevails in the production of yogurt, beer, wine, marmalades, syrups, juices, etc., and the pH greatly affects the shelf-life of a myriad of products [1]. Controlling the pH of domestic water is also important and it is recommended to regulate the pH in the range of 6.5 to 8.5 as high-pH water may have bitter taste whereas low-pH water could affect the distribution-piping system [2].

The regulation of pH is also important in many other industrial sectors: (1) enzyme activity is often optimal at a given pH [3]; (2) the separation of butyric acid from fermentation broths via distillation, membrane pervaporation and adsorption is strongly impacted by the pH of the solution [4]; (3) for the flotation process in the mineral industry to separate different minerals, the pH has a major impact [5]; (4) wastewater from electroplating processes where multiple contaminants of heavy metals are present, the change of pH can be judiciously adapted to induce precipitation [6] [7]; (5) pH is a crucial factor in a microalgae culture where pH conditions are in the vicinity of pH 7, whereas some other biochemical species require either higher pH or lower pH [8]. Generally speaking, the optimum environment for microorganism to grow up is between pH 6.5 and 7.5 [9]; and (6) stringent control of pH is also critical in the production of pharmaceuticals [10].

As seen in the previous paragraphs, the list of processes where pH needs to be controlled is endless. Since pH is very nonlinear, being the logarithmic function of the hydrogen ions, it

is very important to resort to the most appropriate control algorithm to return the pH to its set point value rapidly when a deviation is observed or the set point is changed. The control of pH is highly sensitive especially when it is close to the equilibrium point. This problem has been considered for a long time by many researchers for various applications. In addition to the traditional Proportional-Integral-Derivative (PID) controller, a large number of advanced control algorithms have been proposed successfully for pH control: (1) model predictive control [11], (2) adaptive nonlinear control where the adaptive nonlinear control strategy is obtained by augmenting the non-adaptive controller with an indirect parameter estimation scheme [12], (3) nonlinear Internal Model Control (IMC) applied to a pH neutralization process [13], (4) Zhiyun et al. [14] used a Model Algorithmic Control (MAC) strategy based on nonlinear processes using Hammerstein model, (5) model reference adaptive neural network control strategy [15], (6) the combination of an online identification algorithm and a nonlinear controller [16], (7) different tuning methods based on first-order plus dead time process [17], (8) fractional PID controllers were implemented in a chemical plant with level and pH control [18], (9) the use of multiple linear controllers adapted to the range of pH to be controlled was also suggested [19], and numerous other control algorithms.

In this research project, it was desired to evaluate and compare three different controllers for pH control. One linear controller, the conventional PID controller, and two nonlinear controllers, the fractional PID ( $PI^\lambda D^\mu$ ) and LA controllers, were studied in this investigation.

There are good reasons to use PID,  $PI^\lambda D^\mu$  and LA controllers to control pH in this research. Firstly, PID controller is one of the most popular controllers used for a myriad of control systems due to its efficiency and intuitive design [20]. PID controllers are simple to implement, well understood by process engineers and operators, and offer good performance in process control engineering [21]. PID controllers are known for their wide range of applicability [22], low cost and easy tuning of their parameters [23] [24]. An extension of the linear PID controller has been lately suggested where fractional order integration and derivation are used. The fractional order  $PI^\lambda D^\mu$  offers two additional degrees of freedom, which may help in dealing with the severe nonlinearity of the pH controller. The  $PI^\lambda D^\mu$  controller can help to overcome non-linear conditions in a

neutralization process because it is less sensitive to changes in controller parameters [21]. In addition,  $PI^\lambda D^\mu$  controllers have been showing to have improved performance in controlling non-linear processes when compared to linear PI and PID controllers [25]. On the other hand, the two additional controller parameters of the  $PI^\lambda D^\mu$  add to the complexity in computation and tuning compared to the conventional PID controller. The third controller implemented in this study is the LA controller which was proposed and developed by Lakrori [26]. Similar to PID controllers, LA controllers are very simple to implement and have a strong resemblance to the conventional PID controllers in its development. LA controllers were shown to perform well for the control of chemical processes. LA controllers are described by a nonlinear algorithm and were found to be relatively easy to tune as they have a close association, in an exponentially-transformed domain, to linear PID controllers [26].

Considering the importance of pH control in numerous processes, this study focuses on the control of pH in a simple neutralization process and, more particularly, on the tuning and performances of PID,  $PI^\lambda D^\mu$  and LA controllers.

## **1.2. Research Objectives**

Firstly, this research aims to control the pH of an acidic stream rapidly and smoothly. Controllers developed and tested in this investigation are expected to lead to small response time, low decay ratio if oscillations are present and smooth variation of the manipulated variable. To achieve this objective, three different controllers (linear PID, fractional PID and LA) are implemented and developed on the pH control system and their performances are evaluated and compared over a wide range of pH set point values both for set point changes and disturbances.

## **1.3. Structure of the Thesis**

This thesis is organized using the following structure:

1. Chapter 1 – Introduction: Justifications are provided as to the reasons why this research focuses on pH control and the motivations to compare PID, fractional PID and LA controllers. Chapter 1 also provides the objectives of the study.

2. Chapter 2 – pH Control System: This chapter explains a description of the simple pH control system used in this study. Chapter 2 also presents the schematic diagram of the simple pH control system, the main elements of the neutralization process and pH measurement.
3. Chapter 3 – PID,  $PI^{\lambda}D^{\mu}$  and LA Controllers and Tuning Method: This chapter presents a detailed description of PID,  $PI^{\lambda}D^{\mu}$  and LA controller algorithms. Since this study is based on the simulation of a simple neutralization process, a description of the simulation program for the three controllers is provided. In addition, the controller tuning methods and its implementation in the simulation program are also described.
4. Chapter 4 – Results and Discussion: This chapter presents the series of numerical simulations that were performed for the pH control using the three controllers over a wide range of pH set point values. Results are compared and discussed.
5. Chapter 5 – Conclusion, Recommendations and Future Works: Some general conclusions are drawn with respect to the performance of the three controllers. Some recommendations and potential future works are discussed.

## Chapter 2

### pH Control System

#### 2.1. Description of the pH Control System

In this research, the pH control system was simulated using Visual Basic for Applications (VBA) within the platform of Microsoft Office Excel. The schematic diagram of a typical pH control system is given in Figure 1.

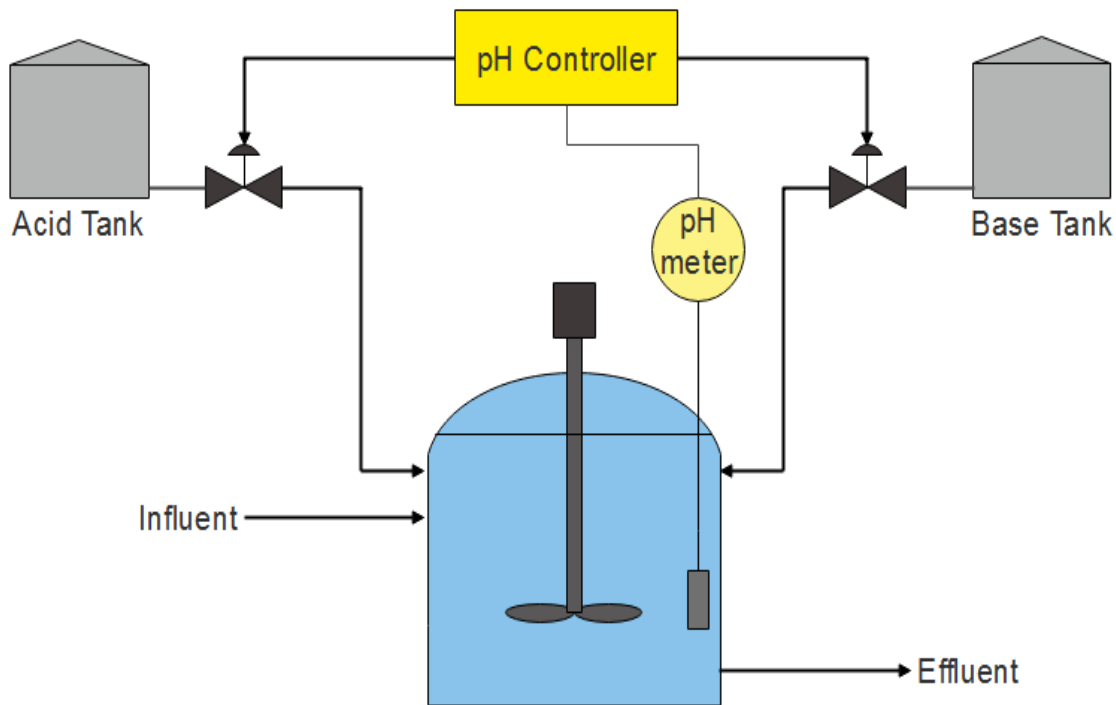


**Figure 1** Schematic diagram of a typical pH control system.

The system of Figure 1 consists of a reaction tank, which receives an influent stream at some pH level and releases essentially the same quantity of solution at a different pH level depending on the flow rate of acid or base added into the reaction tank. The flow rate of acid or base is the manipulated variable corresponding to the controller output. The control loop consists of a pH meter normally installed on the effluent line or inside the neutralization tank, a comparator to calculate the error in pH, a controller (PID,  $PI^{\lambda}D^{\mu}$  or LA) that transforms the series of errors into a control signal and an actuator that implements the control output in a way to bring the pH to its set point value as rapidly as possible. The actuator in this case is a control valve that adjusts the flow rate of the acid or

base solution depending on which direction, the pH needs to move to reach its set point value. The block diagram of the closed-loop system is presented in Figure 2. The pH control system can be used to increase or decrease the pH of the entering liquid stream because both the base and the acid can be used. However, in many processes, the pH is only controlled in one direction. This is the case of this investigation where the pH of the entering stream needs to be increased such that only a base tank is used.

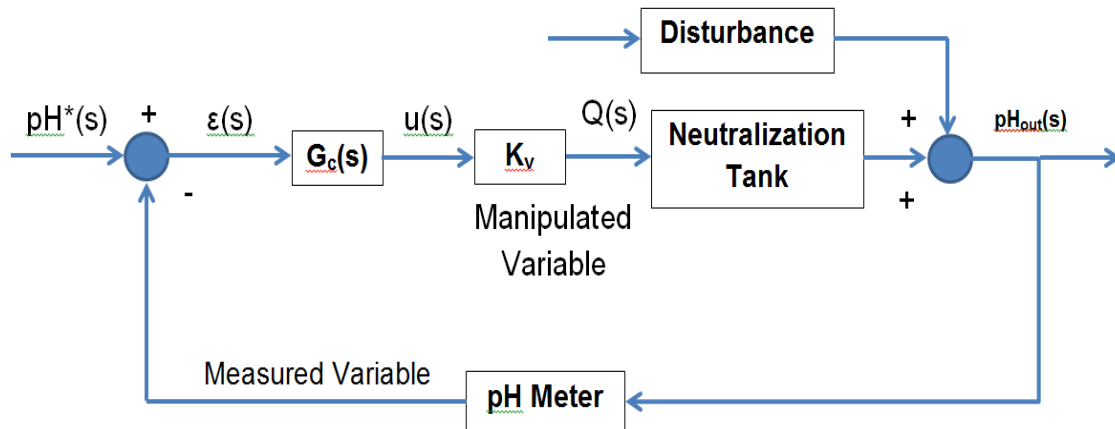


**Figure 2** Block diagram of the control loop of a pH control system.

The current investigation places an emphasis on the type of controllers used to maintain the pH of the effluent stream at the set point values. The response of the controller is based on the current error in pH values and a number of past pH error values. The error is defined as the difference between the desired pH ( $pH^*$ ) and the measured pH (effluent pH). The different controllers use the errors in different ways. The PID and  $PI^\lambda D^\mu$  controllers use the error directly in their algorithm whereas the LA controller uses the errors indirectly in an exponentially-transformed domain, which then become ratios of pH values in the actual domain. More details on the three controller algorithms will be given in the next chapter.

## 2.2. pH Measurement Device and Actuator

The pH control system is comprised of two physical elements in addition to the neutralization tank. These elements will be briefly discussed before providing the necessary information and related mass balance equations that were used to simulate the neutralization process.

A critical instrumentation in the control loop is the measuring device where the output of the process is measured. In the case of the control of pH, a pH meter is used. The continuous analog signal is sent to an Analog-to-Digital Converter (ADC) where it is converted, upon proper calibration, to a binary value corresponding to the current pH value. The pH meter is normally installed on the effluent line of the system.

The most common type of pH meter used in industries is the pH meter with pH sensitive glass electrode. pH sensitive glass electrode generates a potential difference that is a function of  $H^+$  ions activity. Some glass materials, such as  $SiO_2$ ,  $LiO_2$  and  $BaO$ , are known to give a potential difference following Nernst's potential as a result of  $H^+$  ions activity [27].

The typical structure of a glass electrode pH meter is shown on Figure 3.

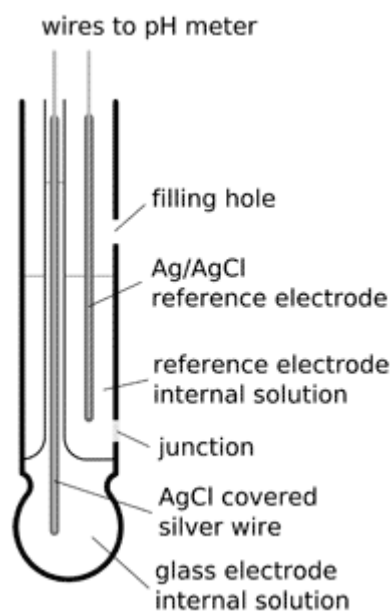


**Figure 3** Structure of a glass electrode pH meter (Source: <http://www.ph-meter.info/pH-electrode-construction>).

Generally, a glass electrode consists of a glass tube body, which is strong and thick, a thin bulb shape membrane attached to the glass tube body, a silver wire (Ag) covered with AgCl salt and connected to the pH meter, a buffer solution, and a reference electrode. The buffer solution usually filling the electrode contains  $Cl^-$  ions and it has a pH value of 7 [27].

The inner electrode constructed of a silver wire and covered by AgCl salt (Ag-AgCl electrode) is connected to the pH meter.

On the surface of a bulb glass, there is an exchange between glass metal ions and  $H^+$  ions of the measured solution when the electrode is immersed in the solution. This exchange activity gives a potential difference that is detected by the electrode. Then, the datum of the activity will be sent to the pH meter through the inner electrode and converted into a pH value by implementing Nernst equation. The Ag/AgCl reference electrode inside the glass electrode is used to obtain a reference potential which must be constant when the measured solution properties change [27].

The pH meter has an inherent time constant that may affect the dynamics of the closed-loop system. It is therefore important to have a pH meter with a small time constant, especially if the dynamics of the neutralization tank is fast.

The value of the current pH available in the computer is subtracted from the desired pH (set point) to generate the current error. The current and past errors are used to calculate a new flow rate of the base solution, known as the control action. The value the control action calculated in the computer must then be converted to an analog signal using a Digital-to-Analog Converter (DAC). In the case of the pH control system, the analog signal is used to adjust the opening of a valve or the speed of a pump to implement the desired flow rate of the base solution. Again, the actuator should have a small time constant and have a range of operation that will lead to good control.

### 2.3. Simulation of the Neutralization Tank

For a one-directional pH control where only a base solution is used and where the pH of the incoming stream needs to be increased, the following mass balance can be derived for a constant neutralization tank volume.

$$FC_{in} + QC_{reagent} - (F + Q)C_{out} - (RV) = V \frac{dC_{out}}{dt} \quad (2.1)$$

where  $F$  and  $Q$  are the influent and base solution flow rates (L/s), and  $C_{in}$ ,  $C_{reagent}$  and  $C_{out}$  are the concentrations (mol/L) of the influent stream, base solution and output streams. Concentrations of the hydrogen ion are used in the mass balance calculations. Concentrations are then converted to pH in the computer program since it is the value of

the pH that is controlled. Since the two incoming streams are mixed with the solution contained in the neutralization tank, a simple neutralization reaction will take place in order to satisfy the water dissociation constant ( $K_w = 1.0 \times 10^{-14}$ ). In Equation (2.1), the rate of reaction  $R$  is therefore calculated to obtain instantaneously the equilibrium between the acid and the base. The last term of Equation (2.1) is the accumulation term.

In this investigation, since the purpose was to evaluate the performance of various controllers, it was assumed that the solution to be neutralized is water such that there is no solution buffering and only the water dissociation constant needs to be considered. Equation (2.1) would also apply to the neutralization a solution where more than one weak acid or a buffering agent would be present. In that case, the reaction rate would be calculated to satisfy simultaneously all equilibrium constants. It was further assumed that the dynamics of the actuator and the measuring device are negligible compared to the dynamics of the neutralization process.

## Chapter 3

### PID, $PI^\lambda D^\mu$ and LA Controllers and Tuning Methods

In this chapter, the three control algorithms, namely the linear PID, fractional  $PI^\lambda D^\mu$  and LA controllers, are presented. Then, the procedure to perform the complete simulation of the closed-loop process is described, followed by the presentation of the methods used to tune the three controllers.

#### 3.1. Proportional, Integral and Derivative (PID) Controller

The Proportional-Integral-Derivative (PID) controller is one of the most popular controllers used in numerous process control systems due to its simplicity and good control performance [28]. It is therefore important to use a linear PID controller for this neutralization process in order to compare its performance with the other two nonlinear controllers. In a PID controller, there are three parts that use the controlled output errors in different ways: a first one that is proportional to the current error, a second one that integrates the errors as a function of time to help tracking the steady state output, and a third one that acts on the derivative of the error. It is the sum of the three actions that provide the controller output or control action.

The first component of the PID controller is the proportional (P) part, which calculates a control action proportional to the error. The proportional constant is the gain ( $K_C$ ) of the control. If  $K_C$  is very high, the controller will be very sensitive to the small deviations from the set point and would resemble an on-off controller. As a result, the actuator (valve, pump) will move from one extreme to the other leading to a very small error. Of course, an appropriate value of the controller gain will need to be found to obtain good performance.

Secondly, the integral (I) part of the PID controller performs the integration of the error as a function of time. The integrative action of the controller has an objective to achieve a steady-state error of zero by determining the new value of the manipulated variable [29]. This is an essential part of the PID controller in order to eliminate a process offset.

The third additional action of a PID controller is the derivative (D) part where the derivative of the error is a measure of the rate of variation of the error as a function of time. If the error changes rapidly, the derivative portion of the controller will produce a larger

control action in order to correct rapidly the deviations of the controlled variable from the set point value [29].

Combining all of the three parts together, the algorithm of the PID controller can be described in the time domain using Equation (3.1). In the Laplace domain, expressed as a transfer function, this equation assumes the form of Equation (3.2) [30]. This is one of the forms that a PID controller can take. There are other expressions but they boil essentially to the same equation. The form of Equation (3.1) is used in this investigation.

$$p = p_0 + K_c \cdot \varepsilon + \frac{K_c}{\tau_I} \int_0^t \varepsilon dt + K_c \cdot \tau_D \frac{d\varepsilon}{dt} \quad (3.1)$$

$$\frac{P(s)}{\varepsilon(s)} = K_c \left( 1 + \frac{1}{\tau_I s} + \tau_D s \right) \quad (3.2)$$

For the tuning of the linear PID controller, the three controller parameters need to be determined: controller gain  $K_c$ , the integration time parameter  $\tau_I$ , and the derivative time parameter  $\tau_D$ .

### 3.2. Fractional PID ( $PI^\lambda D^\mu$ ) Controller

Since the neutralization process is a very nonlinear process and the pH changes very rapidly near pH 7, it was therefore desired to implement a new type of controller, the fractional  $PI^\lambda D^\mu$  controller that has some resemblance to the linear PID controller but uses a fractional integration and derivation. It has been shown that the fractional  $PI^\lambda D^\mu$  controller is less sensitive to changes in the process and controller parameters [28]. Based on experimental results presented in the literature, the  $PI^\lambda D^\mu$  controller was found to perform very well for higher order systems [28] and show good stability [31]. The fractional  $PI^\lambda D^\mu$  controller is obviously more complex to implement and one of the objective of this thesis is to determine under which condition, it would provide sufficient gain in performance to compensate for the implementation difficulty and increased computation time compared to a linear PID controller. The numerical form of the Grünwald-Letnikov, which will be discussed later, is used to implement the fractional calculus  $PI^\lambda D^\mu$  controller for the pH control system.

Like the linear PID controller, the fractional  $PI^\lambda D^\mu$  controller has basically the same controller structure with the three summative controller actions with associated controller

parameters. The fractional  $PI^\lambda D^\mu$  controller has five parameters, namely  $K_c$ ,  $\tau_I$ ,  $\tau_D$ ,  $\lambda$  and  $\mu$ . This controller is therefore an extension of the linear PID controller with the first three controller parameters being the same to provide proportional, integral and derivative actions. Moreover, two additional parameters, namely the fractional order constants  $\lambda$  and  $\mu$  for the order of the integration and the derivation. These two fractional order parameters provide two additional degrees of freedom of the controller. When the values of the fractional orders  $\lambda$  and  $\mu$  are unity, the fractional  $PI^\lambda D^\mu$  controller reduces to a linear PID controller. The fractional  $PI^\lambda D^\mu$  controller will be tuned to optimize the performance of the controller for the pH control system by determining the best five parameters.

In the fractional  $PI^\lambda D^\mu$  controller,  $\lambda$  and  $\mu$  are the orders of integration and the order of differentiator, respectively. It has been suggested that the fractional  $PI^\lambda D^\mu$  controller, with its two additional parameters, is more robust and stable than classical PID controller under similar conditions [21] [32] [33]. The typical range of values that  $\lambda$  and  $\mu$  can assume is between 0 and 2 [28]. Figure 4 shows the full range of values that  $\lambda$  and  $\mu$  can adopt even though for controllers, the orders have rarely exceeded unity by much.

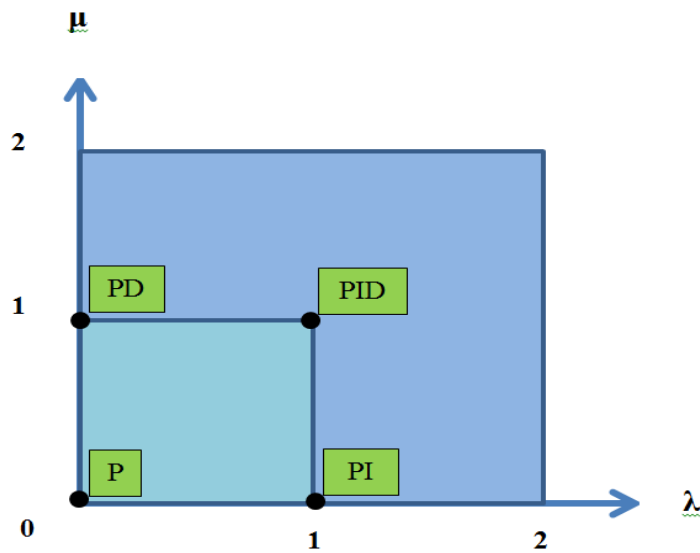


**Figure 4** Typical range of fractional orders  $\lambda$  and  $\mu$  values of the fractional  $PI^\lambda D^\mu$  controller.

The linear PID controller is a subset of the fractions  $PI^\lambda D^\mu$  controller and only the four corner points of the interior square of Figure 4 can prevail for the linear PID controller. Indeed, a linear PID controller is obtained when  $\lambda$  and  $\mu$  are equal to 1. When  $\lambda = 1$  and  $\mu =$

0, a PI controller is obtained whereas for  $\lambda = 0$  and  $\mu = 1$ , a PD controller prevails. Finally, if  $\lambda$  and  $\mu$  are both equal to 0, the resulting controller is a proportional-only controller.

Akin to the linear PID controller, the fractional  $PI^\lambda D^\mu$  controller can be described using equations in the time domain and in the Laplace domain, including  $\lambda$  and  $\mu$  as the fractional orders, respectively in Equations (3.3) and (3.4) [25]:

$$G_C = K_C(\varepsilon(t) + \frac{1}{\tau_I} \int_0^t \varepsilon(t) dt + \tau_D \frac{d\varepsilon(t)}{dt}) \quad (3.3)$$

$$G_C(s) = \frac{U(s)}{\varepsilon(s)} = K_C \left( 1 + \frac{1}{\tau_I s^\lambda} + \tau_D s^\mu \right) \quad (3.4)$$

The implementation of the fractional  $PI^\lambda D^\mu$  controller in a simulation or in a real process must use a numerical form of the Grünwald-Letnikov equation. The Grünwald-Letnikov approximation is the state of the art method to evaluate numerically both the fractional integral and fractional derivative equations. This numerical method is nothing more than a finite difference method used to approximate the continuous fractional integral. The Grünwald-Letnikov equation can be approximated using Equations (3.5) [34] [35]:

$${}_a D_t^\alpha f(t) = \frac{1}{h^\alpha} \sum_{m=0}^{\lfloor \frac{t-a}{h} \rfloor} \omega_m^{(\alpha)} f(t - mh) \quad (3.5)$$

where

$$\omega_m^{(\alpha)} = (-1)^m \binom{\alpha}{m} \quad (3.6)$$

In fact, the Grünwald-Letnikov equation defines the fractional derivative part. In Equation 3.5, when the integer value of  $\alpha$  is negative, then the equation is equivalent to the approximation of the fractional integral of order  $\alpha$  [36]. To perform the finite difference method on both the fractional integral and the fractional derivative, Equation (3.6) is solved recursively as defined in Equation (3.7). This recursive equation greatly simplifies the numerical solution [35]:

$$\omega_m^{(\alpha)} = \left( 1 - \frac{\alpha+1}{m} \right) \omega_{m-1}^{(\alpha)} \quad (3.7)$$

In terms of the control algorithm, the manipulated variable (flow of reagent) is calculated at each time step based on the series of past errors. The following two equations give the calculation of the manipulated variable using the fractional order integration and derivation whereas the second equation provides the equation that was implemented in the simulation code, where the two derivatives were approximated by two summations (Equation 3.8). This equation is known as the position form algorithm, as it relies on the initial steady state value of the manipulated variable.

$$u_n = u_0 + K_C(\varepsilon_n + \frac{1}{\tau_I} \int_0^n \varepsilon(t) dt + \tau_D \frac{d\varepsilon(t)}{dt})$$

$$u_N = u_0 + K_C(\varepsilon_N + \frac{\Delta t^\lambda}{\tau_I} \sum_{m=0}^N \omega_m^{(\lambda)} \varepsilon_{N-m} + \frac{\tau_D}{\Delta t^\mu} \sum_{n=0}^N \omega_n^{(\mu)} \varepsilon_{N-n}) \quad (3.8)$$

The position form of the control algorithm (Equation 3.8) can be changed to the more flexible form of the velocity form by subtracting the manipulated variables calculated at time N-1 and N in order to obtain an equation that depends only on a reduced number of past errors instead of the sequence of errors going back to time zero. The velocity form of the control algorithm of the fractional PI<sup>λ</sup>D<sup>μ</sup> controller is derived as follows.

$$u_N = u_0 + K_C(\varepsilon_N + \frac{\Delta t^\lambda}{\tau_I} [\omega_0^{(\lambda)} \varepsilon_N + \omega_1^{(\lambda)} \varepsilon_{N-1} + \omega_2^{(\lambda)} \varepsilon_{N-2} + \dots] + \frac{\tau_D}{\Delta t^\mu} [\omega_0^{(\mu)} \varepsilon_N + \omega_1^{(\mu)} \varepsilon_{N-1} + \omega_2^{(\mu)} \varepsilon_{N-2} + \dots])$$

$$u_{N-1} = u_0 + K_C(\varepsilon_{N-1} + \frac{\Delta t^\lambda}{\tau_I} [\omega_0^{(\lambda)} \varepsilon_{N-1} + \omega_1^{(\lambda)} \varepsilon_{N-2} + \omega_2^{(\lambda)} \varepsilon_{N-3} + \dots] + \frac{\tau_D}{\Delta t^\mu} [\omega_0^{(\mu)} \varepsilon_{N-1} + \omega_1^{(\mu)} \varepsilon_{N-2} + \omega_2^{(\mu)} \varepsilon_{N-3} + \dots])$$

$$u_N - u_{N-1} = K_C([\varepsilon_N - \varepsilon_{N-1}] + \frac{\Delta t^\lambda}{\tau_I} [\omega_0^{(\lambda)} \varepsilon_N + (\omega_1^{(\lambda)} - \omega_0^{(\lambda)}) \varepsilon_{N-1} + (\omega_2^{(\lambda)} - \omega_1^{(\lambda)}) \varepsilon_{N-2} + \dots] + \frac{\tau_D}{\Delta t^\mu} [\omega_0^{(\mu)} \varepsilon_N + (\omega_1^{(\mu)} - \omega_0^{(\mu)}) \varepsilon_{N-1} + (\omega_2^{(\mu)} - \omega_1^{(\mu)}) \varepsilon_{N-2} + \dots]) \quad (3.9)$$

$$\begin{aligned}
u_N = u_{N-1} + K_C \left( \left[ 1 + \frac{\Delta t^\lambda}{\tau_I} \omega_0^{(\lambda)} + \frac{\tau_D}{\Delta t^\mu} \omega_0^{(\mu)} \right] \varepsilon_N + \left[ -1 + \frac{\Delta t^\lambda}{\tau_I} (\omega_1^{(\lambda)} - \omega_0^{(\lambda)}) + \right. \right. \\
\left. \left. \frac{\tau_D}{\Delta t^\mu} (\omega_1^{(\mu)} - \omega_0^{(\mu)}) \right] \varepsilon_{N-1} + \left[ \frac{\Delta t^\lambda}{\tau_I} (\omega_2^{(\lambda)} - \omega_1^{(\lambda)}) + \frac{\tau_D}{\Delta t^\mu} (\omega_2^{(\mu)} - \omega_1^{(\mu)}) \right] \varepsilon_{N-2} + \dots \right)
\end{aligned}
\tag{3.10}$$

The velocity form of Equation (3.10) calculates the next manipulated variable at the current process time  $t$  based on the manipulated variable at time  $t-1$ .

As can be seen from Equation (3.10), the determination of the control action is significantly more complex than the linear PID control algorithm in terms of algorithm development and computation time. In addition, the tuning the fractional  $PI^\lambda D^\mu$  controller, with its additional two parameters for five parameters, will be significantly more challenging.

### 3.3. LA Controller

The LA controller is a simple nonlinear controller that was proposed and developed by Lakrori [37], which finds its origin in a linear PID controller derived an exponentially-transformed domain. The acronym LA stands for the names of the two sons of Mako Lakrori: Leand and Artan. The LA control algorithm was implemented in this investigation along with PID and fractional  $PI^\lambda D^\mu$  controllers.

Because of its simplicity, ease of implementation and structurally adapted for controlling nonlinear chemical processes, the LA controller was also selected for the neutralization process. Lakrori has developed many forms of the LA controller. Lakrori had the brilliant idea to use the quotient of the controlled variable and the set point instead of the difference as it is commonly performed in the linear PID and the fractional  $PI^\lambda D^\mu$  controllers. Then, based on this idea, he formalized the algorithm and was able to find a close relationship with the linear PID controller.

To provide a conceptual idea of the LA controller, consider the main term of the LA controller that is formed is ratio of the set point value of the controlled variable and the controlled variable. If this ratio is larger than unity, signifies the controlled variable is lower than the set point value, which will induce an increase in the values of the manipulated variable, and vice versa if the ratio is larger than unity. The block diagram of LA controller, as proposed by Lakrori, is presented on Figure 5.

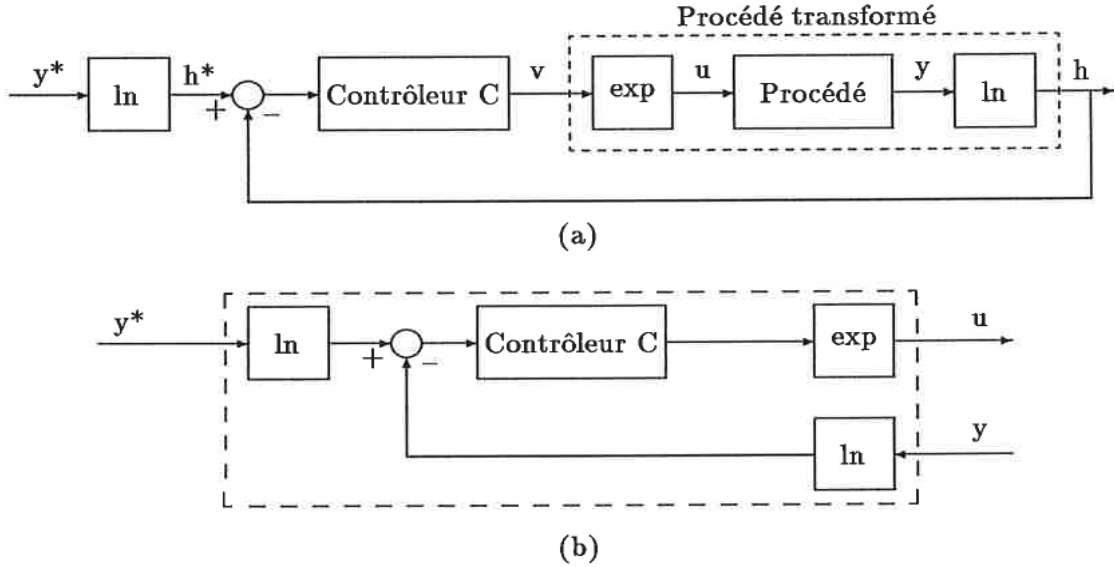


**Figure 5** Block diagram of LA controller [37]

The control algorithm of the LA controller is similar to the linear PID algorithm. In the LA controller, the linear PID controller is derived in an exponentially-transformed domain and then the inverse transformation is performed to return to the time domain. As shown in Figure 5a, the natural logarithm of the set point and the measured controlled variable is calculated. The control algorithm (in this case a linear PID) is derived in this fictitious domain. Using the control algorithm (typically a PID), the manipulated variable is calculated in the fictitious domain before taking its exponential function to return to the real domain. This procedure appears, a priori, somewhat complex but the implementation of the algorithm is relatively simple and equivalent in complexity to the linear PID.

Consider the manipulated variable  $U(t)$ , the controlled variable  $Y(t)$  and the set point value  $Y^*(t)$  which prevails in the time domain. In the fictitious logarithm-exponential domain, the corresponding variables are  $v(t)$ ,  $z(t)$  and  $z^*(t)$ . The relationship of these variables in the two domains is given in Equations (3.11)-(3.13).

$$v(t) = \ln U(t), \quad U(t) = e^{v(t)} \quad (3.11)$$

$$z(t) = \ln Y(t), \quad Y(t) = e^{z(t)} \quad (3.12)$$

$$z^*(t) = \ln Y^*(t), \quad Y^*(t) = e^{z^*(t)} \quad (3.13)$$

The determination of the manipulated variable in the LA controller in its PI form can be performed by implementing the following numerical procedure. We will only use the PI form in this investigation but the extension of a PID form would be obtained in a similar manner. In Equation (3.14a), the manipulated variable is calculated in the fictitious domain using the velocity form of a PI controller. The difference ( $z_n^* - z_n$ ) in Equation (3.14a) corresponds to the error calculated in the fictitious domain. Equation (3.14a) can be simplified to Equation (3.14b). Replacing each of the three variables in the fictitious domain by their corresponding logarithmic transformation, Equation (3.14c) is obtained. It is then possible to regroup the variables to lead to Equation (3.14d) and then take the exponential of the whole equation to give Equation (3.14e) that can be directly implemented in the computer code. Similar equations could be derived for a P, PD and PID forms of the LA controller.

$$v_n = v_{n-1} + K_C \left[ (z_n^* - z_n) - (z_n^* - z_{n-1}) + \frac{\Delta t}{\tau_I} (z_n^* - z_n) \right] \quad (3.14a)$$

$$v_n = v_{n-1} + K_C \left[ (z_{n-1} - z_n) + \frac{\Delta t}{\tau_I} (z_n^* - z_n) \right] \quad (3.14b)$$

$$\ln U_n = \ln U_{n-1} + K_C \left[ (\ln Y_{n-1} - \ln Y_n) + \frac{\Delta t}{\tau_I} (\ln Y_n^* - \ln Y_n) \right] \quad (3.14c)$$

$$\begin{aligned} \ln \left( \frac{U_n}{U_{n-1}} \right) &= K_C \left[ \ln \left( \frac{Y_{n-1}}{Y_n} \right) + \frac{\Delta t}{\tau_I} \ln \left( \frac{Y_n^*}{Y_n} \right) \right] = \ln \left( \frac{Y_{n-1}}{Y_n} \right)^{K_C} + \ln \left( \frac{Y_n^*}{Y_n} \right)^{\frac{K_C \Delta t}{\tau_I}} = \\ \ln \left[ \left( \frac{Y_{n-1}}{Y_n} \right)^{K_C} \left( \frac{Y_n^*}{Y_n} \right)^{\frac{K_C \Delta t}{\tau_I}} \right] & \end{aligned} \quad (3.14d)$$

$$\left( \frac{U_n}{U_{n-1}} \right) = \left( \frac{Y_{n-1}}{Y_n} \right)^{K_C} \left( \frac{Y_n^*}{Y_n} \right)^{\frac{K_C \Delta t}{\tau_I}} \quad (3.14e)$$

The exponents of the two ratios on the left-hand side of Equation (3.14e) are related to the PI controller parameters that were defined in the fictitious domain. These two exponents will be replaced in this investigation as simple controller parameters of the LA controller. In term of the neutralization process where the pH of the effluent needs to be controlled, Equation (3.15) is obtained and could be used in the simulation program for this specific controller.

$$Q_n = Q_{n-1} \left( \frac{pH^*}{pH_n} \right)^{n_1} \left( \frac{pH_{n-1}}{pH_n} \right)^{n_2} \quad (3.15)$$

Equation (3.15) can be used in its current form. However, depending on the magnitude of the variables, it may be necessary to add an offset to set point and controlled variables. This additional parameter may be necessary to avoid variables to reach zero or negative values as well as to decrease the sensitivity of the algorithm. The sensitivity parameter  $\theta$  could take negative values as well if it was desired to increase the sensitivity of the controller. A simple example to comprehend the need to use a sensitivity parameter is in the control of temperature where the temperature could be expressed in degree Celsius or Kelvin. For the same temperature error, the controller would be significantly less sensitive when the temperature is expressed in degrees Kelvin. An increase in the offset parameter  $\theta$ , as shown in Equation (3.16), leads to a decrease in controller sensitivity.

$$Q_n = Q_{n-1} \left( \frac{pH^* + \theta}{pH_n + \theta} \right)^{n_1} \left( \frac{pH_{n-1} + \theta}{pH_n + \theta} \right)^{n_2} \quad (3.16)$$

Despite its simple design, LA controllers have been implemented successfully for the control of few nonlinear systems. Surprisingly, the number of applications using LA controllers remain limited even though LA controllers have shown good performance and stability in controlling nonlinear behavior in a bioprocess system, a chemical reactor and a distillation pilot-scale column [37] [38].

### 3.4. Simulation Program of PID, PI<sup>λ</sup>D<sup>μ</sup> and LA Controllers

The simulation of the neutralization process with the implementation of PID, PI<sup>λ</sup>D<sup>μ</sup> and LA controllers was coded on Visual Basic for Application (VBA) on Microsoft Excel. The procedure used to simulate the three controllers for the pH control system is as follows:

1. The simulation of the neutralization process is initiated by specifying the simulation conditions: neutralization tank volume, the pH set point values, the time step size to perform one iteration and the duration of the simulation.
2. The initial conditions are then specified: the pH and flow rate of the influent stream, the initial pH of the solution in the neutralization tank, the pH and initial flow rate of the reagent solution. In most cases, it was assumed that the system operated under steady

state at the beginning of the numerical experiment and, at time zero, a step change in the pH set point value or in the influent pH (i.e. a disturbance) was made.

3. The PID parameters ( $K_c$ ,  $\tau_I$  and  $\tau_D$ ),  $PI^\lambda D^\mu$  parameters ( $K_c$ ,  $\tau_I$ ,  $\tau_D$ ,  $\lambda$  and  $\mu$ ) or LA parameters ( $n_1$ ,  $n_2$  and  $\theta$ ) are specified. When the simulator is used in conjunction with an optimization subroutine, the parameters are given by the optimization routine as the optimization subroutine attempts to determine the best set of controller parameters to minimize the specified objective function.
4. At each time interval  $\Delta t$ , the effluent pH is calculated using the mass balance of the hydrogen ions (Equation (2.1)). However, Equation (2.1) cannot be used directly because the reaction is not known a priori. The mass balance is therefore performed first without the term of the reaction. Then the reaction occurring between the acid and the base in the tank is iterated such that the concentrations of both  $[H^+]$  and  $[OH^-]$  in the tank or the effluent stream satisfy the equilibrium dissociation constant of water.

$$C_{OUT A} = Conc_{(3)} + ((Flow_{(1)} * Conc_{(1)}) - ((Flow_{(1)} + Flow_{(2)}) * Conc_{(3)}) + (Flow_{(2)} * Conc_{(2)})) * \frac{DT}{V} \quad (3.17)$$

$$C_{OUT B} = Conc_{(4)} + ((Flow_{(1)} * \left(\frac{10^{-14}}{Conc_{(1)}}\right)) - ((Flow_{(1)} + Flow_{(2)}) * Conc_{(4)}) + (Flow_{(2)} * \frac{10^{-14}}{Conc_{(2)}})) * \frac{DT}{V} \quad (3.18)$$

As mentioned before, these equations only account for the mass balance. The reaction is taken into account where the acid and base concentrations are reacted iteratively to determine  $X$  (Equations (3.19) and (3.20)) that satisfies the equilibrium dissociation constant of water. The concentrations of  $[H^+]$  and  $[OH^-]$  are then calculated by these two equations.

$$C_{OUT A} = C_{OUT A} - X \quad (3.19)$$

$$C_{OUT B} = C_{OUT B} - X \quad (3.20)$$

Since, the error is calculated in term of pH, the  $[H^+]$  concentration in the effluent stream is converted into pH:

$$pH_{EFFLUENT} = -\text{Log}_{10} (C_{OUT A}) \quad (3.21)$$

5. For the PID and  $PI^\lambda D^\mu$  controllers, the errors are determined by subtracting the set pH and the effluent pH values:

$$\text{Error} = \text{pH}_{\text{SET}} - \text{pH}_{\text{EFFLUENT}} \quad (3.22)$$

Meanwhile, for the LA controller, the values of the set pH and the effluent pH are directly used in the controller algorithm without calculating an error value (see Equations 3.15 and 3.16).

6. Finally, the reagent flow rate as the manipulated variable or control action is calculated at each  $\Delta t$  according to the error data or measured controlled variables:

- **For the PID controller**, the reagent flow rate is determined by the following equation, expressed in velocity form:

$$Q^t = Q^{t-\Delta t} + (K_C * ((\varepsilon_0 - \varepsilon_1) + \left(\frac{\Delta T * \varepsilon_0}{\tau_I}\right) + \left(\frac{\tau_D * (\varepsilon_0 - 2 * \varepsilon_1 + \varepsilon_2)}{\Delta T}\right))) \quad (3.23)$$

- **For the PI<sup>λ</sup>D<sup>μ</sup> controller**, the reagent flow rate is determined by performing the summation on both fractional integral and fractional derivative. Equation (3.7) is implemented.

#### *Fractional Integral*

For the fractional integral,  $\alpha$  (i.e.  $\lambda$  for the PI<sup>λ</sup>D<sup>μ</sup>) is a negative number and the implementation of Grünwald-Letnikov approximation is written as follows:

$$\omega_m^{(\lambda)} = \left(1 - \left(\frac{1-\lambda}{m}\right)\right) * \omega_{m-1}^{(\lambda)} \quad \text{with } \omega_0^{(\lambda)} = 1 \quad (3.24)$$

Using this series of  $\omega^{(\lambda)}$  coefficients, the following summation is performed and then used in Equation (3.10) in order to calculate the next manipulated variable (Equation 3.28):

$$\sum_{m=0}^N \omega_m^{(\lambda)} \varepsilon_{N-m} = \sum_{m=0}^N \left[ \omega_0^{(\lambda)} \varepsilon_N + \left( \omega_1^{(\lambda)} - \omega_0^{(\lambda)} \right) \varepsilon_{N-1} + \left( \omega_2^{(\lambda)} - \omega_1^{(\lambda)} \right) \varepsilon_{N-2} + \dots \right] \quad (3.25)$$

#### *Fractional Derivative*

For the fractional derivative,  $\alpha$  (i.e.  $\mu$  for the PI<sup>λ</sup>D<sup>μ</sup>) is a positive number and the implementation of Grünwald-Letnikov approximation is written as follows:

$$\omega_m^{(\mu)} = \left(1 - \left(\frac{1+\mu}{m}\right)\right) * \omega_{m-1}^{(\mu)} \quad \text{with } \omega_0^{(\mu)} = 1 \quad (3.26)$$

Using this series of  $\omega^{(\mu)}$  coefficients, the following summation is performed and then used in Equation (3.10) in order to calculate the next manipulated variable based on the series of past errors (Equation 3.28):

$$\sum_{n=0}^N \omega_n^{(\mu)} \varepsilon_{N-n} = \sum_{n=0}^N \left[ \omega_0^{(\mu)} \varepsilon_N + (\omega_1^{(\mu)} - \omega_0^{(\mu)}) \varepsilon_{N-1} + (\omega_2^{(\mu)} - \omega_1^{(\mu)}) \varepsilon_{N-2} + \dots \right] \quad (3.27)$$

Finally, the reagent flow rate or manipulated variable is determined by implementing Equation (3.9):

$$Q^t = Q^{t-\Delta t} + K_C([\varepsilon_N - \varepsilon_{N-1}] + \frac{\Delta t^\lambda}{\tau_I} \sum_{m=0}^N (\omega_m^{(\lambda)} \varepsilon_{N-m})) + \frac{\tau_D}{\Delta t^\mu} \sum_{n=0}^N (\omega_n^{(\mu)} \varepsilon_{N-n}) \quad (3.28)$$

- **For the LA controller**, the reagent flow rate or the manipulated variable is determined by simply applying either Equation (3.15) or Equation (3.16).

### 3.5. Controller Tuning

To obtain the best performance for the process to be controlled, one must determine the best controller parameters that minimize some pre-defined objective function. This procedure is called controller tuning. There are several methods to tune a controller. Some of these are nonlinear least squares methods, grid search method, genetic algorithms (NSGA-III, particle swarm optimization), Ziegler-Nichols, and many others [21] [23]. The methods that were used in this investigation are a combination of grid search method and the steepest gradient method.

One objective function that is often used is the minimization of the sum of squares of the errors (SSQ or ISE) throughout a given time of simulation. The ISE criterion attempts to return the controlled variable to its set point as rapidly as possible since the deviations from the set point are squared and larger deviations greatly penalize this criterion. Controllers tuned with ISE criterion have a tendency to be more oscillatory. Instead, the controller performance metrics that were evaluated in this investigation are the ITAE and the ISDU. The ITAE criterion penalizes more importantly the deviations that occur later in time such that it gives smoother control. The ISDU criterion ensures that the control action is also smooth. To tune the controller parameters for the three controllers, the sum of these two objective criteria, ITAE and ISDU, was minimized.

The ITAE and ISDU performance metrics are defined by the following equations:

$$ITAE = \int_0^t |\varepsilon| t dt \quad (3.29)$$

$$ISDU = \int_0^t \Delta Q^2 dt \quad (3.30)$$

Two methods were used to tune the three controllers under identical operating conditions. Tuning the controllers implies to find the best set of controller parameters that minimize the sum of ITAE and ISDU following a step change in the pH set point. The first tuning method is grid search method. The grid search method is very useful to identify the region where the objective function is minimum. In this method, the multidimensional search space is divided uniformly in a number of search points where minimum ( $X_{\min}$ ) and maximum ( $X_{\max}$ ) values of each dimension of the search space are given. This is a brute force method that enables to locate the optimum region of the controller parameters and allows mapping the variation of the objective function within the search volume.

The other tuning method that was used in this investigation is the simple gradient descent method. In this method, an initial estimate of the controller parameters is given and the objective function is evaluated. Then, each of the controller parameters are changed in turn to determine the one-dimensional gradient relative to each parameter. The combined gradient provides the direction to change all the control parameters over a certain distance of the search space. The procedure is repeated until a point is found where changing the parameters in any direction will not improve the value of the objective function. Reaching a minimum of the objective function does not guarantee that the global minimum has been reached because many local minima may exist.

To increase the probability of reaching the global minimum, the combination of the grid search method and the steepest descent has been used. The grid search is first performed to identify the best set of controller parameters that minimize the objective function. The best set of controller parameters are used as the starting point for the gradient descent method. The parameter optimization search volume was a tridimensional space for the linear PID and LA controllers whereas it was a five dimensional space for the fractional  $PI^\lambda D^\mu$  controller [21].

### 3.6. Simulation Program of Grid and Gradient Search

For more clarity, the procedure used to implement the grid and gradient search methods and how these search methods were coded in VBA are provided in this section. The steps used for combining the two search methods are as follows:

1. The simulation of the grid and gradient search begins with specifying the minimum ( $X_{min}$ ) and maximum ( $X_{max}$ ) values as well as the number of divisions of each controller parameter. It is possible to start with a smaller number of divisions over a large range of parameters to have an idea on the variation of the objective function over the whole search space. However, there is a risk of missing the optimal region if the objective space not smooth such that it is recommended to perform this grid search few times with different numbers of divisions and ranges. When the number of parameters is large, the number of solutions can become excessively large.

2. The grid search is first performed where a series of do loop are used to cover all selected sets of controller parameters. The following equation is used for each dimension:

$$Parm(i) = X_{min}(i) + ((X_{max}(i) - X_{min}(i)) * \left(\frac{I(i)-1}{N(i)-1}\right)) \quad (3.31)$$

3. For each grid point, the objective function is calculated. At the of the grid search, the minimum value of objective function (ITAE + ISDU) is determined. The optimum set of controller parameters from the grid search is thereby identified. If the grid search was sufficiently refined, the best point becomes the desired solution.
4. To obtain a better solution, the optimum set of controller parameters from the grid search are then used as seed for the gradient search method. The steepest descent technique is then used to refine the estimation of the best set of controller parameters.
5. The values of the optimal set of controller parameters, along with the minimum value of the objective function are finally obtained and serve to evaluate de performance of each controller.

## Chapter 4

### Results and Discussion

In this investigation, a series of simulations with three different controllers, namely the linear PID, fractional  $PI^{\lambda}D^{\mu}$  and LA controllers, were performed to control the pH of the effluent of a neutralization process. It is desired to assess the performance of the three controllers for maintaining a constant pH for this very nonlinear process. Since the pH is highly nonlinear, especially near the neutral point [9], the three controllers need to be evaluated, assessed and compared for their ability to control pH over a wide range of pH set point values. The desired pH values were set in the range of 5 to 10. This range corresponds to pH control systems of many industrial sectors, such as food production, biochemical industry, mineral industry and wastewater treatment [2] [3] [5] [8]. For each set point value, a step change of 2 in the pH set point value was performed for every desired pH to compare the performance of controllers under similar conditions. For instance, for a desired pH of 5, the pH of the influent stream was 3; when the pH set point was 6, the pH of the influent stream was 4, and so on. The simulation results will be discussed for each desired pH system in the range of 5 to 10 to assess the performance of each controller at each pH level. For pH control systems, the design of the system is also important for proper control. In the series of simulation performed in this investigation, the maximum flow rate through the control valve needs to be selected for more efficient control. The maximum flow rate should be smaller for pH control around the neutral point whereas it needs to be higher for pH away from the neutral point. In this investigation, the effect of the maximum flow rate will be assessed using four different maximum flow rates (0.5, 1.0, 5.0 and 100 L/s) to obtain the appropriate reagent flow rate for a given desired pH. For all simulations, the reagent pH and the minimum reagent flow rate were set to be constant at 11 and 0.0001 L/s, respectively. A constant reagent pH of 11 was chosen. This reagent pH allowed to control efficiently and with the right sensitivity of the pH in the range of 5 to 10. The volume of the neutralization tank was set constant at 50 L. Most simulations were performed for a change in pH set point. However, the performance of the three controllers was also assessed for a disturbance in the incoming pH.

## 4.1. Simulation Results

### 4.1.1. Desired pH of 5.0

The performances of the linear PID, the fractional  $PI^\lambda D^\mu$  and LA controllers were evaluated for the neutralization process for a desired pH of 5 when the pH of the incoming stream was 3 and with a flow rate of 0.1 L/s. First, it was desired to study the impact of the maximum flow rate ( $Q_{\max}$ ) of the reagent or manipulated variable on the control performance such the controllers would be tested on well-designed conditions. The three performance such the controllers would be tested on well-designed conditions. The three controllers were tested for four different maximum flow rates. Results of these numerical experiments are presented in Figures 6 to 9.

Figures 6 to 8 show that the three controllers were able to bring the pH of the effluent stream from its initial pH of 3 to the desired pH of 5 and to maintain very well the effluent pH at its set point thereafter. When the maximum reagent flow rate  $Q_{\max}$  was set to 0.5 L/s, the time required to reach the pH set point is very long because the rate at which the base is added is too low. In this case, the manipulated variable ( $Q$ ) remained at its maximum value in almost the entire duration of the experiment. When the control valve is chosen to provide a higher flow rate, the system obviously responds faster. With a maximum flow rate of 0.5 L/s, the set point was reached in approximately 75 s, whereas it reached the pH set point value in roughly 36 and 7 s, respectively, for a maximum reagent flow rate of 1.0 and 5.0 L/s. It appears that for this case, a proper selection of valve would be to choose one that provides a maximum flow rate of 5.0 L/s. The responses follow the same pattern where an initial slow increase is observed because a larger quantity of the basic reagent is required to elevate the pH when the solution is near a pH of 3. On the other hand, the pH increases more rapidly at higher value. In all three cases and for the three controllers, the response is very smooth and the pH stabilized readily when the set point is reached. Very small overshoots are observed when the fractional PID and the linear PID controllers are used for  $Q_{\max}$  of 1.0 and 5.0 L/s.

When the neutralization process is designed to give a maximum reagent flow rate,  $Q_{\max}$ , of 100 L/s, the system will obviously react faster to reach the pH set point value. As shown in Figure 9, the linear PID, the fractional  $PI^\lambda D^\mu$  and LA controllers all provide a very smooth and rapid control for the effluent pH response. For the PID controller, there is an overshoot

reaching a process pH of 5.5 before returning slowly via dilution to pH 5. It takes time for the process to return to steady state due to the one-directional control, which for process pH values larger than the set point value will close the valve and let the system return to steady state only by dilution.

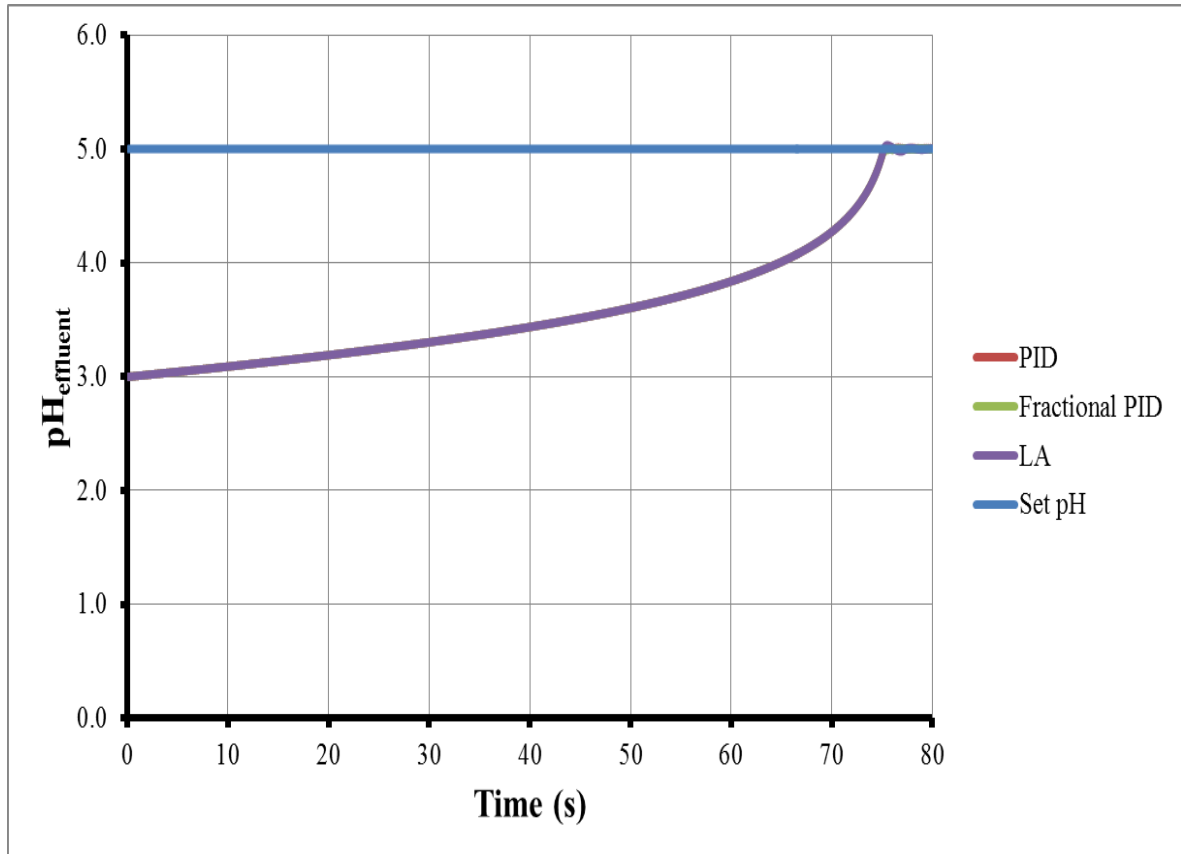


**Figure 6** pH as a function of time for a desired pH of 5.0 with  $Q_{\max} = 0.5$  L/s for the three controllers tuned to minimize the sum of ITAE and ISDU.

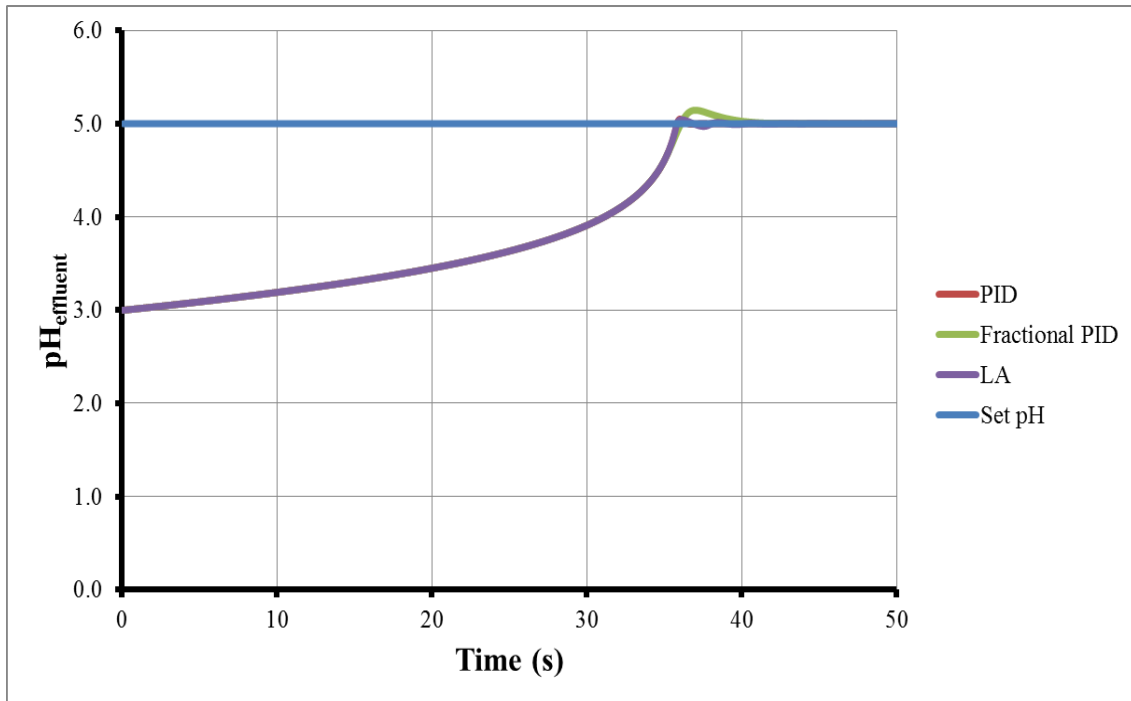


**Figure 7** pH as a function of time for a desired pH of 5.0 with  $Q_{\max} = 1.0$  L/s for the three controllers tuned to minimize the sum of ITAE and ISDU.

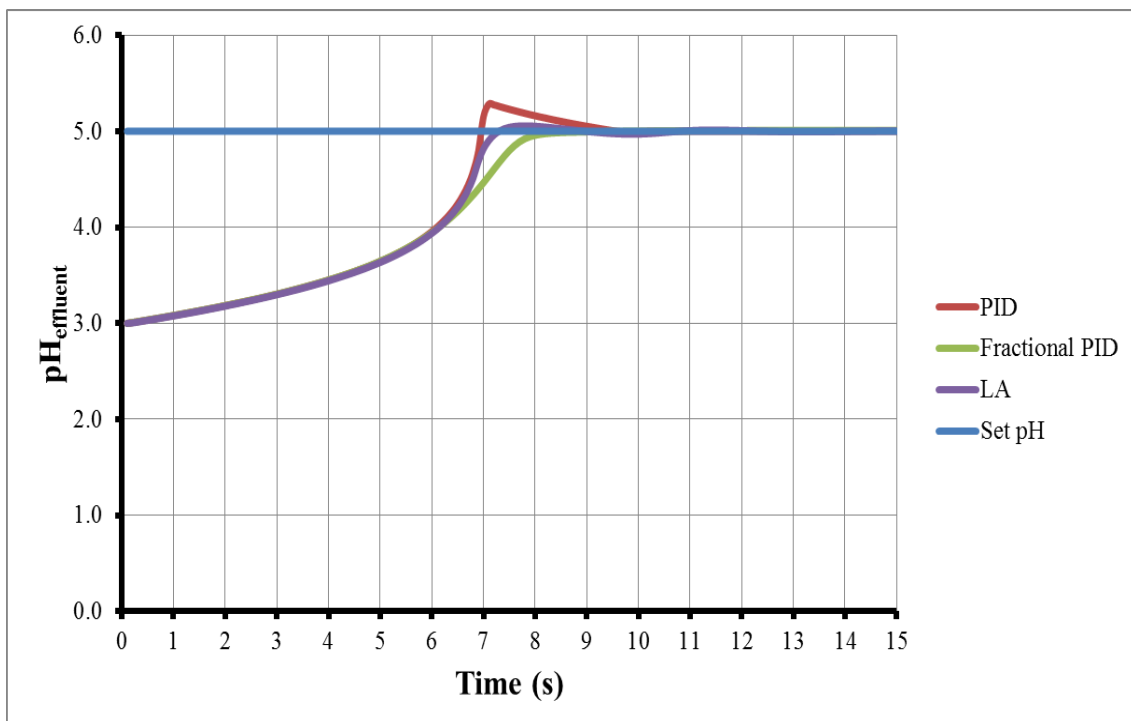


**Figure 8** pH as a function of time for a desired pH of 5.0 with  $Q_{\max} = 5.0$  L/s for the three controllers tuned to minimize the sum of ITAE and ISDU.

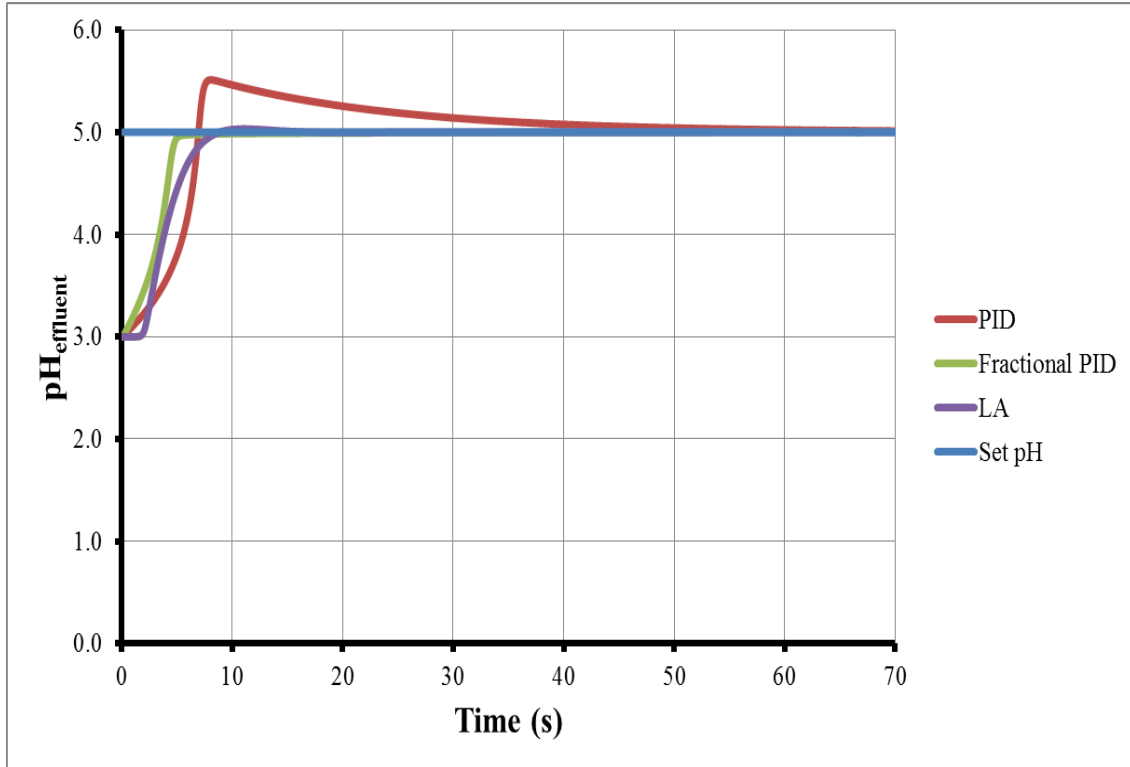


**Figure 9** pH as a function of time for a desired pH of 5.0 with  $Q_{\max} = 100$  L/s for the three controllers tuned to minimize the sum of ITAE and ISDU.

The responses of the effluent pH for the four maximum reagent flow rates  $Q_{\max}$  are presented in Figures 10 to 12 for the linear PID, fractional  $PI^{\lambda}D^{\mu}$  and LA controllers. The maximum reagent flow rate is one of the important design considerations in a neutralization process and similarly for numerical simulations. If the aperture of the flow control valve for the reagent is too large, even though theoretically the control could be very good, the sensitivity of the valve to small pH errors could induce some oscillations because of potential positioning of the valve in real system. In addition, if the maximum flow rate is very high, it could lead to a rapid increase of the pH beyond the set point, which under one-directional control will lead to improper control.

For the neutralization for a pH set point of 5, the responses presented in Figures 10 to 12 showing that there is a small difference between a maximum reagent flow rate of 5.0 and 100 L/s. In fact, for the process response with a maximum flow rate of 100 L/s, the manipulated variable was always well below the maximum. A control valve with a maximum flow rate  $Q_{\max}$  of 5.0 L/s is quite satisfactory given an influent flow rate of 0.1

L/s and a tank volume of 50 L. Choosing a much lower maximum reagent flow rate led to slow controlled variable response.

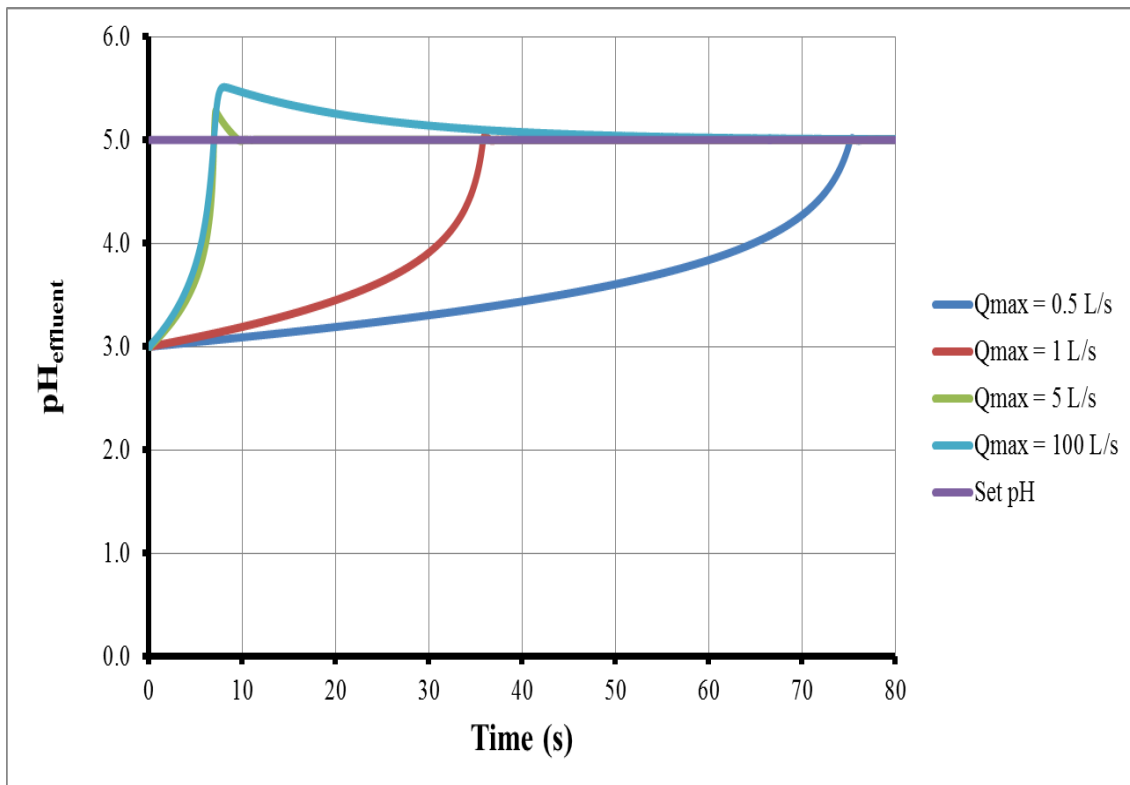


**Figure 10** pH as a function of time for a desired pH of 5.0 with a PID controller for the four different maximum reagent flow rates.

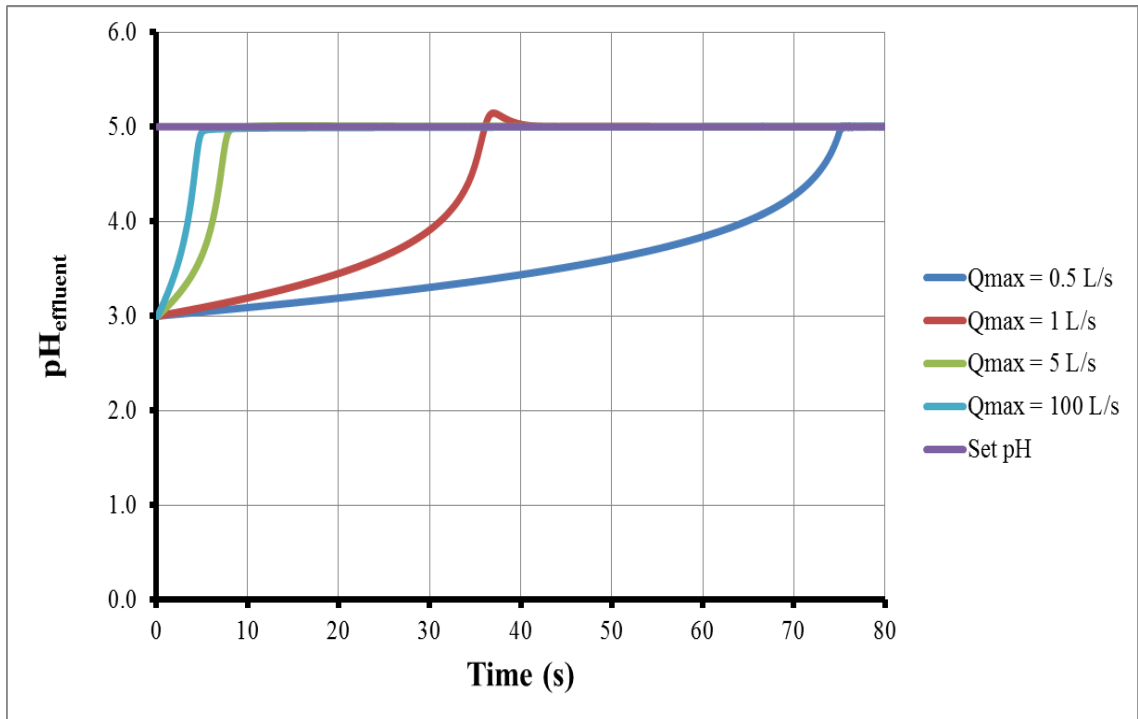


**Figure 11** pH as a function of time for a desired pH of 5.0 with a fractional  $PI^\lambda D^\mu$  controller for the four different maximum reagent flow rates.

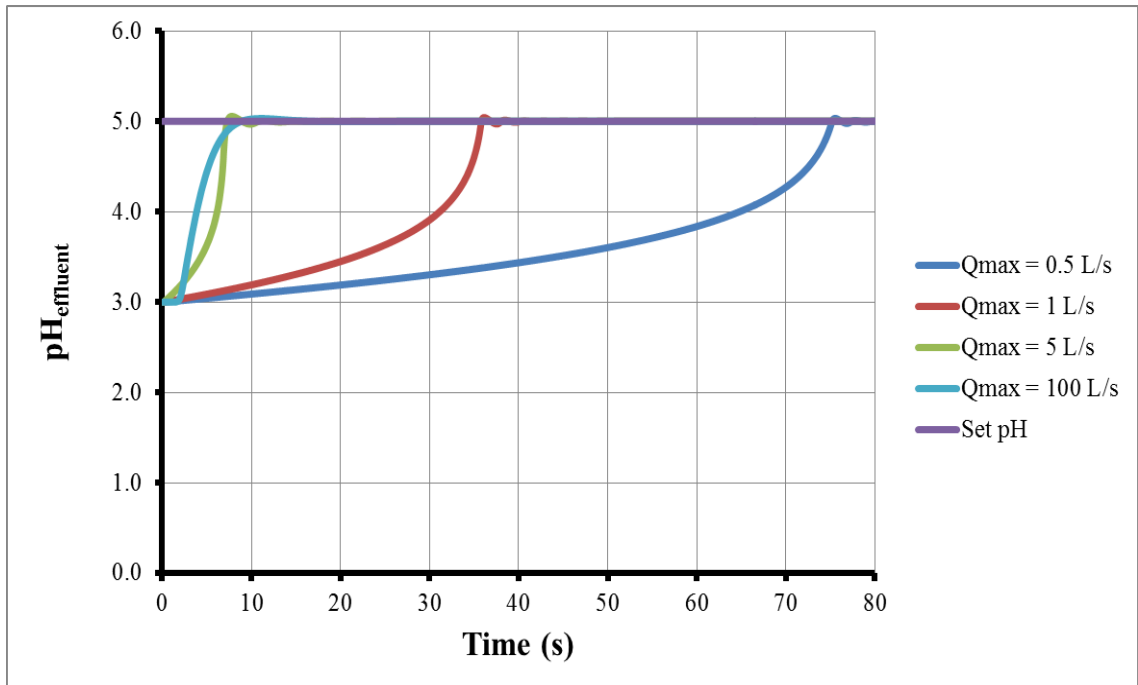


**Figure 12** pH as a function of time for a desired pH of 5.0 with a LA controller for the four different maximum reagent flow rates.

For the neutralization process for a desired pH of 5, it is recommended to use an actuator with a maximum reagent flow rate  $Q_{\max}$  of 5.0 L/s. This maximum flow rate is large enough to allow fast control for all three controllers used in this investigation, and yet small enough to avoid excessive control action.

Table 1 provides a summary of the operating conditions and the optimal controller parameters obtained for the linear PID, the fractional  $PI^\lambda D^\mu$  and the LA controllers for the case study for which the pH set point was 5. Table 1 also gives the response time for the three different controllers. The response time is defined in this work, as the time it takes for the controlled variable to enter the zone of  $\pm 5\%$  of the set point value. The 5% is defined based on the total change in set point that was made. For this case study, the response corresponds to the time that it takes to enter and remain in the zone of 4.9 to 5.1. All response times are approximately 7 s. LA controller has the lowest sum of ITAE and ISDU. On the other hand, the fractional  $PI^\lambda D^\mu$  controller has the highest value of the objective function. All controllers show excellent performance for reaching rapidly the desired pH of 5 when the maximum reagent flow rate  $Q_{\max}$  is 5.0 L/s.

**Table 1** Summary of simulation results for desired pH of 5.0 system for  $Q_{\max} = 5.0$  L/s.

<b>Operating Conditions</b>			
pH <sub>set</sub>	5		
pH <sub>in</sub>	3		
pH <sub>reagent</sub>	11		
Q <sub>min</sub> (L/s)	0.0001		
<b>Parameters</b>	<b>PID</b>	<b>PI<sup>λ</sup>D<sup>μ</sup></b>	<b>LA</b>
t <sub>response</sub> (s)	6.9	7.5	7.0
ITAE + ISDU	36.2	44.0	35.1
Q <sub>max</sub> (L/s)	5.0	5.0	5.0
K <sub>C</sub>	5.73	0.10	-
τ <sub>I</sub>	3.89	0.12	-
τ <sub>D</sub>	0.01	50.00	-
λ	-	1.01	-
μ	-	0.01	-
n <sub>1</sub>	-	-	20.35
n <sub>2</sub>	-	-	51.25

The parameters obtained for the PID controller suggest that the derivative control action is at its minimum set value such the controller is really a PI controller. These parameters were obtained following a combination of the grid search and the steepest decent methods. It is possible that other sets of parameters would lead to similar results.

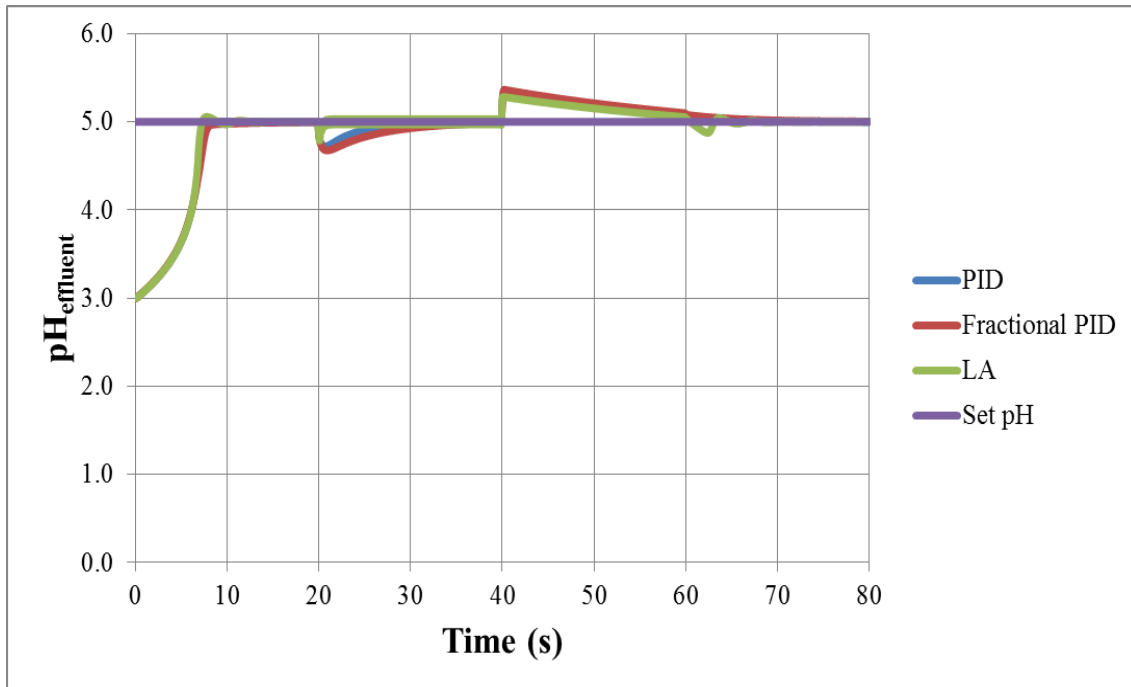
The integration order and the derivative order of the fractional  $PI^\lambda D^\mu$  controller, being 1.01 and 0.01, indicating that the controller is really a PI controller. However, the controller gain is very small being at its minimum set value whereas the integration time is nearly equal to the controller gain. Since the derivative order  $\mu$  can be considered zero and the integration order  $\lambda$  can be considered to be unity, the  $PI^\lambda D^\mu$  controller can be easily transformed into a simple PI controller as shown in Equation (4.1). If the values of  $K_c$ ,  $\tau_I$  and  $\tau_D$  are substituted in the expression of  $K_c^*$  and  $\tau_I^*$ , the values of 5.1 and 6.12 will be the values of  $K_c$  and  $\tau_I$  for the equivalent PI controller. The equivalent controller gain  $K_c^*$  is nearly the same as the PID controller whereas the equivalent integration time  $\tau_I^*$  is slightly larger. The larger value for the equivalent integration time is due to the minimum value imposed in the optimization algorithm. The higher equivalent integration time led to a higher value of the objective function (Table 1).

$$\begin{aligned}
 G_c(s) &= K_c \left( 1 + \frac{1}{\tau_I s^\lambda} + \tau_D s^\mu \right) = K_c \left( 1 + \frac{1}{\tau_I s} + \tau_D \right) = K_c \left( (1 + \tau_D) + \frac{1}{\tau_I s} \right) \\
 &= (1 + \tau_D) K_c \left( 1 + \frac{1}{(1 + \tau_D) \tau_I s} \right) \quad \text{with} \quad \begin{aligned} K_c^* &= (1 + \tau_D) K_c \\ \tau_I^* &= (1 + \tau_D) \tau_I \end{aligned}
 \end{aligned} \tag{4.1}$$

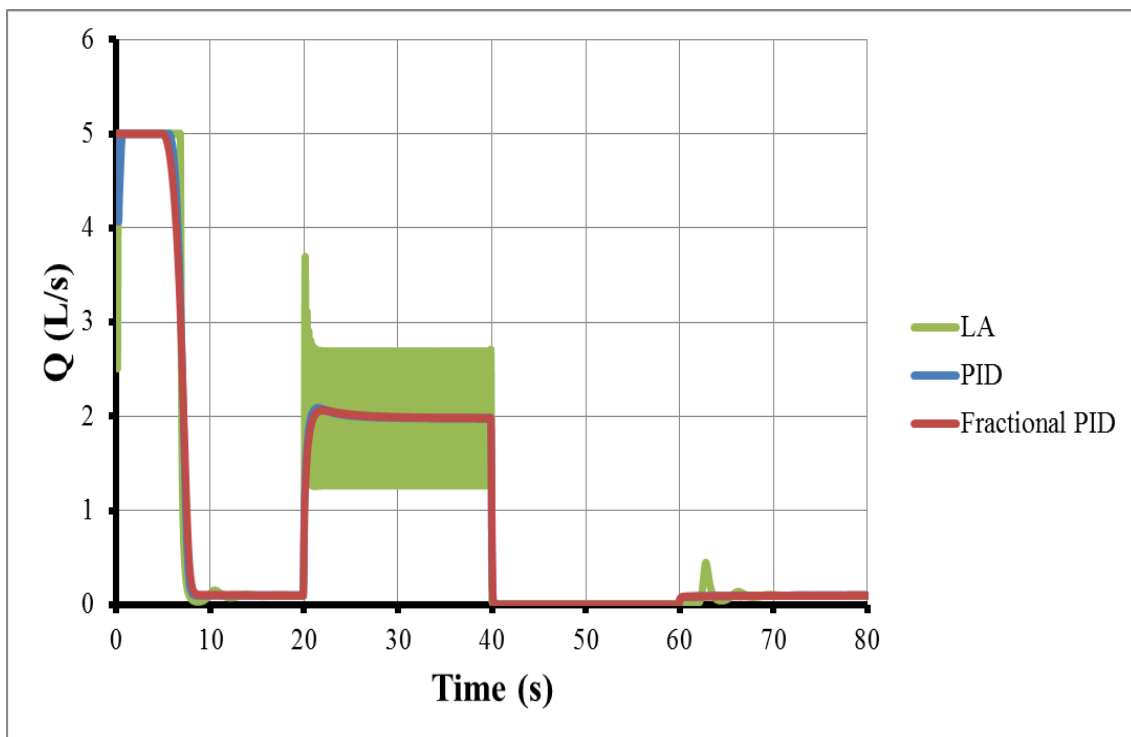
The parameters for the LA controller were obtained to minimize the objective function. Relatively high values of  $n_1$  and  $n_2$  were obtained, whereas the third parameter  $\theta$  (Equation 3.16) was determined to be negligible for all cases considered in this investigation. For this particular case study, the LA controller provided the smoothest control with the lowest objective function value.

Figure 13 displays the responses of PID, fractional  $PI^\lambda D^\mu$  and LA controllers to a disturbance occurring in the influent pH for the case of a desired pH of 5.0. The controller parameters are those that were determined in Table 1. For these simulations, the pH of the inlet stream was initially equal to be 3.0 for the first 20 s. It was subsequently changed to 1.7, 4.0 and 3.0, respectively at 20, 40 and 60 s. The first portion of the responses on Figure

13 corresponds to the results presented above. When the influent pH is changed to 1.7, the pH decreases as expected but the control system is able to recover rapidly to bring back the pH of the effluent stream to 5.0. At 40 s, when the influent stream suddenly went from 1.7 to 4, the pH increased and then decreased slowly to the pH of 5.0 by dilution with the minimum reagent flow rate as it is a one-directional control system. At 40 s, the pH of the influent stream was changed from 4.0 to 3.0 and the control system was able to recover very rapidly to return to its set point value. Figure 14 shows the plot of the manipulated variable, i.e. the reagent flow rate, for the simulation runs presented in Figure 13. For the first 20 s, the valve reaches its maximum value to increase the pH as rapidly as possible and, as the pH gets closer to the set point, the reagent flow rate is reduced progressively to achieve the desired pH. Between 20 and 40 s, the important decrease in the pH of influent stream induces a decrease in the pH of the effluent pH such that the reagent flow rate needs to increase on average to 2 L/s on PID and fractional  $PI^{\lambda}D^{\mu}$  to accommodate the additional amount of hydrogen to neutralize. On LA controller, the base flow rate oscillates between 1 and 3 L/s. The reason for these oscillations is due to the parameters of the controller which were tuned for a pH of 5.0 but for an influent pH of 3.0. The concentration of hydrogen ions of the incoming flow rate has increased by a factor of 20 (pH of 3.0 to 1.7) such the controller would need to be adjusted for these new conditions. At 40 s, the influent pH is increased from 1.7 to 4.0 such that the pH of the effluent will increase and again the controller is able to return the effluent pH to its set point. In this case, the base flow rate is at its minimum value (Figure 14) and the pH only decreases by dilution since it is a one-directional control. At 60 s, the influent pH is returned to 3 and the effluent pH returns rapidly to pH 5.0 following a small decrease. Results clearly show that the three controllers are able to return the pH of the system rapidly to its set point value without a large overshoot.



**Figure 13** Response of the effluent pH as a function of time for a series of disturbances in the influent pH for a desired pH of 5.0 for the three controllers.



**Figure 14** Variation of the reagent flow rate as a function of time for a series of disturbances in the influent pH for a desired pH of 5.0 for the three controllers.

#### 4.1.2. Desired pH of 6.0

The performances of the linear PID, the fractional  $PI^\lambda D^\mu$  and LA controllers were also investigated for the neutralization process for a desired pH of 6.0 when the pH of the incoming stream was 4.0 and with a flow rate of 0.1 L/s. The three controllers were also tested for four different maximum reagent flow rates as they were assessed on the system of the desired pH of 5.0 in the previous section. Results of these numerical experiments are presented in Figures 15 to 18. Meanwhile, the responses of the effluent pH for the four maximum reagent flow rates  $Q_{\max}$  are presented in Figures 19 to 21 for the linear PID, fractional  $PI^\lambda D^\mu$  and LA controllers, respectively. As it was mentioned earlier, the maximum reagent flow rate should be considered in the design of a neutralization process and similarly for the numerical simulations.

Figures 15 to 18 show that the three controllers were able to bring the pH of the effluent stream from its initial pH of 4.0 to the desired pH of 6.0 and then to maintain it at its set point very well. When the maximum reagent flow rate  $Q_{\max}$  was set to 0.5 L/s, the time required to reach the pH set point was much longer than the response time when the maximum reagent flow rates were set to 1, 5 and 100 L/s. When the control valve is chosen to provide a higher base flow rate, the system obviously responds faster. With a maximum flow rate of 0.5 L/s, the set point was reached in approximately 10 s, whereas it reached the pH set point value in around 5 s for a maximum reagent flow rate of 1.0 L/s. The responses presented in Figures 19 to 21 show that the maximum flow rates of 5.0 L/s and 100 L/s give similar results for the response time to reach the set point value is between 1 s and 5 s. Instead of using 100 L/s, a maximum reagent flow rate of 5 L/s was found to be large enough to control the system rapidly for all three controllers. Therefore, it is recommended to use an actuator with a maximum reagent flow rate  $Q_{\max}$  of 5.0 L/s with the current influent flow rate of 0.1 L/s and a tank volume of 50 L. In all four cases and for the three controllers, the pH response is very smooth and stabilized readily when the set point is reached.

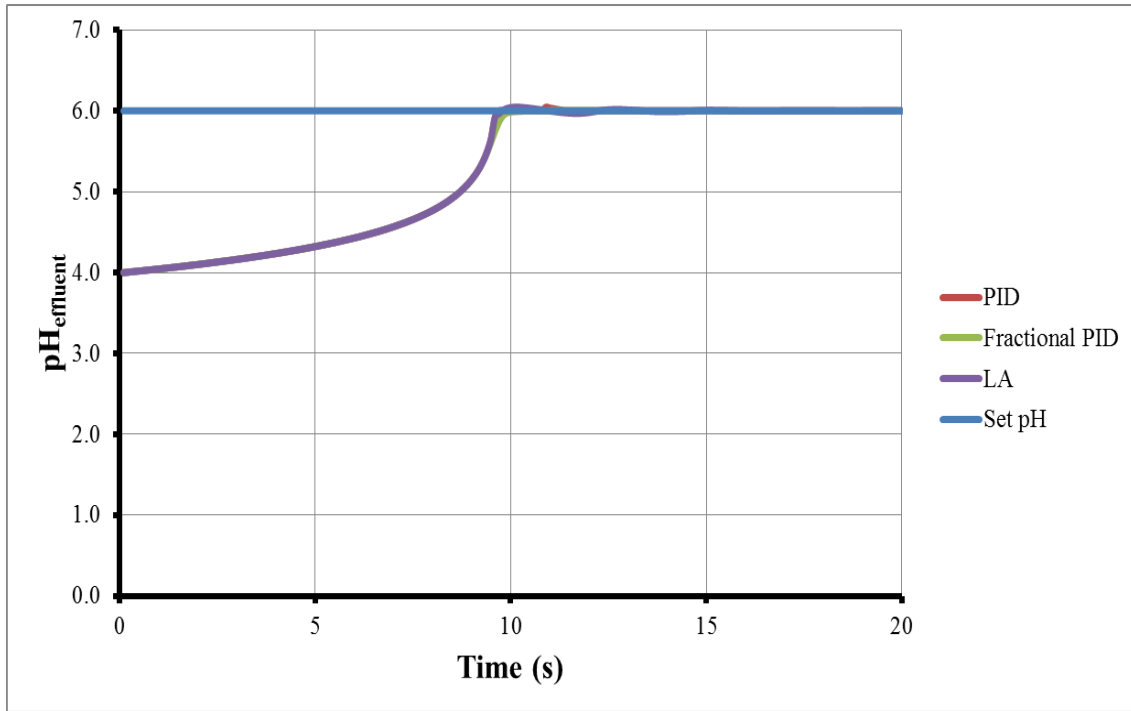


**Figure 15** pH as a function of time for a desired pH of 6.0 with  $Q_{\max} = 0.5$  L/s for the three controllers tuned to minimize the sum of ITAE and ISDU.

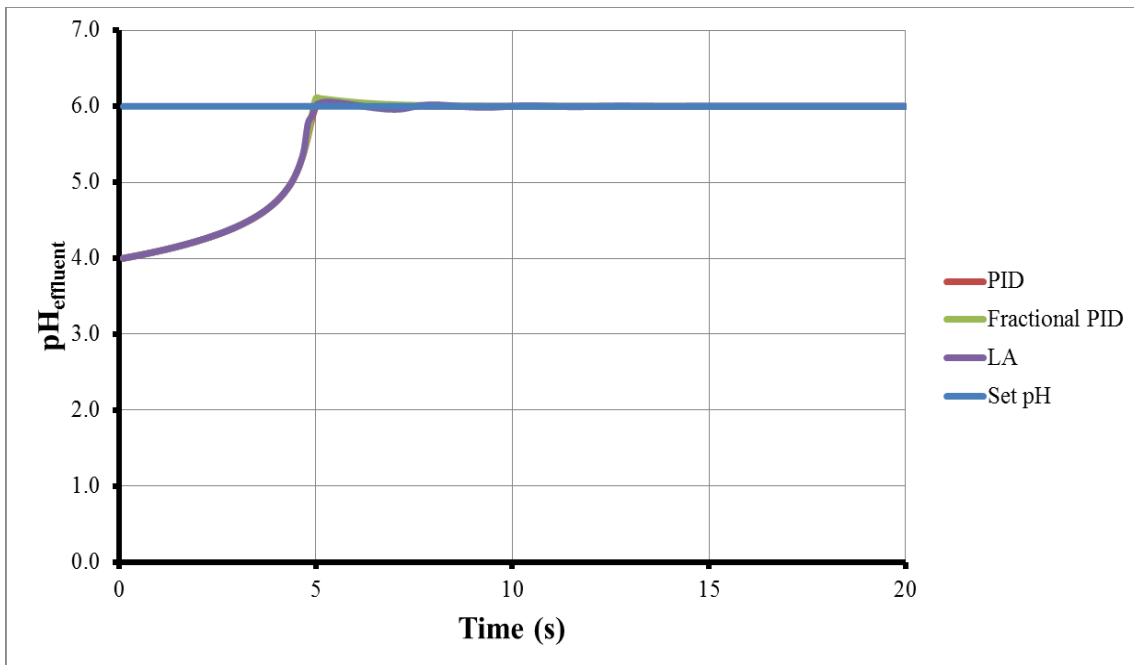


**Figure 16** pH as a function of time for a desired pH of 6.0 with  $Q_{\max} = 1.0$  L/s for the three controllers tuned to minimize the sum of ITAE and ISDU.

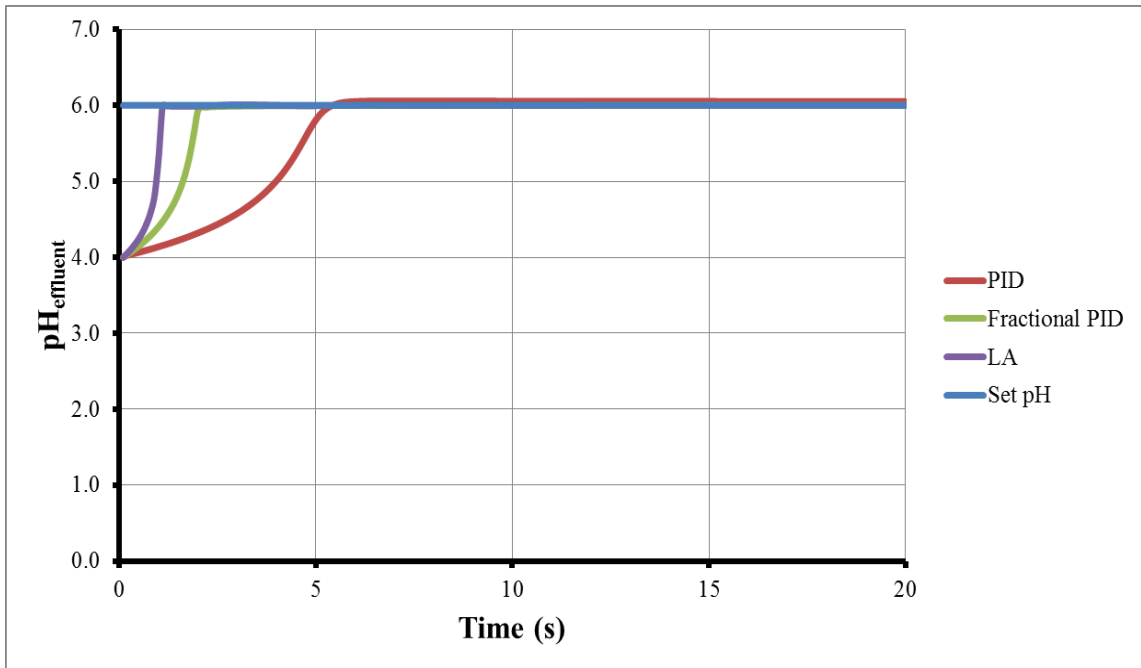


**Figure 17** pH as a function of time for a desired pH of 6.0 with  $Q_{\max} = 5.0$  L/s for the three controllers tuned to minimize the sum of ITAE and ISDU.

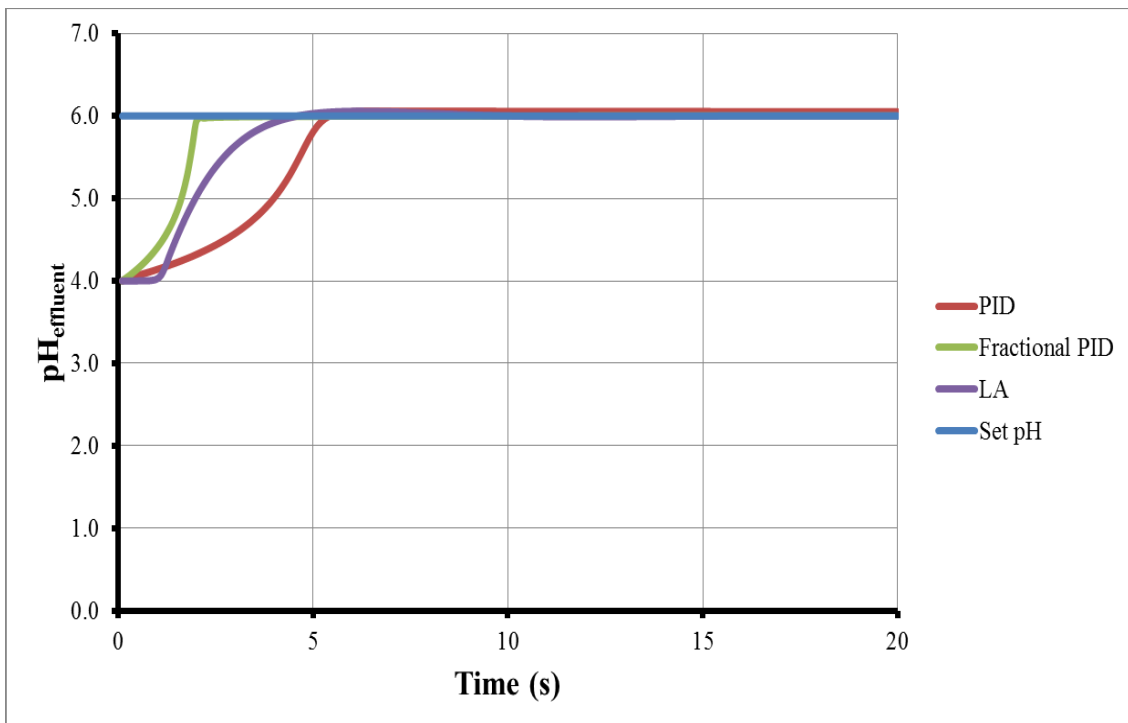


**Figure 18** pH as a function of time for a desired pH of 6.0 with  $Q_{\max} = 100$  L/s for the three controllers tuned to minimize the sum of ITAE and ISDU.

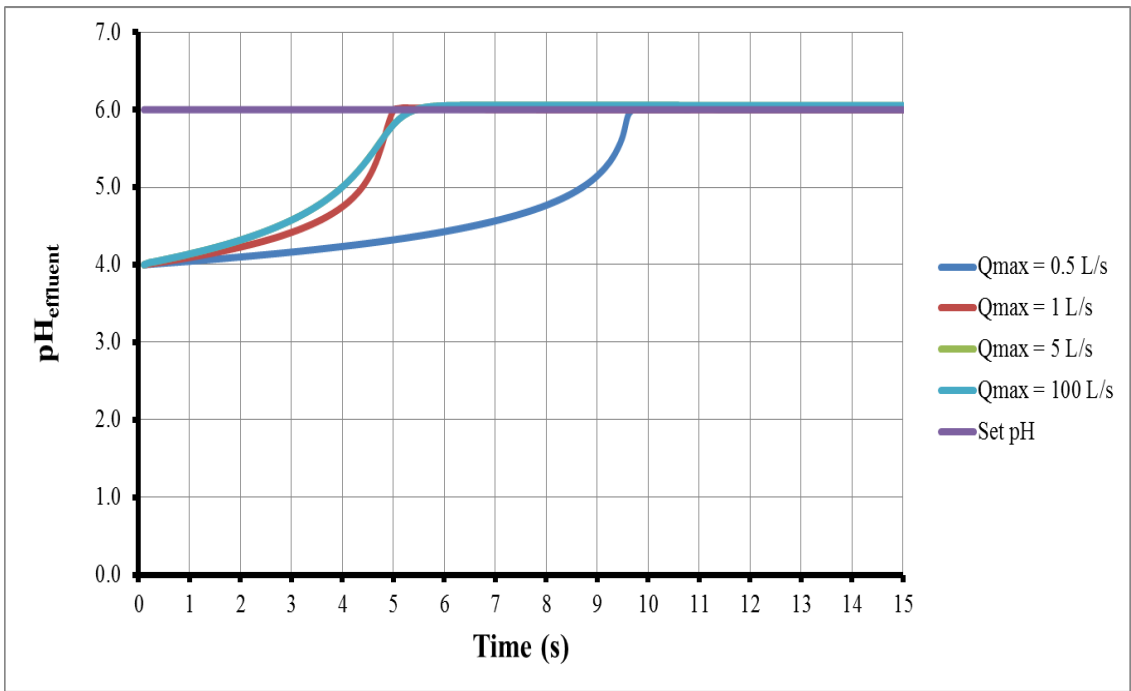


**Figure 19** pH as a function of time for a desired pH of 6.0 with a PID controller for the four different maximum reagent flow rates.

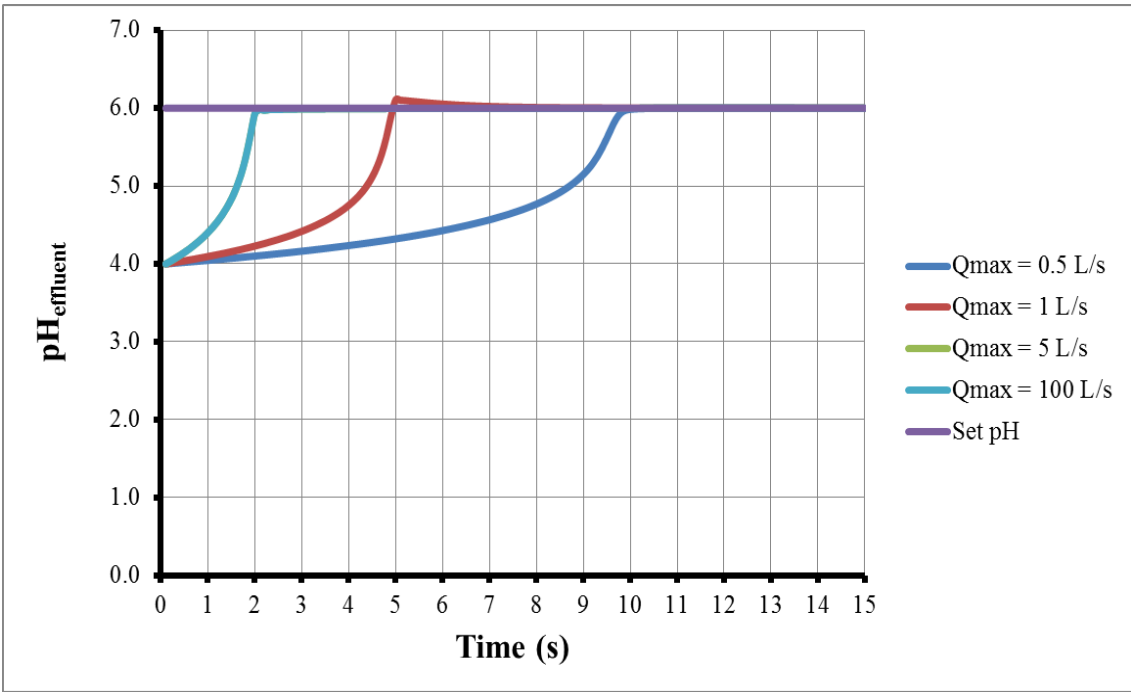


**Figure 20** pH as a function of time for a desired pH of 6.0 with a fractional  $PI^{\lambda}D^{\mu}$  controller for the four different maximum reagent flow rates.

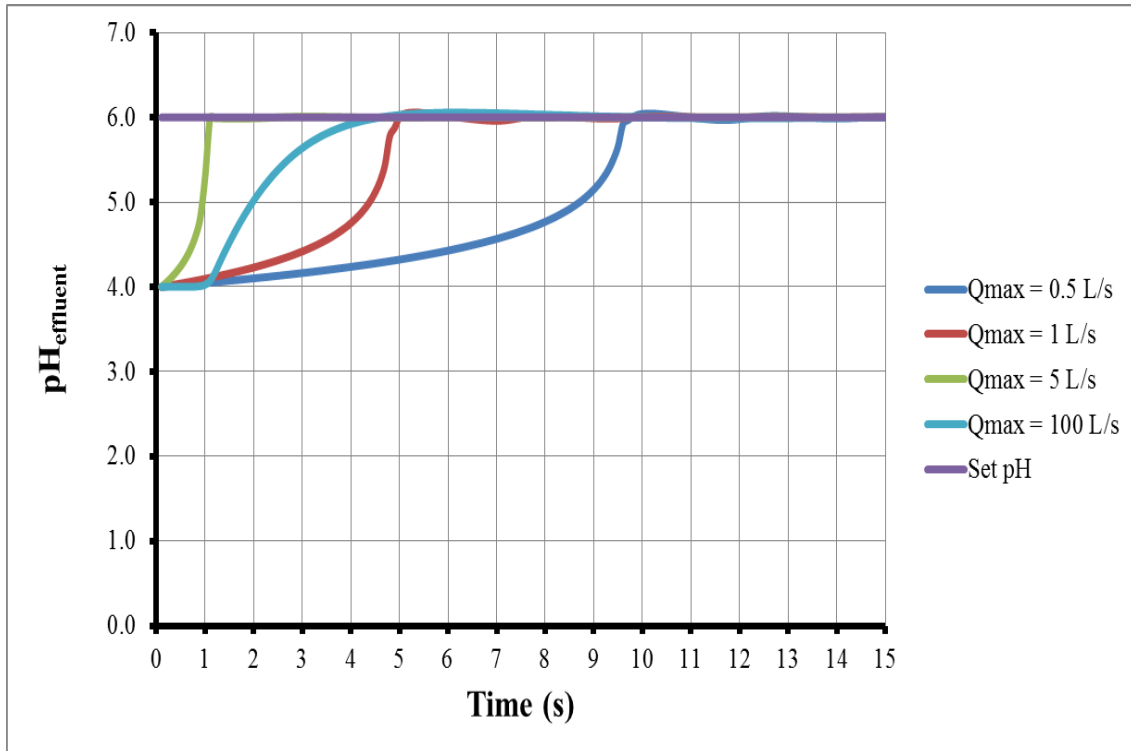


**Figure 21** pH as a function of time for a desired pH of 6.0 with a LA controller for the four different maximum reagent flow rates.

Table 2 provides a summary of the operating conditions and the optimal controller parameters obtained for the linear PID, the fractional  $PI^{\lambda}D^{\mu}$  and the LA controllers for the case study for which the pH set point was 6.0. In Table 2, it is clearly shown that all controllers give a fast response with a response time ranging between 1 and 5 s. The objective function for the PID controller is the highest while the fractional  $PI^{\lambda}D^{\mu}$  and LA controllers have a relatively small sum of ITAE and ISDU. All controllers show excellent performance for reaching rapidly the desired pH of 6.0 when the maximum reagent flow rate  $Q_{max}$  is 5.0 L/s.

**Table 2** Summary of simulation results for the desired pH of 6.0 for  $Q_{\max} = 5.0$  L/s.

<b>Operating Conditions</b>			
$\text{pH}_{\text{set}}$	6		
$\text{pH}_{\text{in}}$	4		
$\text{pH}_{\text{reagent}}$	11		
$Q_{\text{min}}$ (L/s)	0.0001		
<b>Parameters</b>	<b>PID</b>	<b><math>\text{PI}^{\lambda}\text{D}^{\mu}</math></b>	<b>LA</b>
$t_{\text{response}}$ (s)	4.9	2.0	1.1
ITAE + ISDU	69.8	4.0	4.7
$Q_{\text{max}}$ (L/s)	5.0	5.0	5.0
$K_C$	0.65	0.12	-
$\tau_I$	96	24.54	-
$\tau_D$	0.1	13.46	-
$\lambda$	-	0.85	-
$\mu$	-	0.01	-
$n_1$	-	-	28.85
$n_2$	-	-	47.10

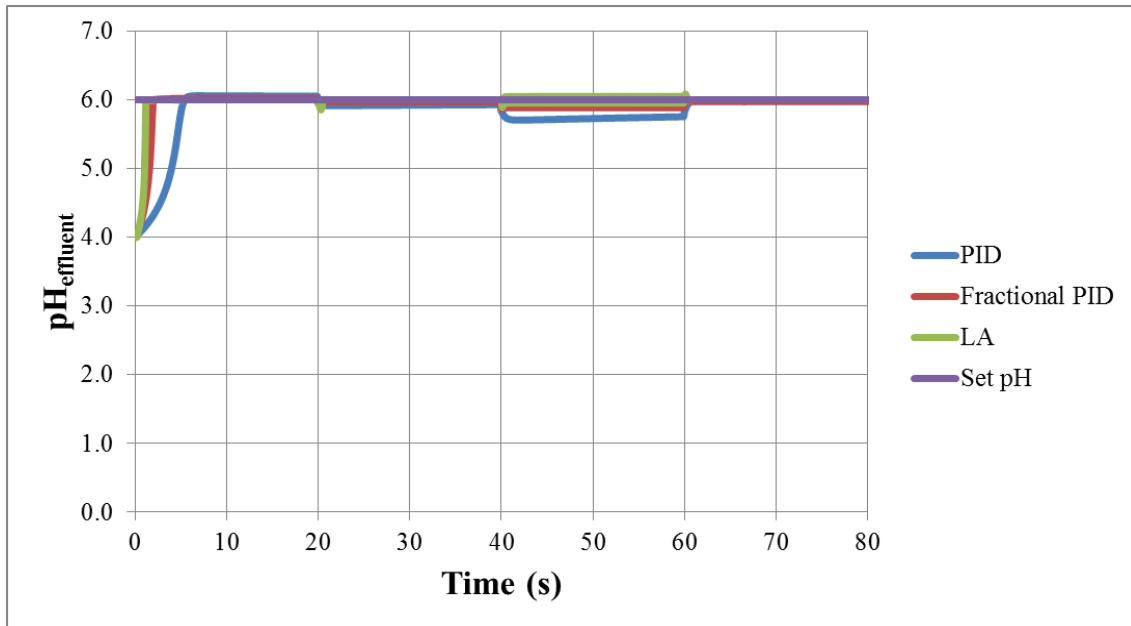
The parameters obtained for the PID controller suggest that the derivative control action is at its minimum set value such the controller is a PI controller. These parameters were obtained following a combination of the grid search and the steepest decent methods.

For the fractional  $\text{PI}^{\lambda}\text{D}^{\mu}$  controller, the integration order and the derivative order are 0.85 and 0.01, respectively. These results therefore suggest a fractional  $\text{PI}^{\lambda}$  controller. The controller gain is very small whereas the integration time parameter is relatively high. Since the derivative order  $\mu$  can be considered zero, the derivative time becomes a constant and if similar calculations, as it was performed in Equation (4.1) are performed, the control gain and integration time of the equivalent fractional  $\text{PI}^{\lambda}$  controller are 1.74 and 354.8, respectively.

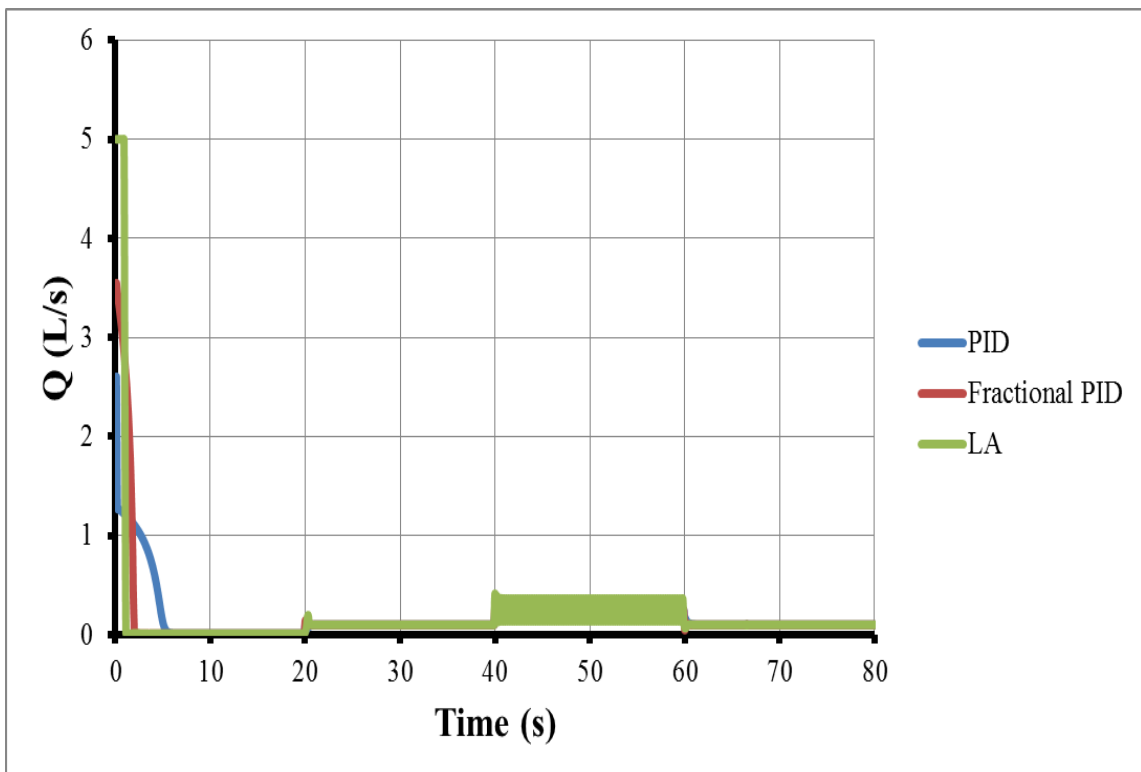
The parameters for the LA controller were obtained to minimize the objective function. Relatively high values of  $n_1$  and  $n_2$  were obtained, whereas the third parameter  $\theta$  (Equation 3.16) was determined to be negligible for all cases considered in this case study.

Figure 22 displays the responses of PID, fractional  $\text{PI}^{\lambda}\text{D}^{\mu}$  and LA controllers for the pH of the effluent stream following a series of disturbances occurring in the pH of the influent

stream when the desired pH is 6.0. For these simulated experiments, the pH of the influent stream was initially set to 4.0 for the first 20 s. The pH of the influent stream was then changed to 3.0, 2.6 and 3.0, respectively at 20, 40 and 60 s. Results of the simulations for the series of disturbances for the three controllers are presented in Figure 22. In these simulations, the controller parameters of Table 2 were used. The responses for the first 20 s of Figure 22 corresponds to the results presented before and used to tune the controllers. When the influent pH is changed to 3.0 and then to 2.6, the pH decreases as expected but the control system is able to recover rapidly to bring back the pH of the effluent stream to 6.0. When at 60 s, the influent pH is set at 3.0, the process returns rapidly to its set point value. Figure 23 shows plot of the manipulated variable, i.e. the reagent flow rate, for the simulation runs presented in Figure 22. Between 20 and 40 s, the manipulated variable of the base flow rate settles rapidly around 0.1 L/s. At 40 s, the influent pH decreases to 2.6 thereby triggering the controller to admit a larger reagent flow rate to return the process output to its set point value. In that segment of the experiment, the base flow rate shows some oscillations and it would necessary to detune slightly the controller to obtain a smoother variation of the base flow rate. Finally, when the influent pH is changed to 3.0 at 60 s, the effluent pH returns rapidly to its set point. It can be postulated that PID, fractional  $PI^{\lambda}D^{\mu}$  and LA controllers are all able to control the pH of the neutralization tank at the desired pH of 6.0 even in the presence of disturbances.



**Figure 22** Response of the effluent pH as a function of time for a series of disturbances in the influent pH for a desired pH of 6.0 for the three controllers.



**Figure 23** Variation of the reagent flow rate as a function of time for a series of disturbances in the influent pH for a desired pH of 6.0 for the three controllers.

#### 4.1.3. Desired pH of 7.0

Figures 24 to 27 present the results of the numerical experiments for the control of the pH of the effluent at pH 7.0 using PID, fractional  $PI^\lambda D^\mu$  and LA controllers. Similar to previous sections, the three controllers were tested for four different maximum base flow rates. The pH and flow rate of the incoming stream were 5 and 0.1 L/s, respectively. Meanwhile, the responses of the effluent pH for the four maximum reagent flow rates  $Q_{\max}$  are presented in Figures 28 to 30 for the linear PID, fractional  $PI^\lambda D^\mu$  and LA controllers.

Figures 24 to 27 show that the three controllers were able to bring the pH of the effluent stream from its initial pH of 5.0 to the desired pH of 7.0 and maintain the effluent pH very well at its set point. The time required to reach the pH set point is between 1 and 3 s for the maximum reagent flow rates of 0.5, 1.0, 5.0 and 100 L/s (Figures 28 to 30). In Figures 24 and 25, the PID controller takes the longest time while the LA controller takes the fastest time to bring up the initial pH of 5.0 to the desired pH of 7.0 when the maximum reagent flow rates of 0.5 L/s and 1 L/s are used. Meanwhile, when the maximum reagent flow rate is increased to 5.0 L/s and 100 L/s, the performance of PID, fractional  $PI^\lambda D^\mu$  and LA controllers is very similar. For the neutralization process for a pH set point of 7.0, the responses presented in Figures 28 to 30 show that there is not much difference between a maximum reagent flow rate of 5.0 and 100 L/s. In fact, for the process response with a maximum flow rate of 100 L/s, the manipulated variable was always well below the maximum. A control valve with a maximum base flow rate  $Q_{\max}$  of 5.0 L/s is quite satisfactory given an influent flow rate of 0.1 L/s and a tank volume of 50 L. In addition, a control valve with a maximum flow rate  $Q_{\max}$  of 5.0 L/s gives a relatively small sum of ITAE and ISDU compared to other maximum base flow rates in every controller in the simulation. In all four base flow rates and for the three controllers, the response is very smooth and the pH stabilized readily when the set point is reached.

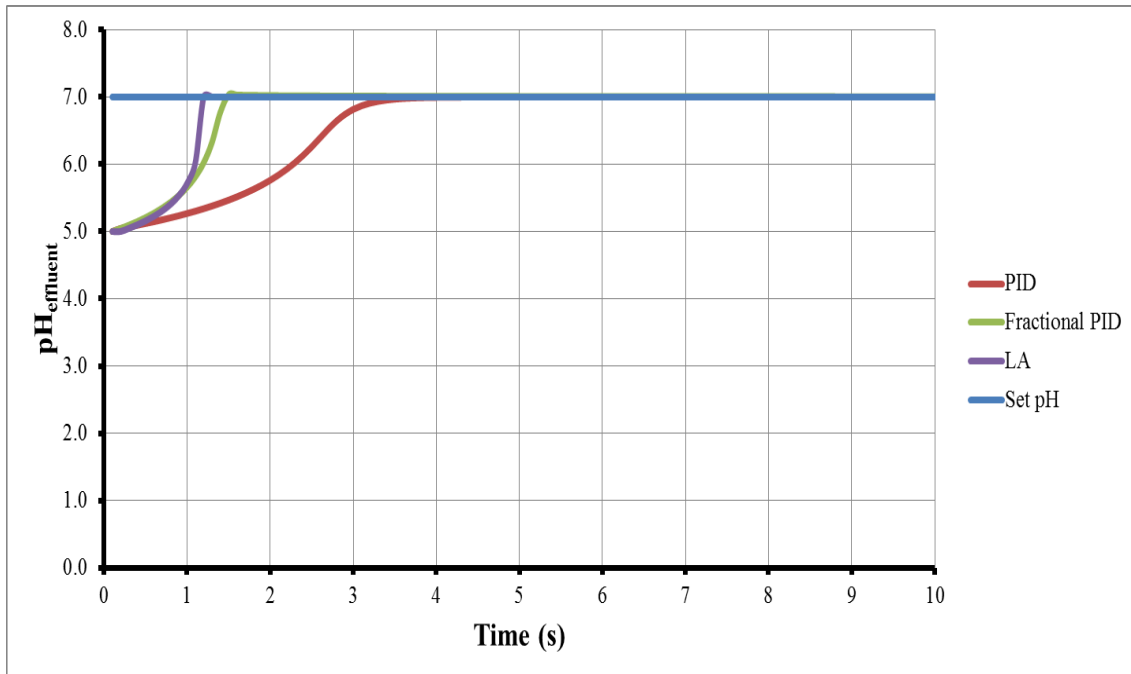


**Figure 24** pH as a function of time for a desired pH of 7.0 with  $Q_{\max} = 0.5$  L/s for the three controllers tuned to minimize the sum of ITAE and ISDU.

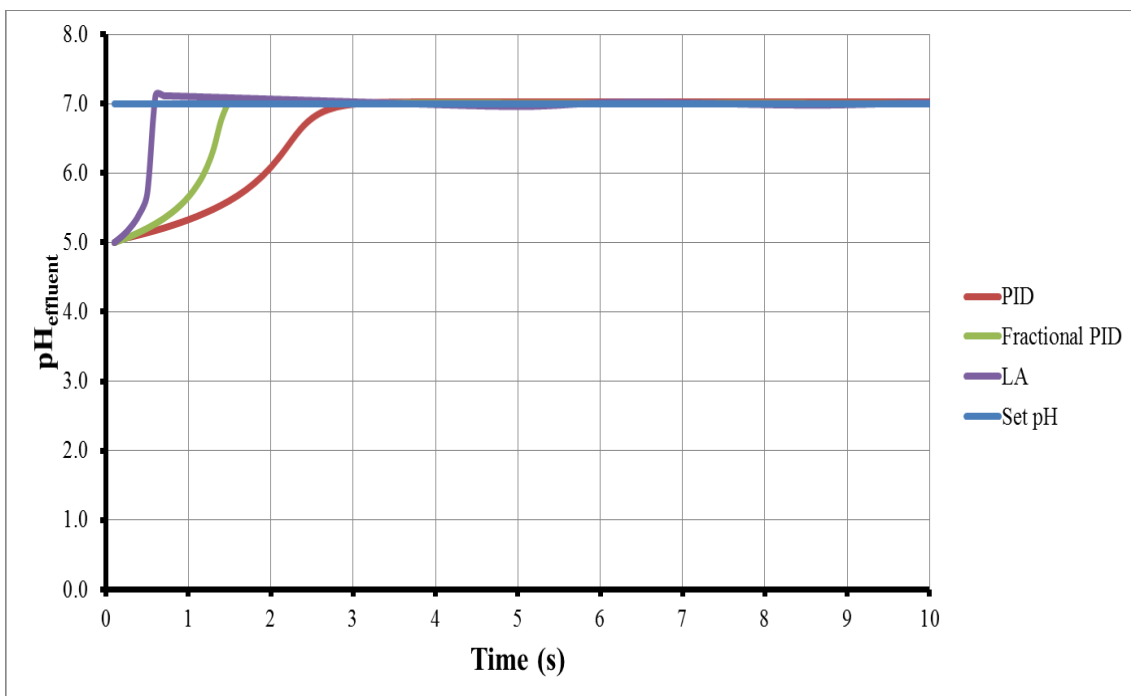


**Figure 25** pH as a function of time for a desired pH of 7.0 with  $Q_{\max} = 1.0$  L/s for the three controllers tuned to minimize the sum of ITAE and ISDU.

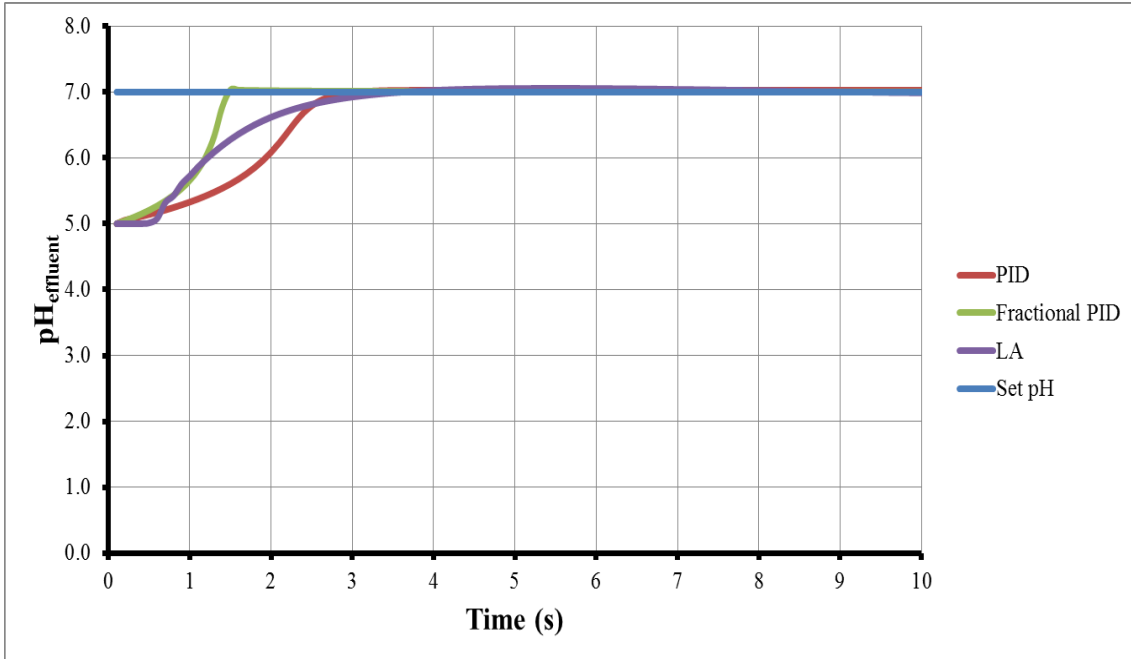


**Figure 26** pH as a function of time for a desired pH of 7.0 with  $Q_{\max} = 5.0$  L/s for the three controllers tuned to minimize the sum of ITAE and ISDU.

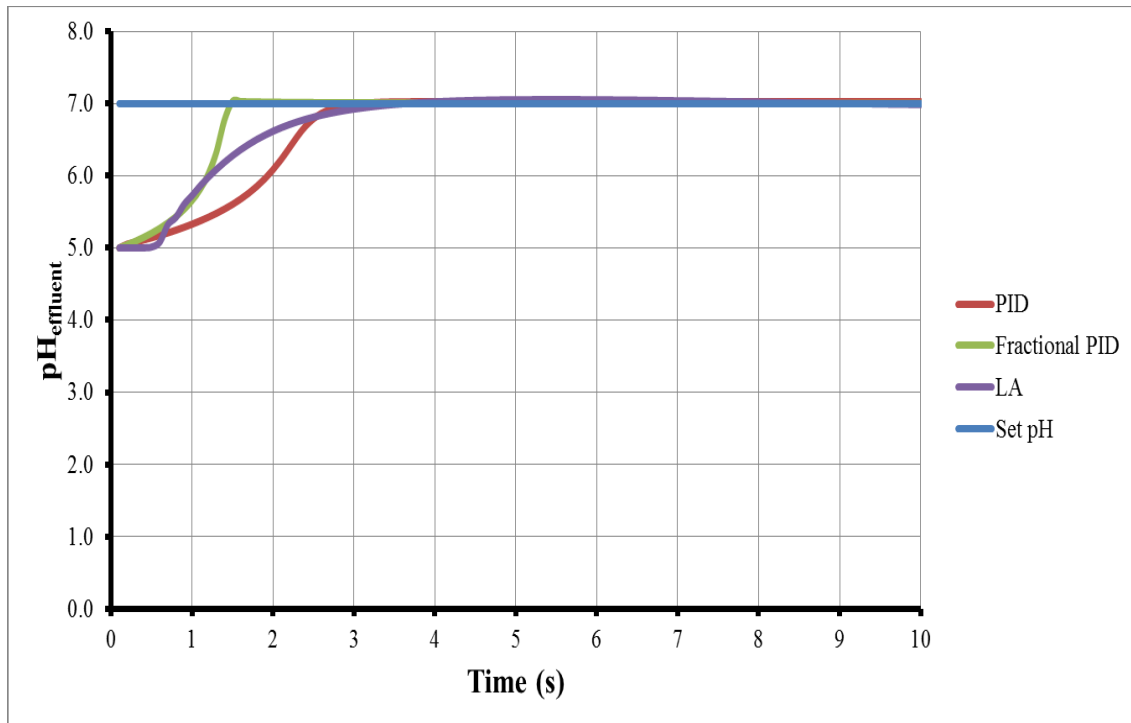


**Figure 27** pH as a function of time for a desired pH of 7.0 with  $Q_{\max} = 100$  L/s for the three controllers tuned to minimize the sum of ITAE and ISDU.

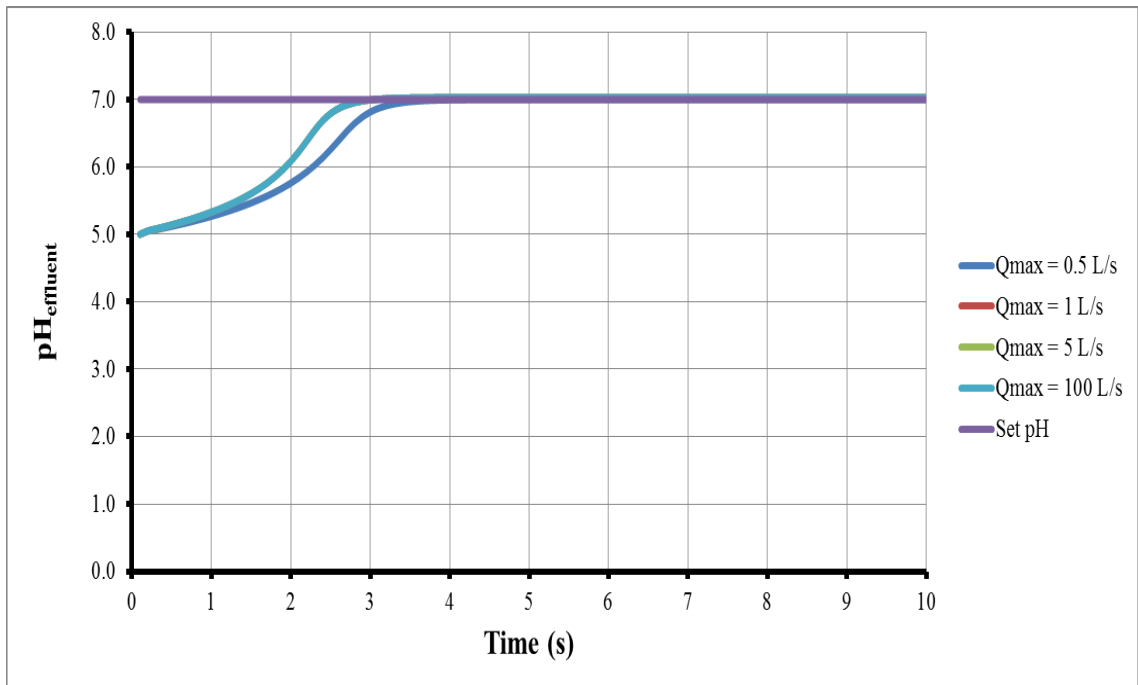


**Figure 28** pH as a function of time for a desired pH of 7.0 with a PID controller for the four different maximum reagent flow rates.

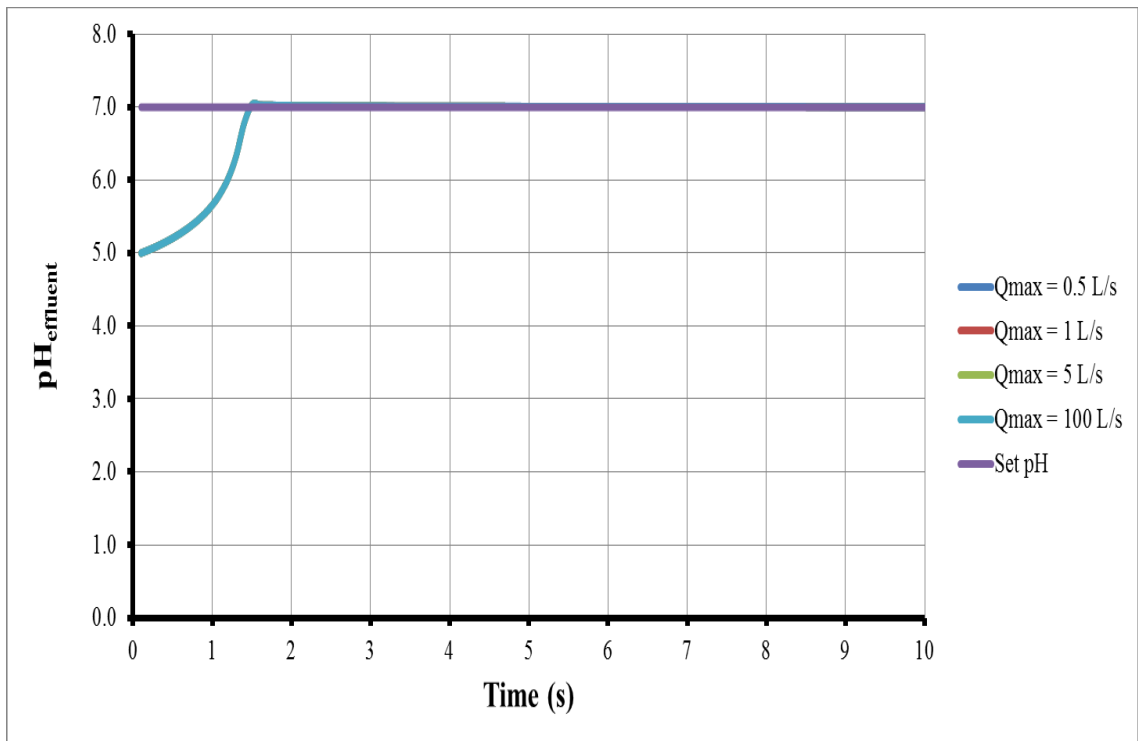


**Figure 29** pH as a function of time for a desired pH of 7.0 with a fractional PI<sup>λ</sup>D<sup>μ</sup> controller for the four different maximum reagent flow rates.

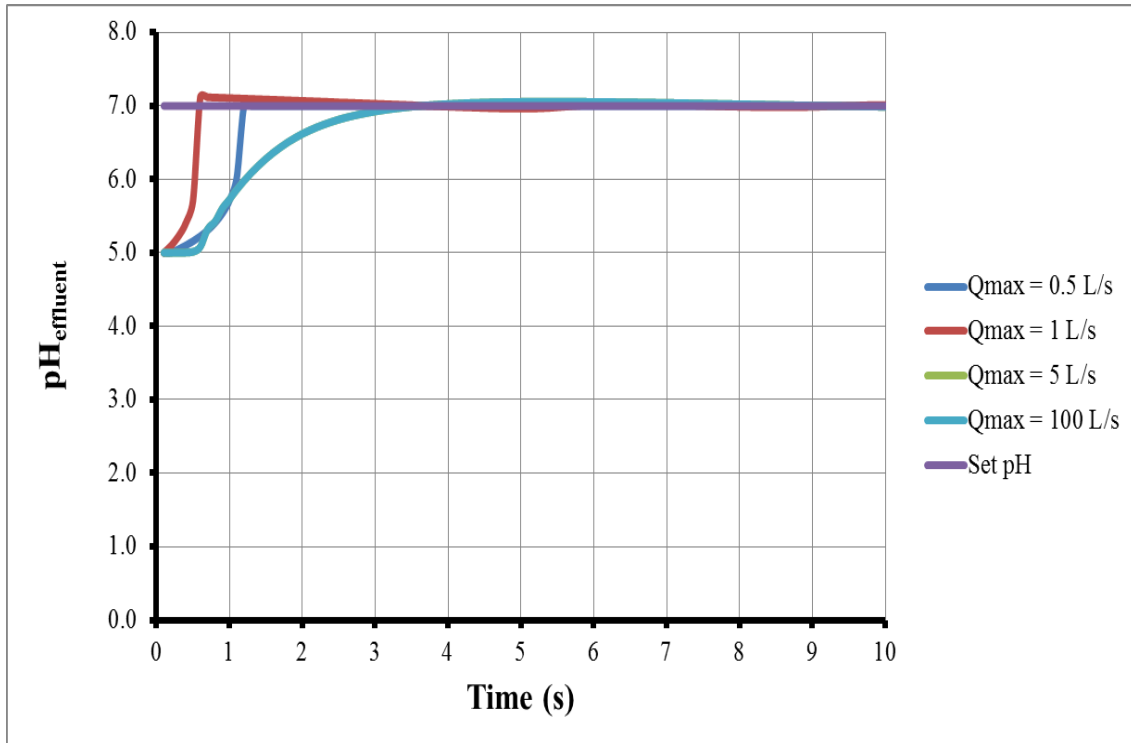


**Figure 30** pH as a function of time for a desired pH of 7.0 with a LA controller for the four different maximum reagent flow rates.

Table 3 provides a summary of the operating conditions and the optimal controller parameters obtained for the linear PID, the fractional  $PI^\lambda D^\mu$  and the LA controllers for the case study for which the pH set point was 7.0. As shown in Table 3, all controllers respond quickly with an approximate response time between 1 and 3 s. The objective function of PID controller is the highest whereas the fractional  $PI^\lambda D^\mu$  and LA controllers have lower sum of ITAE and ISDU, with the fractional  $PI^\lambda D^\mu$  controller having the best performance. Based on the very small difference in the objective function, it can be postulated that all controllers show excellent performance for reaching rapidly the desired pH of 7.0 when the maximum reagent flow rate  $Q_{max}$  is 5.0 L/s.

**Table 3** Summary of simulation results for a desired pH of 7.0 for  $Q_{\max} = 5.0$  L/s.

<b>Operating Conditions</b>			
pH <sub>set</sub>	7		
pH <sub>in</sub>	5		
pH <sub>reagent</sub>	11		
Q <sub>min</sub> (L/s)	0.0001		
<b>Parameters</b>	<b>PID</b>	<b>PI<sup>λ</sup>D<sup>μ</sup></b>	<b>LA</b>
t <sub>response</sub> (s)	2.4	1.4	2.1
ITAE + ISDU	30.6	2.3	5.7
Q <sub>max</sub> (L/s)	5.0	5.0	5.0
K <sub>c</sub>	0.14	0.21	-
τ <sub>I</sub>	96.00	27.98	-
τ <sub>D</sub>	0.10	0.11	-
λ	-	0.40	-
μ	-	0.01	-
n <sub>1</sub>	-	-	5.45
n <sub>2</sub>	-	-	60.00

The parameters obtained for the PID controller show that the derivative control action is at its minimum set value such the resulting controller is a PI controller. As expected, results show small controller gain and high integration time compared to controllers tuned for lower pH because at a pH at the neutralization point, the controller needs to be significantly detuned.

The integration order and the derivative order of the fractional PI<sup>λ</sup>D<sup>μ</sup> controller are 0.4 and 0.01, respectively. The controller gain is very small whereas the integration time is high. The derivative order μ can be considered zero such that the resulting controller is a PI<sup>λ</sup> controller. The PI<sup>λ</sup>D<sup>μ</sup> controller can be transformed into a simple PI<sup>λ</sup> controller akin to what was done in Equation (4.1) to give values of K<sub>c</sub><sup>\*</sup> and τ<sub>I</sub><sup>\*</sup> of 0.23 and 30.8 respectively for the equivalent PI<sup>λ</sup> controller.

The parameters for the LA controller were obtained to minimize the objective function. A relatively low value of n<sub>1</sub> is obtained because the controller needs to be detuned compared to the controller parameters at lower pH. The value of n<sub>2</sub> remains high. Again the third parameter θ (Equation 3.16) was determined to be negligible.

Figure 31 displays the response of the pH of the effluent when using PID, fractional  $PI^{\lambda}D^{\mu}$  and LA controllers following a series of disturbances in the influent pH while the desired pH remains at 7.0. The initial inlet stream pH was set to be 5 and kept constant for the first 20 s. The pH of the influent stream was then changed to 4.0, 3.6 and 5.0 at 20, 40 and 60 s respectively. Generally speaking the PID, fractional  $PI^{\lambda}D^{\mu}$  and LA controllers respond efficiently, rapidly and with minimum overshoot to disturbances in the influent pH when the desired pH is 7.0. However, since the controllers are significantly detuned at the desired pH 7, the controller could not cope adequately with a disturbance for an influent pH of less than 3.0.

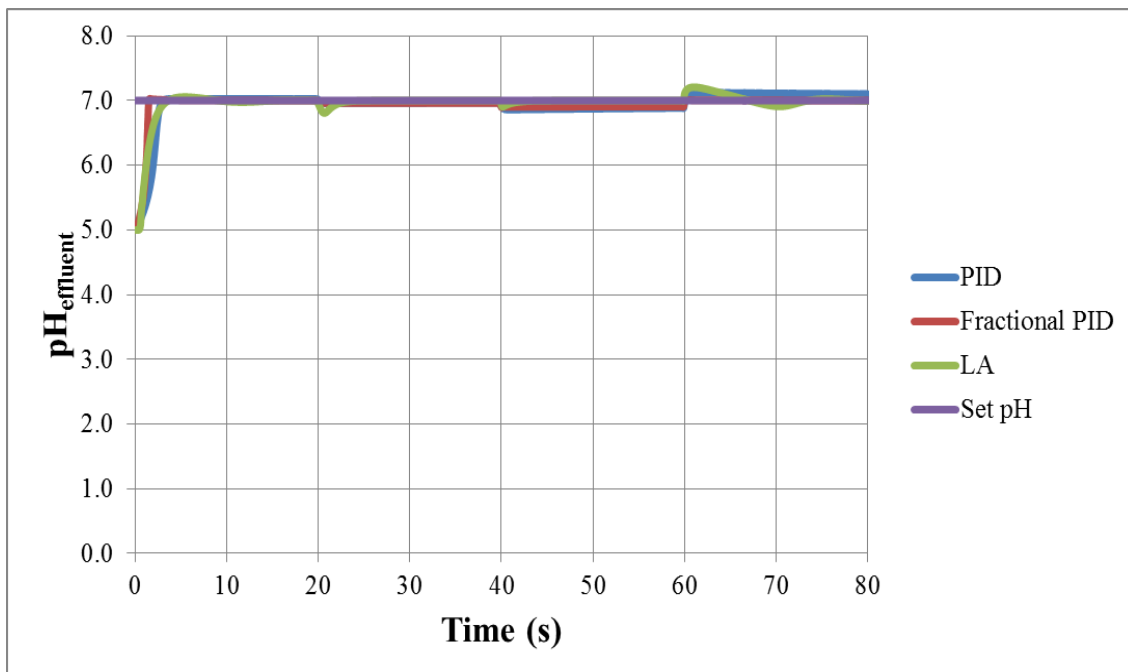


**Figure 31** Response of the effluent pH as a function of time for a series of disturbances in the influent pH for a desired pH of 7.0 for the three controllers.

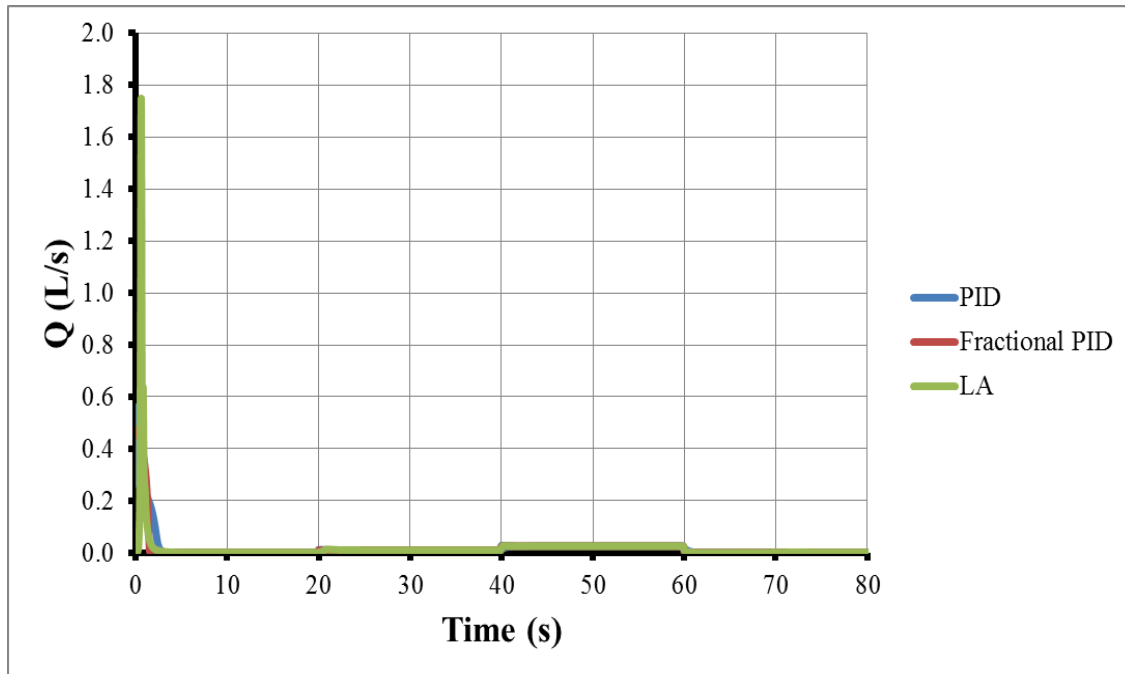


**Figure 32** Variation of the reagent flow rate as a function of time for a series of disturbances in the influent pH for a desired pH of 7.0 for the three controllers.

#### 4.1.4. Desired pH of 8.0

The results of the numerical experiments for the control of pH in the neutralization tank using PID, fractional  $PI^{\lambda}D^{\mu}$  and LA controllers for four different maximum base solution flow rates for the desired pH of 8.0 are shown in Figures 33 to 36. In addition, the responses of the effluent pH for the four maximum reagent flow rates  $Q_{\max}$  are presented in Figures 37 to 39 individually for the linear PID, fractional  $PI^{\lambda}D^{\mu}$  and LA controllers. The three controllers were simulated and evaluated for the pH of an incoming stream having a pH of 6.0 and a flow rate of 0.1 L/s. Figures 33 to 36 show that the three controllers were able to bring the pH of the effluent stream from an initial pH of 6.0 to the desired pH of 8.0 and to maintain the pH at its set point. The time required to reach the pH set point on the three controllers is very fast, being less than 3 seconds. For the neutralization tank with a pH set point of 8.0 and the maximum reagent flow rates of 0.5, 1.0, 5.0 and 100 L/s, each controller nearly leads to the same results in the pH effluent response. Since pH 8.0 is close to the neutralization point and the distance between the set pH and the pH of the base solution is closer, it is preferable for this case study to use a control valve giving a

maximum flow rate  $Q_{\max}$  of 1.0 L/s. This is also justified by the relatively small sum of ITAE and ISDU compared to the other maximum flow rates. No noticeable overshoots were observed in the process response when PID, fractional  $PI^{\lambda}D^{\mu}$  and LA controllers were used for  $Q_{\max}$  of 0.5, 1.0, 5.0 and 100 L/s at a desired pH of 8.0. The response obtained with the PID controller was exactly the same for all maximum base flow rates and, in fact, the same controller parameters were obtained.

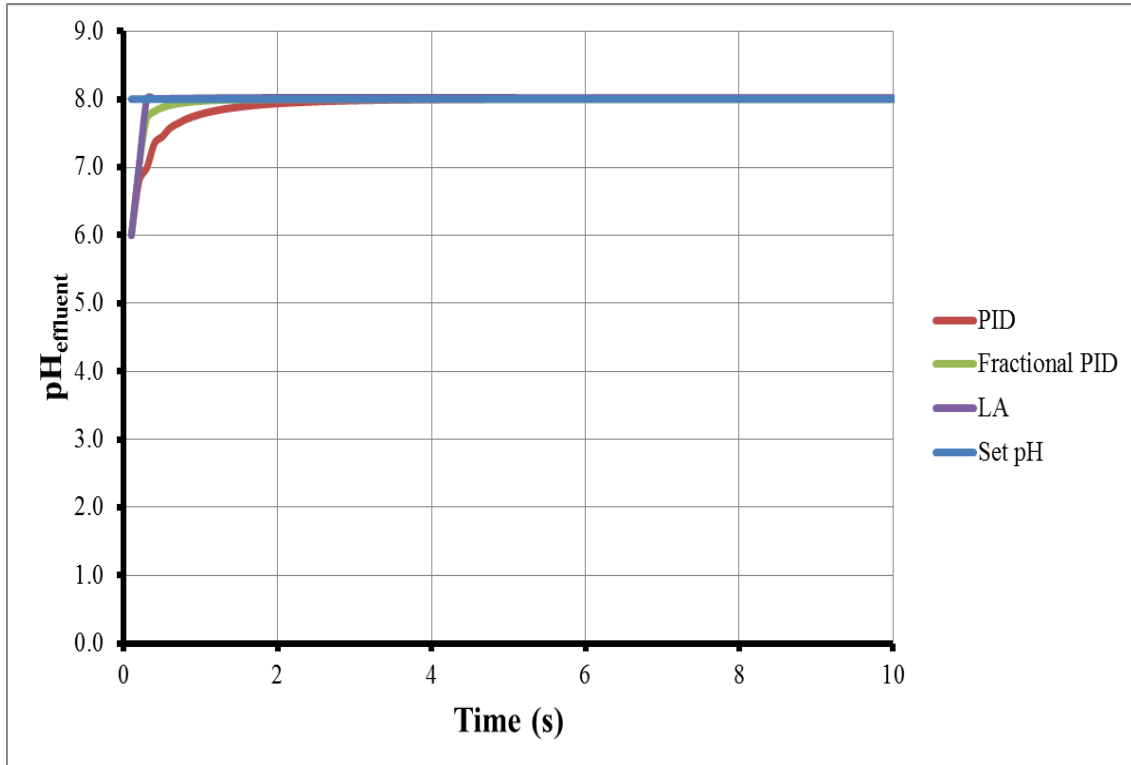


**Figure 33** pH as a function of time for a desired pH of 8.0 with  $Q_{\max} = 0.5$  L/s for the three controllers tuned to minimize the sum of ITAE and ISDU.

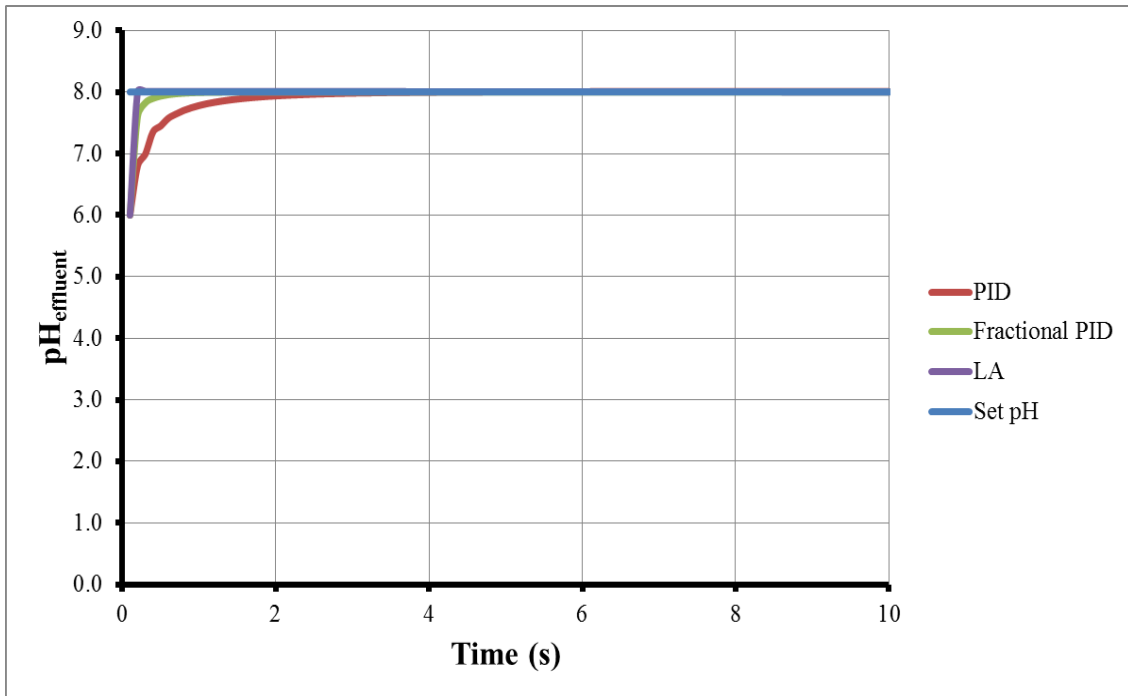


**Figure 34** pH as a function of time for a desired pH of 8.0 with  $Q_{\max} = 1.0$  L/s for the three controllers tuned to minimize the sum of ITAE and ISDU.

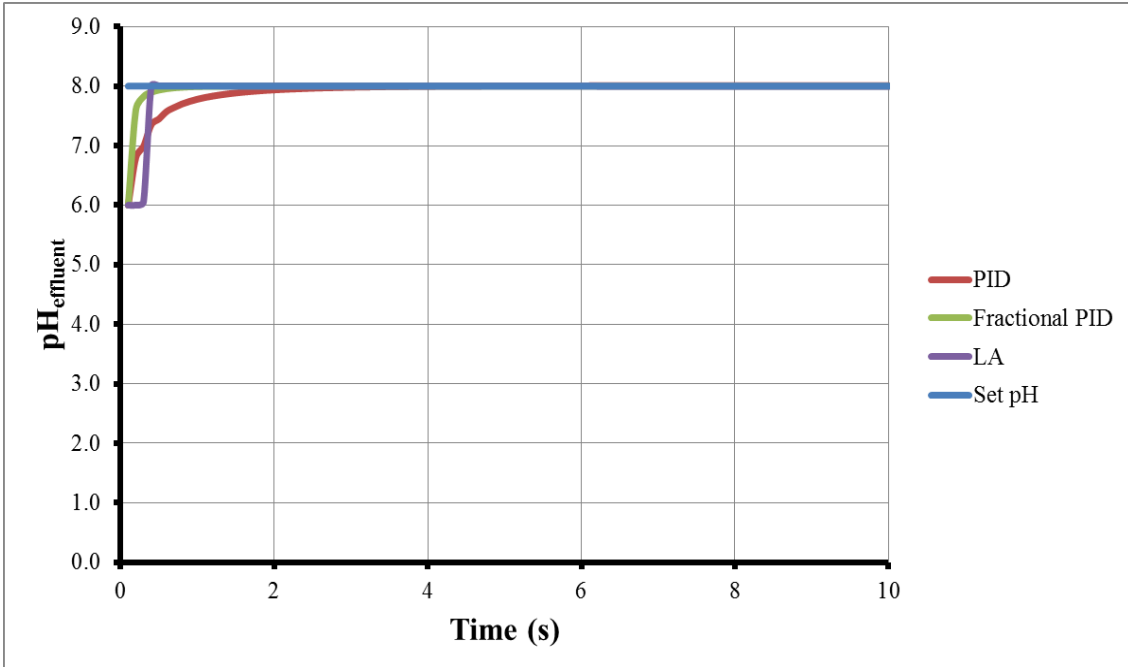


**Figure 35** pH as a function of time for a desired pH of 8.0 with  $Q_{\max} = 5.0$  L/s for the three controllers tuned to minimize the sum of ITAE and ISDU.

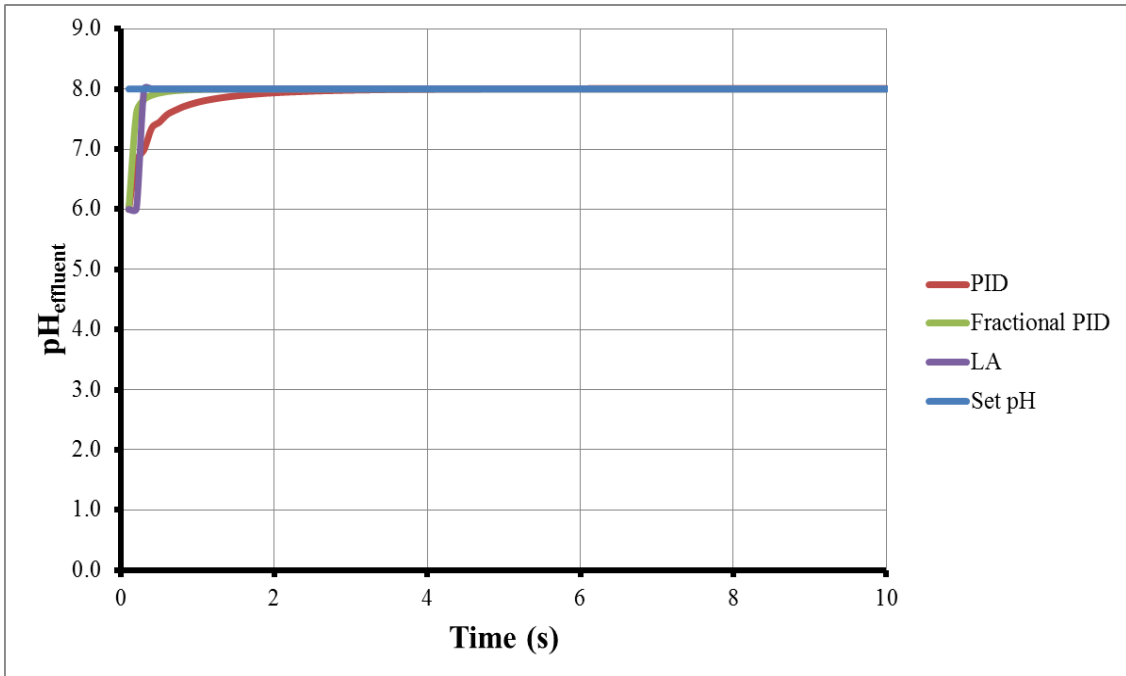


**Figure 36** pH as a function of time for a desired pH of 8.0 with  $Q_{\max} = 100$  L/s for the three controllers tuned to minimize the sum of ITAE and ISDU.

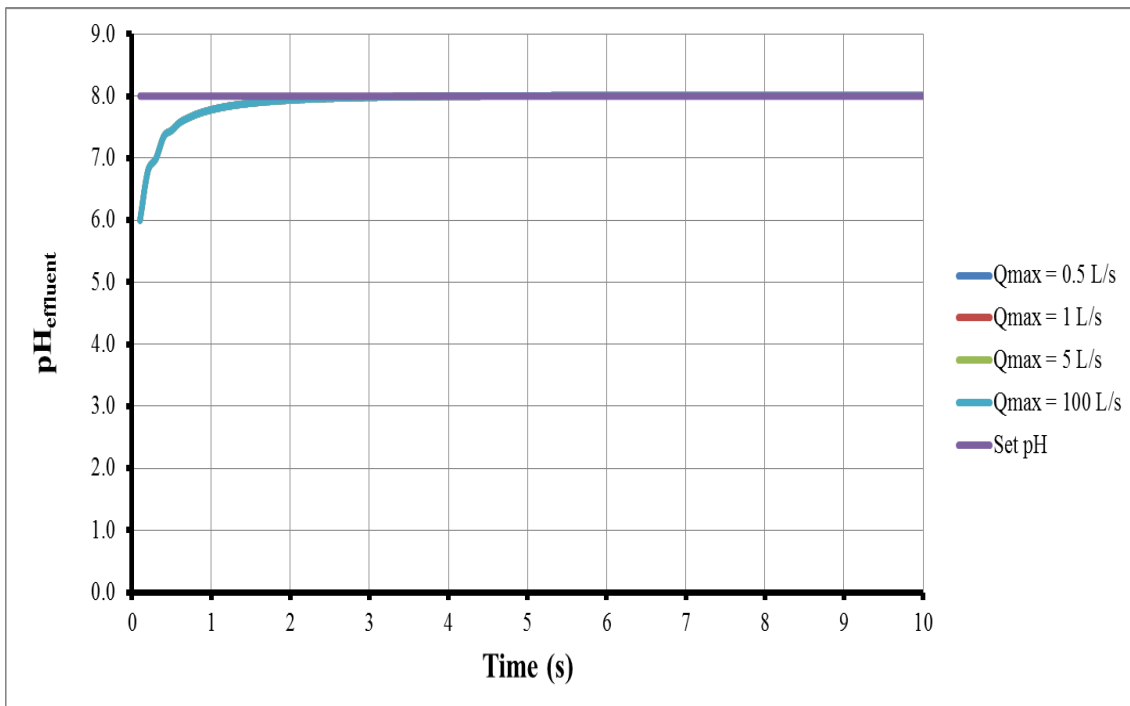


**Figure 37** pH as a function of time for a desired pH of 8.0 with a PID controller for the four different maximum reagent flow rates.

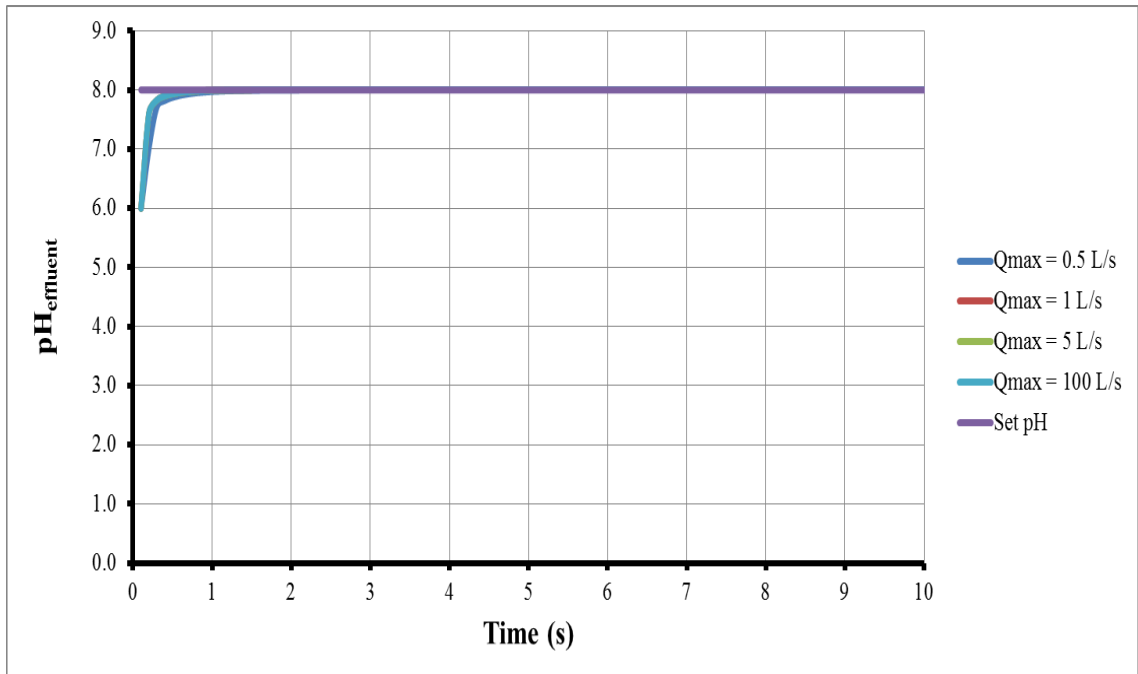


**Figure 38** pH as a function of time for a desired pH of 8.0 with a fractional  $PI^\lambda D^\mu$  controller for the four different maximum reagent flow rates.

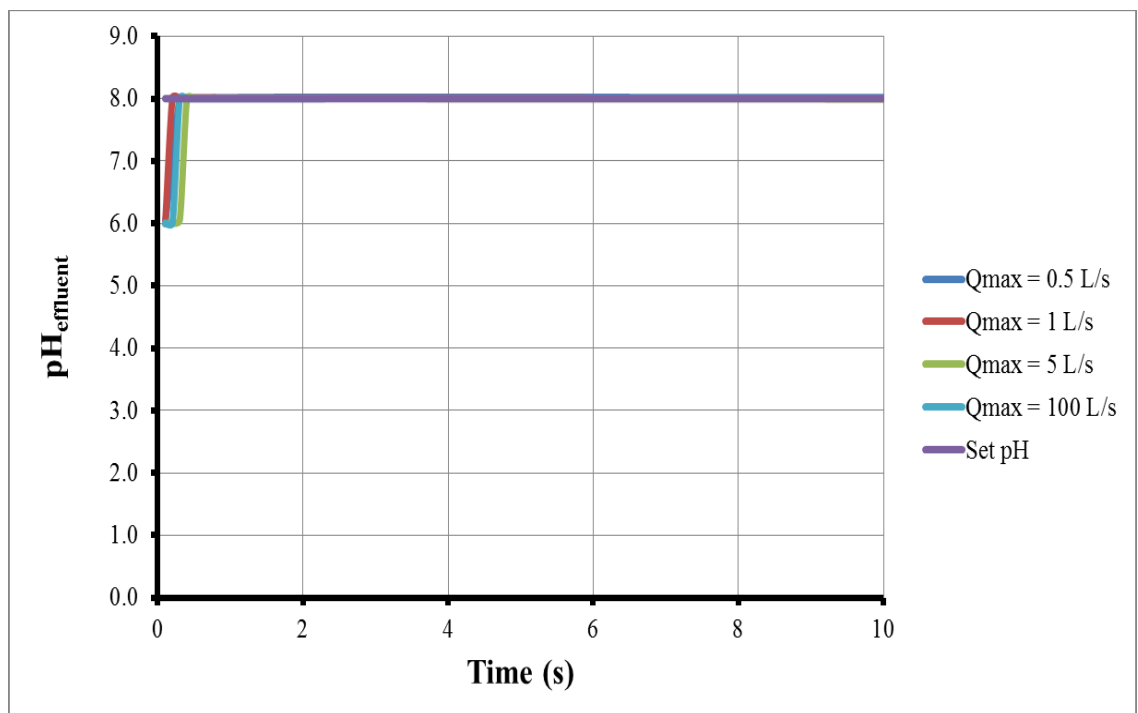


**Figure 39** pH as a function of time for a desired pH of 8.0 with a LA controller for the four different maximum reagent flow rates.

Table 4 provides a summary of the operating conditions and the optimal controller parameters obtained for the linear PID, the fractional  $PI^\lambda D^\mu$  and the LA controllers for the case study for which the pH set point was 8.0. Results show that all controllers provide a very fast response time which is less than 0.6 s. The objective function of the PID controller is the highest while the fractional  $PI^\lambda D^\mu$  controller has the lowest sum of ITAE and ISDU. All controllers show excellent performance for reaching rapidly the desired pH of 8.0 when the maximum reagent flow rate  $Q_{\max}$  is 1.0 L/s.

**Table 4** Summary of simulation results for the desired pH of 8.0 for  $Q_{\max} = 1.0$  L/s.

<b>Operating Conditions</b>			
pH <sub>set</sub>	8		
pH <sub>in</sub>	6		
pH <sub>reagent</sub>	11		
Q <sub>min</sub> (L/s)	0.0001		
<b>Parameters</b>	<b>PID</b>	<b>PI<sup>λ</sup>D<sup>μ</sup></b>	<b>LA</b>
t <sub>response</sub> (s)	0.6	0.2	0.2
ITAE + ISDU	8.1	0.2	2.3
Q <sub>max</sub> (L/s)	1.0	1.0	1.0
K <sub>C</sub>	0.11	0.30	-
τ <sub>I</sub>	96.00	36.51	-
τ <sub>D</sub>	0.10	0.12	-
λ	-	0.36	-
μ	-	0.01	-
n <sub>1</sub>	-	-	60.00
n <sub>2</sub>	-	-	50.00

The parameters obtained for the PID controller suggest that the derivative control action is at its minimum set value such the controller is a PI controller with small value of K<sub>C</sub>. The integration time is very close to its upper limit.

The integration order and the derivative order of the fractional  $PI^\lambda D^\mu$  controller, being 0.36 and 0.01. The controller gain is very small and the derivative time is at its minimum value. The derivative order  $\mu$  can therefore be considered zero. The  $PI^\lambda D^\mu$  controller can be transformed into a simple  $PI^\lambda$  controller akin to what was shown in Equation (4.1). If the

values of  $K_c$ ,  $\tau_I$  and  $\tau_D$  are substituted in the expression of  $K_c^*$  and  $\tau_I^*$ , the values of 0.34 and 40.9 are obtained for  $K_c$  and  $\tau_I$ , respectively, for the equivalent  $PI^\lambda$  controller.

Relatively high values of parameters of  $n_1$  and  $n_2$  for the LA controller were obtained, whereas the third parameter  $\theta$  (Equation 3.16) was determined to be negligible as in all the other cases.

Figure 40 displays the pH effluent response for PID, fractional  $PI^\lambda D^\mu$  and LA controllers following a series of inlet pH disturbances when the desired pH is 8.0. The initial pH of the influent was set equal to 6.0 for the first 20 s. Subsequently, the inlet stream pH was changed to 5.0, 4.6 and then 6.0 at, respectively, 20, 40 and 60 s. Results of Figure 40 show that PID, fractional  $PI^\lambda D^\mu$  and LA controllers were excellent to control the effluent stream at the desired pH of 8.0 despite the presence of disturbances.

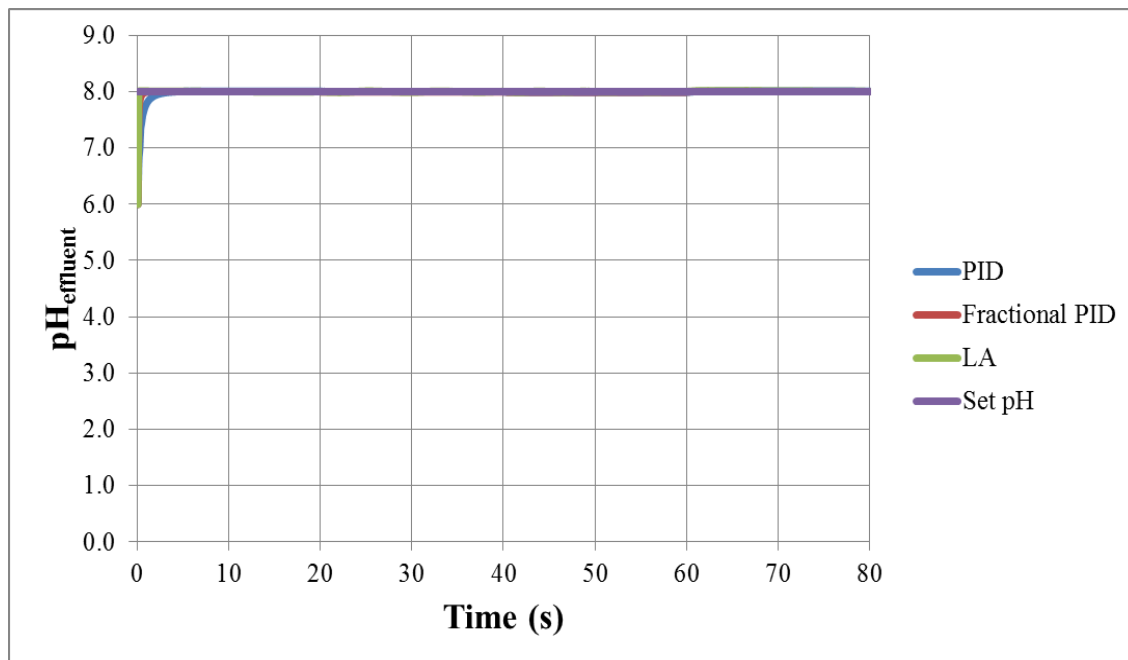


**Figure 40** Response of the effluent pH as a function of time for a series of disturbances in the influent pH for a desired pH of 8.0 for the three controllers.

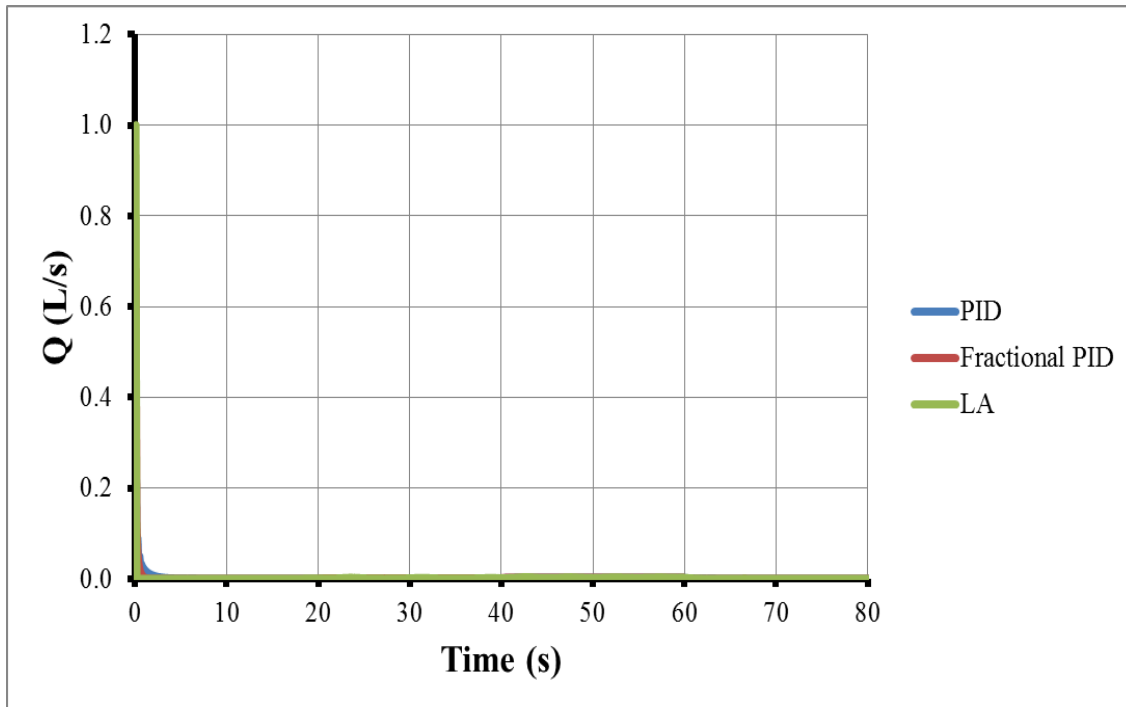


**Figure 41** Variation of the reagent flow rate as a function of time for a series of disturbances in the influent pH for a desired pH of 8.0 for the three controllers.

#### 4.1.5. Desired pH of 9.0

The results of the numerical experiments for the control of the effluent pH of a neutralization tank using PID, fractional  $PI^{\lambda}D^{\mu}$  and LA controllers for four different maximum flow rates for a desired pH of 9.0 are presented in Figures 42 to 45. In addition, the responses of the effluent pH for the four maximum reagent flow rates  $Q_{\max}$  are presented in Figures 46 to 48 for individual linear PID, fractional  $PI^{\lambda}D^{\mu}$  and LA controllers. The neutralization process was simulated and evaluated for an incoming stream having a pH of 7 and a flow rate of 0.1 L/s. Figures 42 to 45 show that the three controllers were able to bring the pH of the effluent stream from its initial pH of 7.0 to the desired pH of 9.0 and maintain very well the pH at its set point. The time required to reach the pH set point was longer with the PID controller, at around 6 s, while the response time for the fractional  $PI^{\lambda}D^{\mu}$  and LA controllers were less than 2 s. Results of Figure 46 show that for the PID controller, responses of the effluent pH are identical for all maximum base solution flow rates. Meanwhile the effluent pH responses when using fractional  $PI^{\lambda}D^{\mu}$  and LA controllers with maximum reagent flow rates of 0.5, 1.0, 5.0 and 100 L/s are very similar. A control

valve with a maximum base flow rate  $Q_{\max}$  of 1.0 L/s provided a relatively small sum of ITAE and ISDU compared to other responses obtained for other maximum base flow rates for all controllers. Thus, for the neutralization process for a desired pH of 9.0, a maximum reagent flow rate  $Q_{\max}$  of 1.0 L/s was chosen. This maximum base flow rate is large enough to allow fast control for all three controllers used in the system of the desired pH of 9.0. No noticeable overshoots were observed when PID, fractional  $PI^{\lambda}D^{\mu}$  and LA controllers were used for all values of  $Q_{\max}$ .

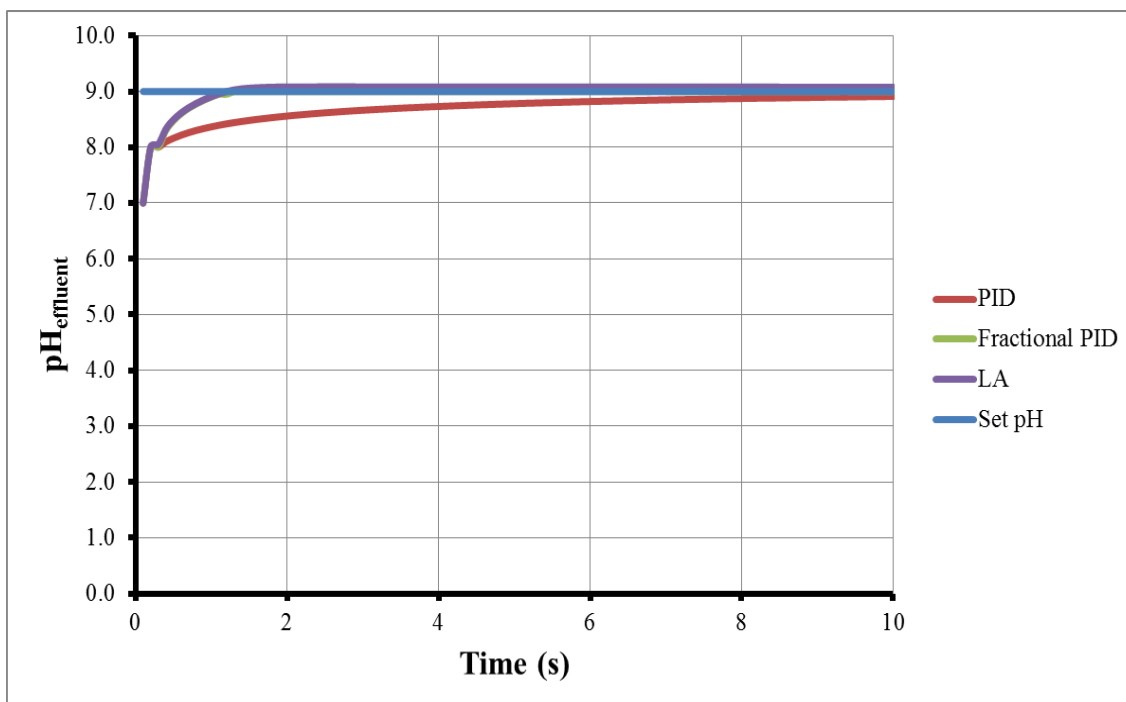


**Figure 42** pH as a function of time for a desired pH of 9.0 with  $Q_{\max} = 0.5$  L/s for the three controllers tuned to minimize the sum of ITAE and ISDU.

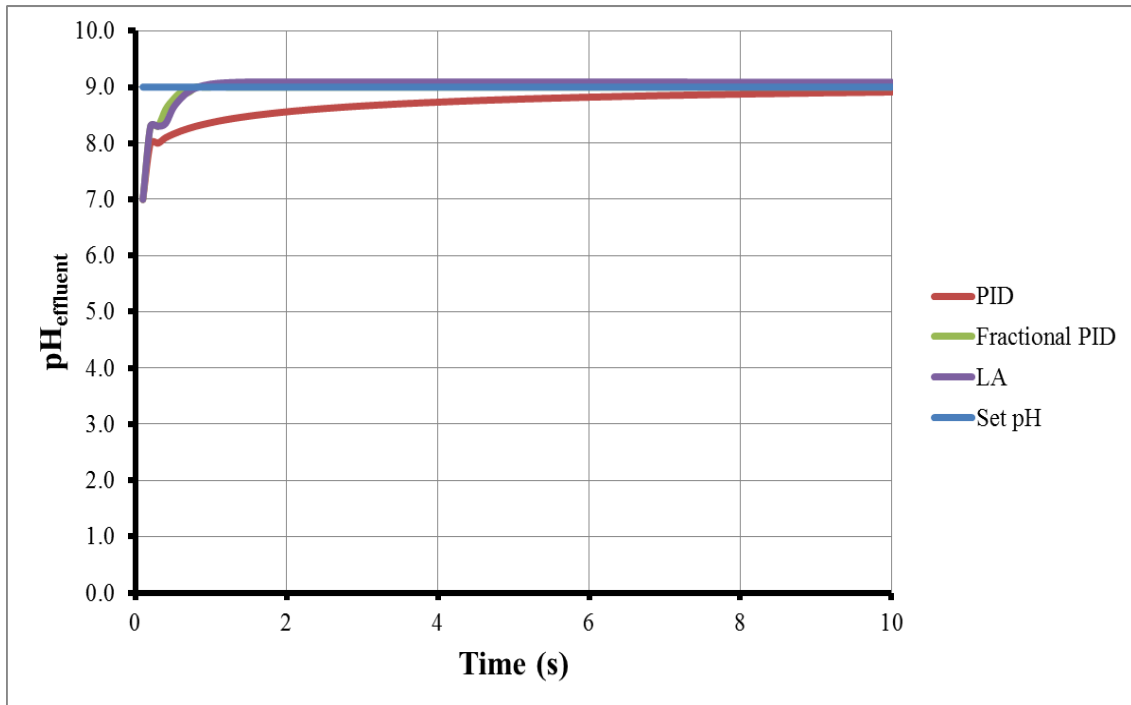


**Figure 43** pH as a function of time for a desired pH of 9.0 with  $Q_{\max} = 1.0$  L/s for the three controllers tuned to minimize the sum of ITAE and ISDU.

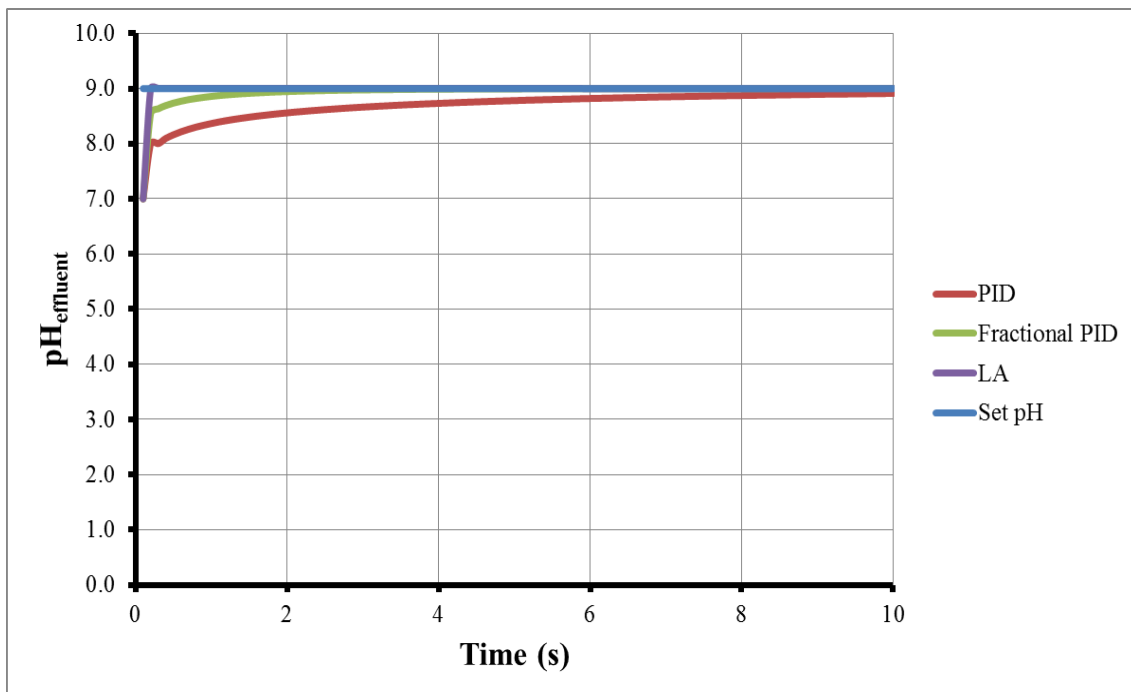


**Figure 44** pH as a function of time for a desired pH of 9.0 with  $Q_{\max} = 5.0$  L/s for the three controllers tuned to minimize the sum of ITAE and ISDU.

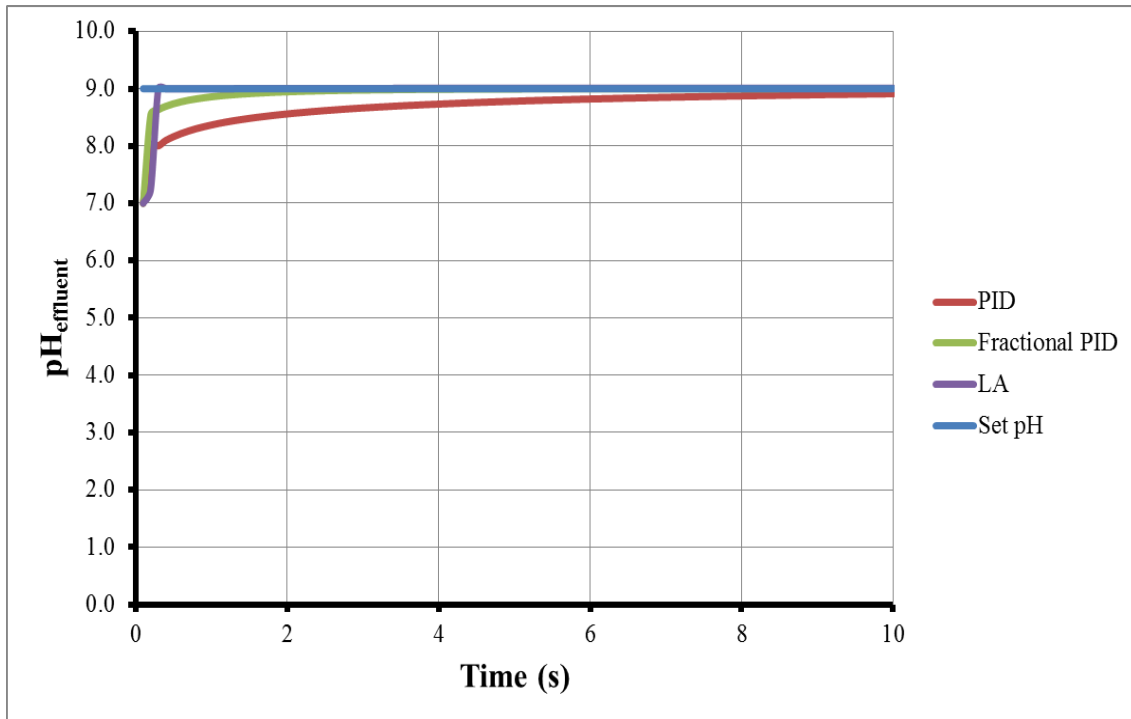


**Figure 45** pH as a function of time for a desired pH of 9.0 with  $Q_{\max} = 100$  L/s for the three controllers tuned to minimize the sum of ITAE and ISDU.

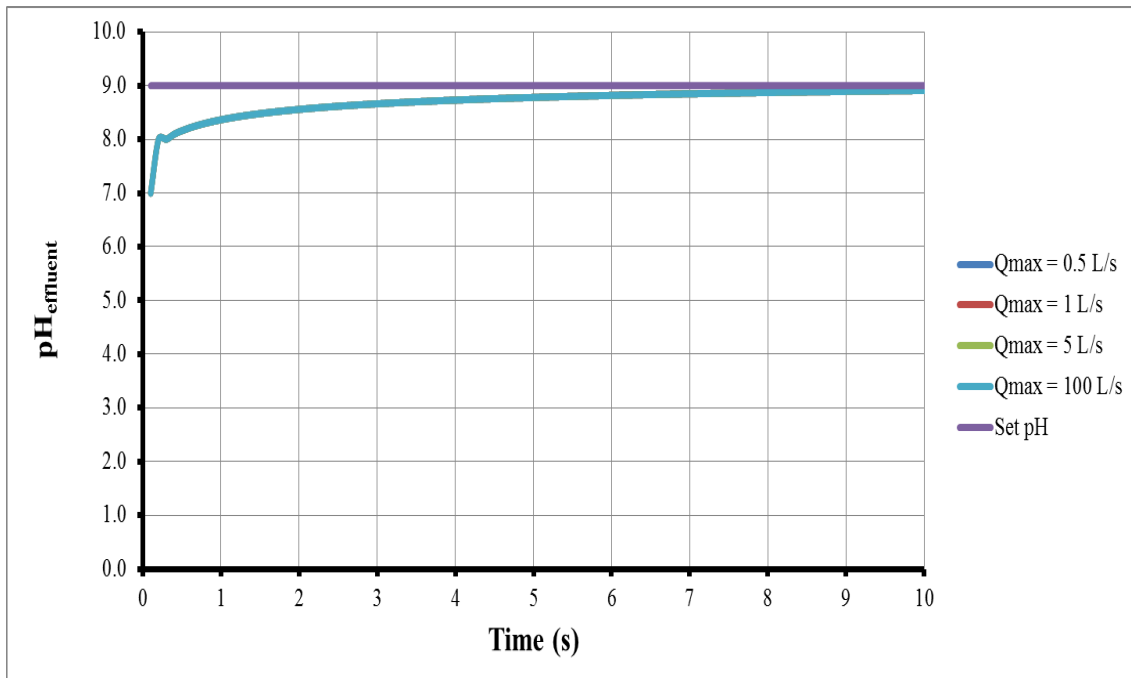


**Figure 46** pH as a function of time for a desired pH of 9.0 with a PID controller for the four different maximum reagent flow rates.

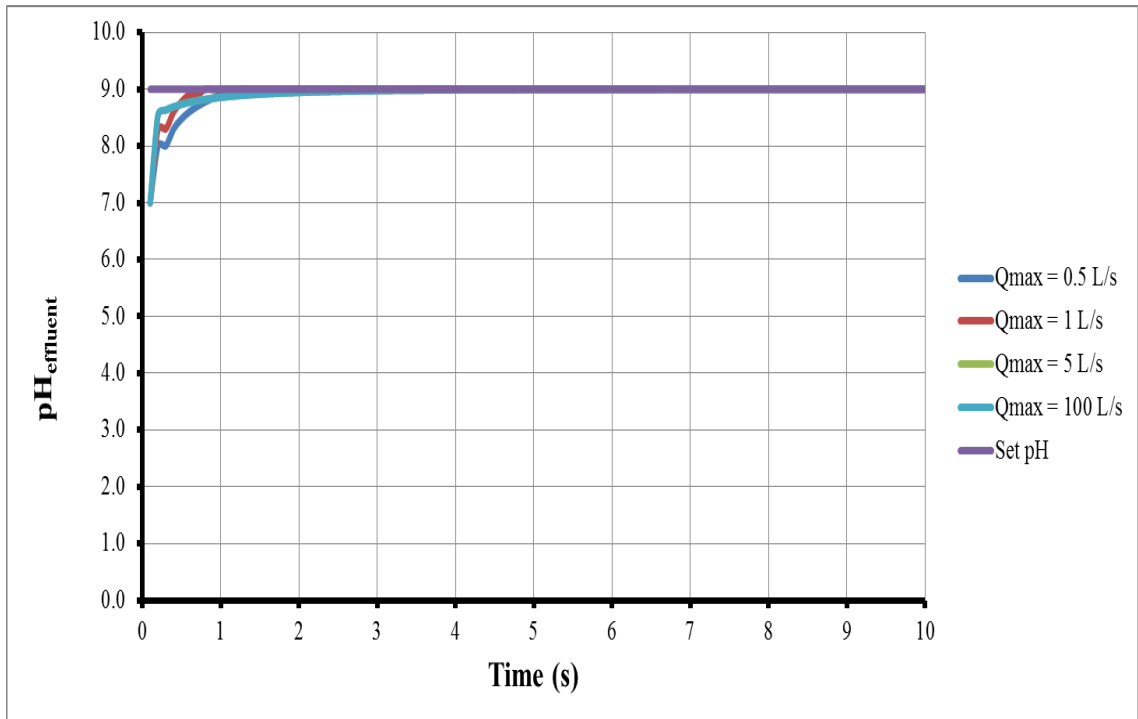


**Figure 47** pH as a function of time for a desired pH of 9.0 with a fractional  $PI^\lambda D^\mu$  controller for the four different maximum reagent flow rates.

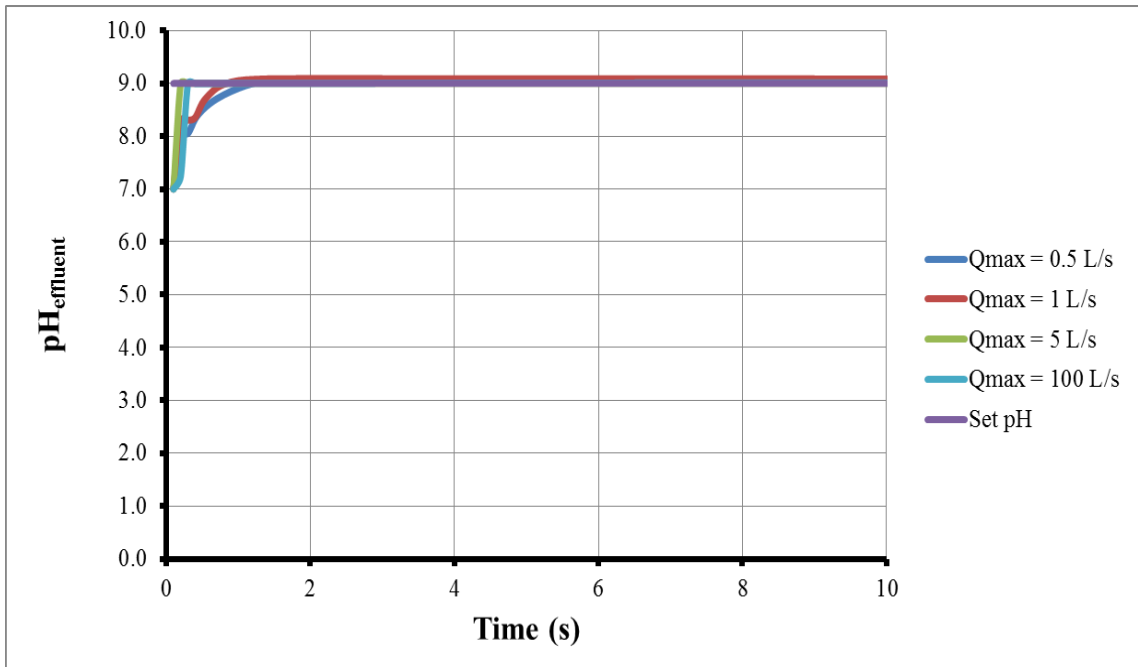


**Figure 48** pH as a function of time for a desired pH of 9.0 with a LA controller for the four different maximum reagent flow rates.

Table 5 provides a summary of the operating conditions and the optimal controller parameters obtained for the linear PID, the fractional  $PI^\lambda D^\mu$  and the LA controllers for the case study for which the pH set point was 9.0. Results in Table 5 show that the response time obtained with all controllers are fast with values less than 2 s. The objective function (sum of ITAE and ISDU) obtained with the LA controller is the highest while the one for the fractional  $PI^\lambda D^\mu$  controller is the lowest. All controllers show a rapid response and were able to reach efficiently the desired pH of 9.0 when the maximum reagent flow rate  $Q_{\max}$  is 1.0 L/s.

**Table 5** Summary of simulation results for desired pH of 9 system for  $Q_{\max} = 1.0$  L/s.

<b>Operating Conditions</b>			
pH <sub>set</sub>	9		
pH <sub>in</sub>	7		
pH <sub>reagent</sub>	11		
Q <sub>min</sub> (L/s)	0.0001		
<b>Parameters</b>	<b>PID</b>	<b>PI<sup>λ</sup>D<sup>μ</sup></b>	<b>LA</b>
t <sub>response</sub> (s)	2	0.4	0.5
ITAE + ISDU	3.2	0.8	5.0
Q <sub>max</sub> (L/s)	1.0	1.0	1.0
K <sub>C</sub>	9.94	98.54	-
τ <sub>I</sub>	80	0.10	-
τ <sub>D</sub>	0.10	0.10	-
λ	-	0.99	-
μ	-	0.01	-
n <sub>1</sub>	-	-	50.00
n <sub>2</sub>	-	-	60.00

The parameters obtained for the PID controller suggest that the derivative control action is at its minimum set value such the controller is a PI controller. The controller gain is much higher compared to the ones that were obtained when the pH set points were closer to the neutralization set point. This was expected.

The parameters obtained for the fractional  $PI^\lambda D^\mu$  controller suggest that the controller is really a PI controller since the integral order is nearly unity and the derivative order is zero. The  $PI^\lambda D^\mu$  controller can be therefore easily transformed into a simple PI controller as

shown in Equation (4.1). If the values of  $K_c$ ,  $\tau_I$  and  $\tau_D$  are substituted in the expression of  $K_c^*$  and  $\tau_I^*$ , the values of 108.4 and 0.11 will be the values of  $K_c$  and  $\tau_I$  for the equivalent PI controller.

For the LA controller, relatively high values of  $n_1$  and  $n_2$  were obtained, whereas the third parameter  $\theta$  (Equation 3.16) was determined to be negligible.

Figure 49 displays the response of the effluent pH as a function of time when PID, fractional  $PI^{\lambda}D^{\mu}$  and LA controllers are used to maintain the pH constant following a series of disturbances in the pH of the influent stream for a desired pH of 9.0. The initial pH of the inlet stream was set to be 7.0 for the first 20 s before being changed to 6.0, 5.6, and 7.0 at, respectively 20, 40 and 60 s. Results of Figure 49 show that PID, fractional  $PI^{\lambda}D^{\mu}$  and LA controllers are able to efficiently and rapidly control the effluent pH at the desired pH of 9.0 despite the series of disturbances. Figure 50 shows the variation of the reagent flow rate as a function of time for a series of disturbances in the influent pH for a desired pH of 9.0 for the three controllers.

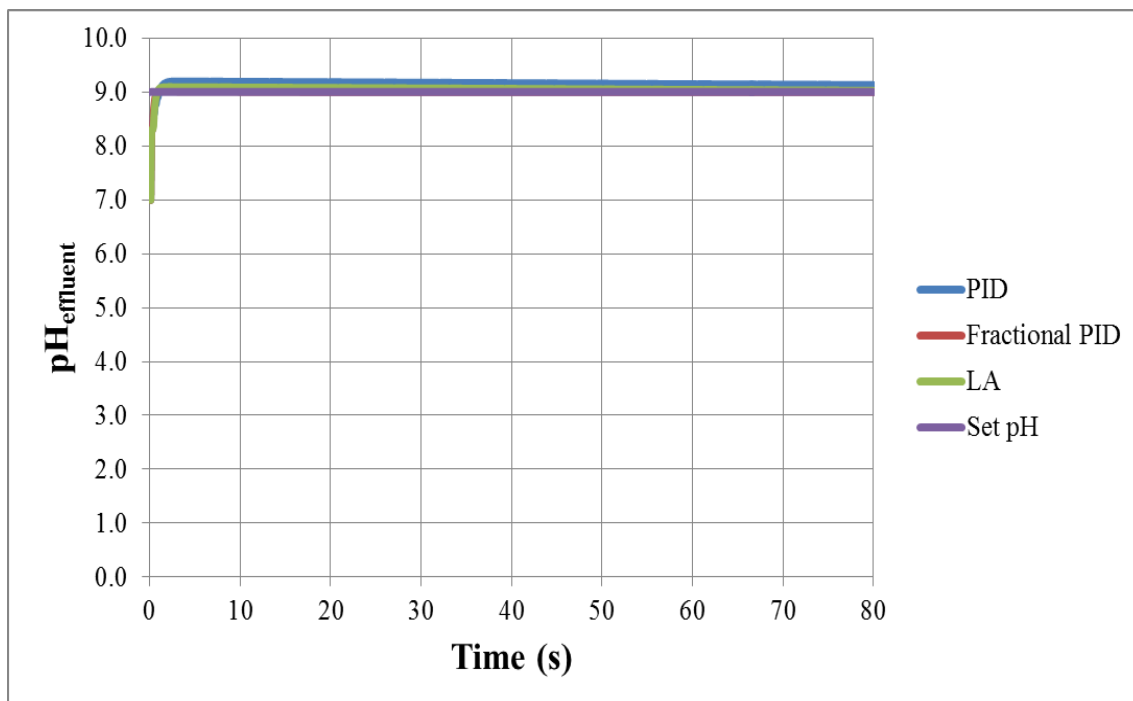


**Figure 49** Response of the effluent pH as a function of time for a series of disturbances in the influent pH for a desired pH of 9.0 for the three controllers.

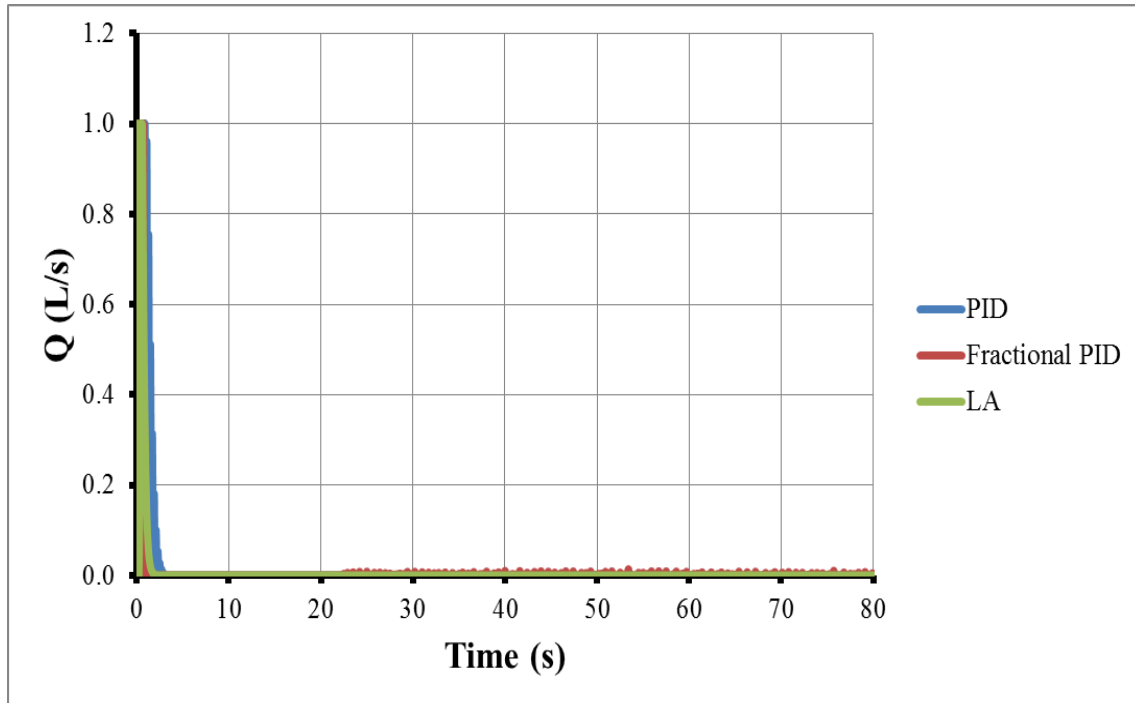


**Figure 50** Variation of the reagent flow rate as a function of time for a series of disturbances in the influent pH for a desired pH of 9.0 for the three controllers.

#### 4.1.6. Desired pH of 10.0

The results of the numerical experiments for the control of the effluent pH of a neutralization tank using PID, fractional  $PI^{\lambda}D^{\mu}$  and LA controllers for four different maximum reagent flow rates for a desired pH of 10.0 are presented in Figures 51 to 54. In addition, the responses of the effluent pH as a function of time for the four maximum reagent flow rates  $Q_{\max}$  are presented in Figures 55 to 57 individually for the linear PID, fractional  $PI^{\lambda}D^{\mu}$  and LA controllers. The three controllers were evaluated for the neutralization tank with the incoming stream having a pH of 8 and a flow rate of 0.1 L/s. Figures 51 to 54 show that the three controllers were able to bring the pH of the effluent stream from its initial pH of 8.0 to the desired pH of 10.0 and maintain very well the pH at its set point. All controllers lead to identical responses for this case study. The time required to reach the pH set point with the three controllers is approximately 6 s when a maximum reagent flow of 0.5 L/s was used. Meanwhile it takes less than 2 s for all controllers to bring up the initial pH of 8.0 to 10.0 when the maximum reagent flow rates

are 1.0, 5.0 and 100 L/s. A control valve with a maximum flow rate  $Q_{\max}$  of 1.0 L/s gives a relatively small sum of ITAE and ISDU and it was chosen for these series of tests.

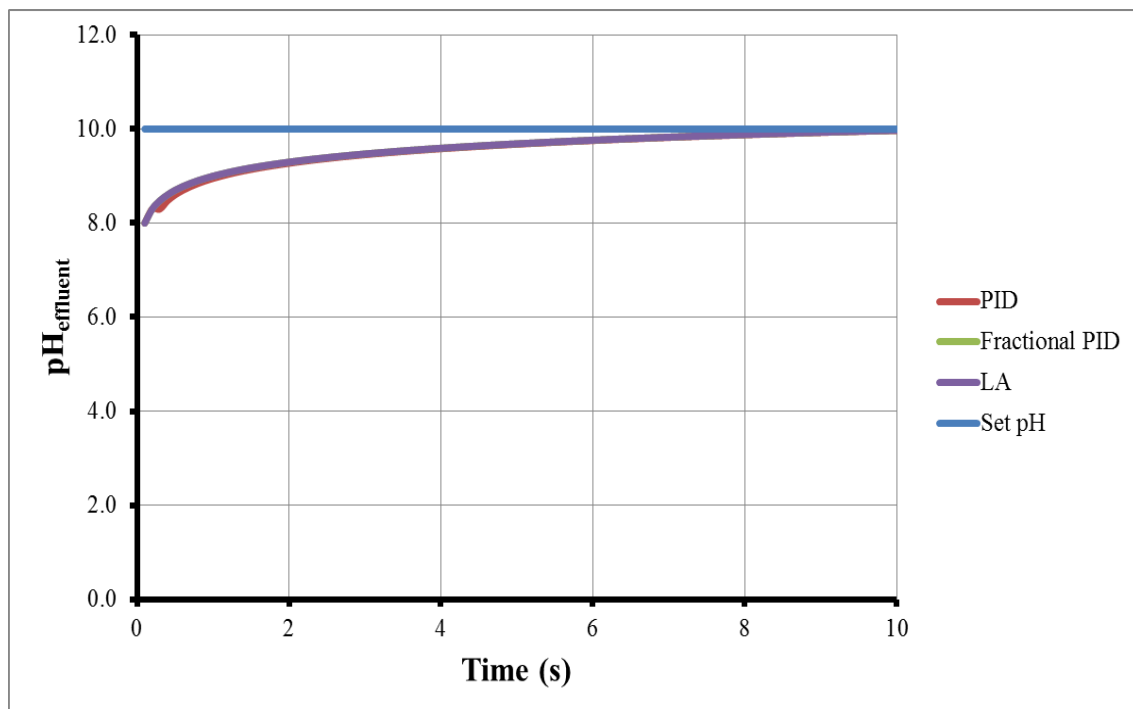


**Figure 51** pH as a function of time for a desired pH of 10.0 with  $Q_{\max} = 0.5$  L/s for the three controllers tuned to minimize the sum of ITAE and ISDU.

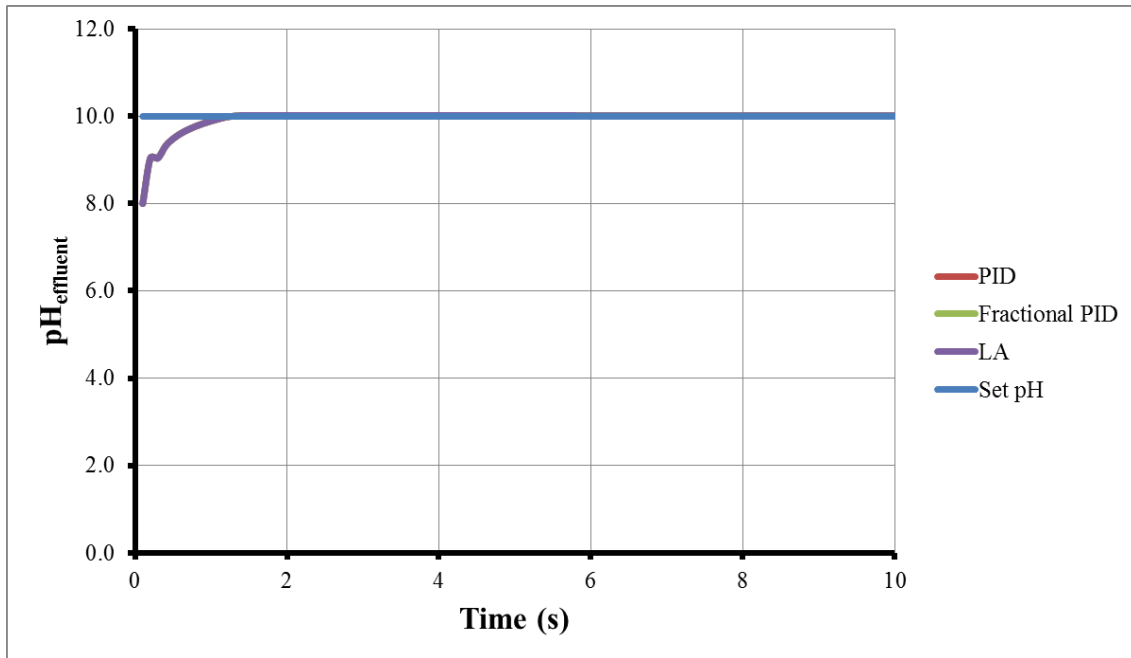


**Figure 52** pH as a function of time for a desired pH of 10.0 with  $Q_{\max} = 1.0$  L/s for the three controllers tuned to minimize the sum of ITAE and ISDU.

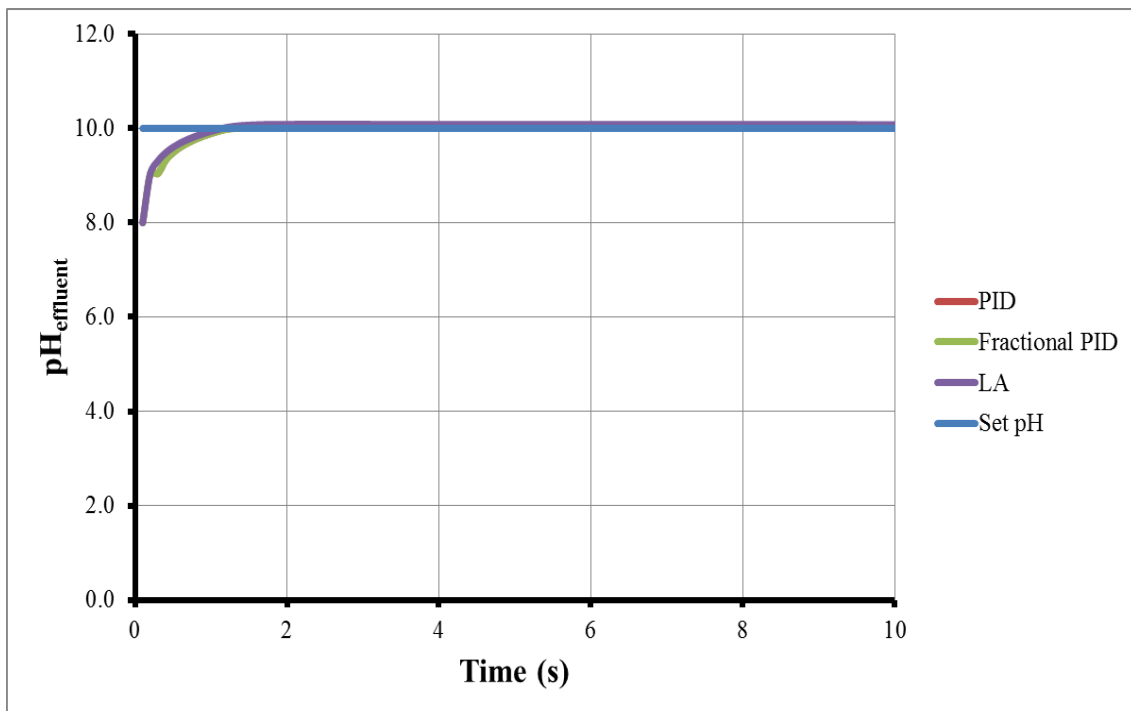


**Figure 53** pH as a function of time for a desired pH of 10.0 with  $Q_{\max} = 5.0$  L/s for the three controllers tuned to minimize the sum of ITAE and ISDU.

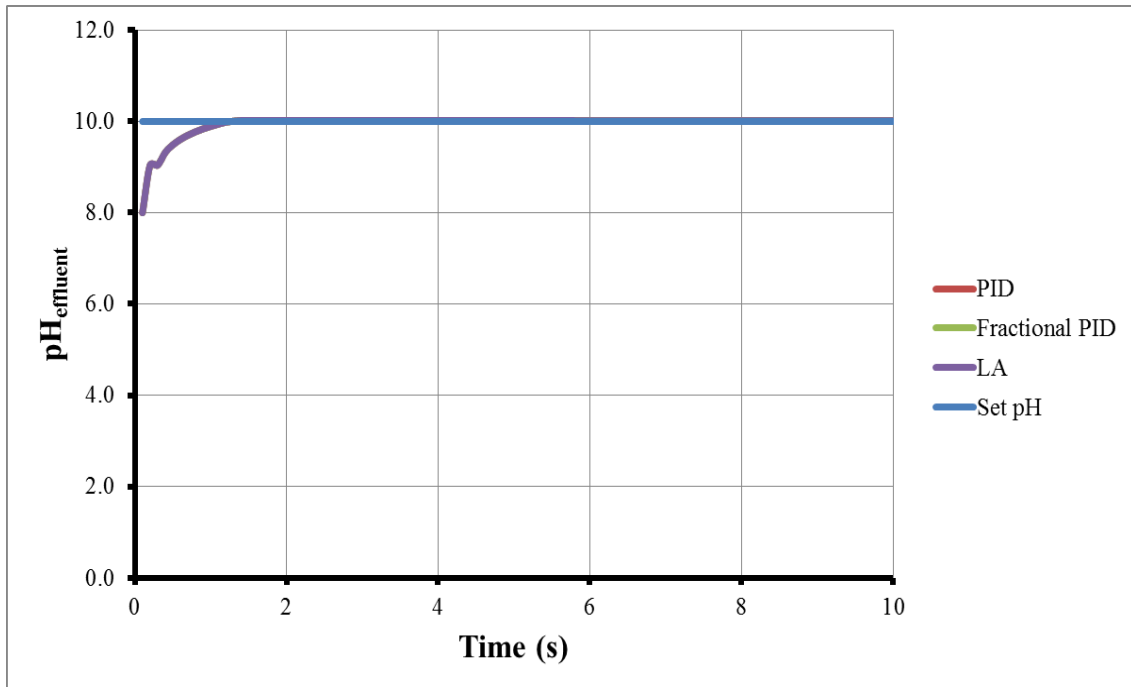


**Figure 54** pH as a function of time for a desired pH of 10.0 with  $Q_{\max} = 100$  L/s for the three controllers tuned to minimize the sum of ITAE and ISDU.

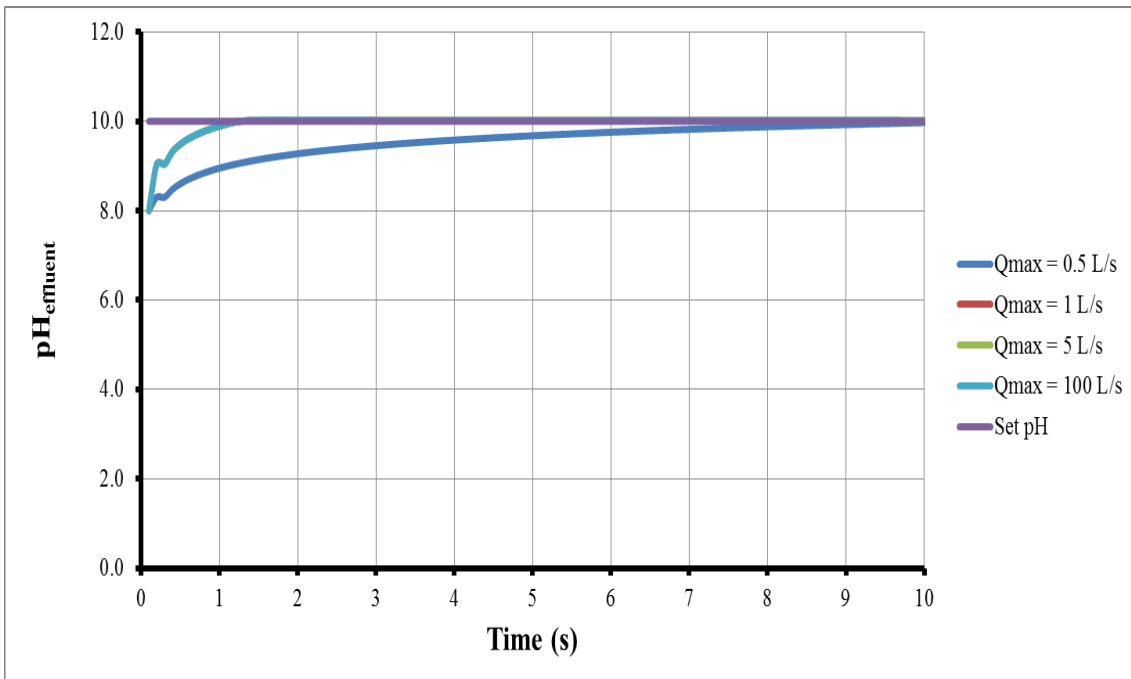


**Figure 55** pH as a function of time for a desired pH of 10.0 with a PID controller for the four different maximum reagent flow rates.

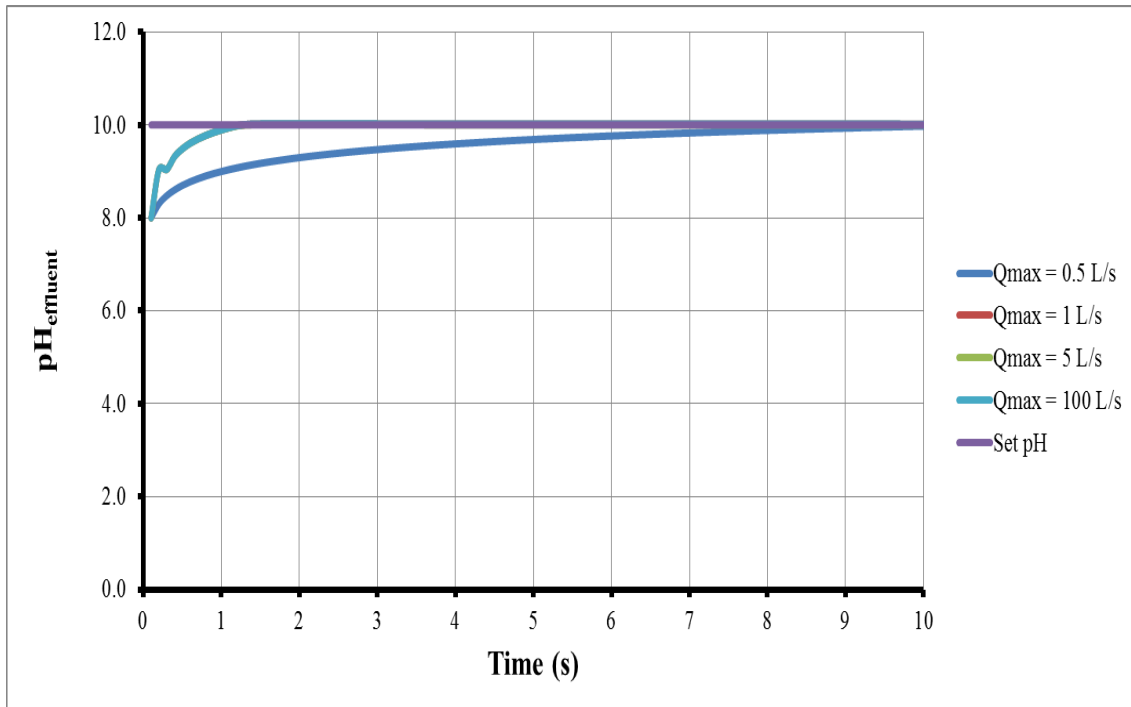


**Figure 56** pH as a function of time for a desired pH of 10.0 with a fractional  $PI^\lambda D^\mu$  controller for the four different maximum reagent flow rates.

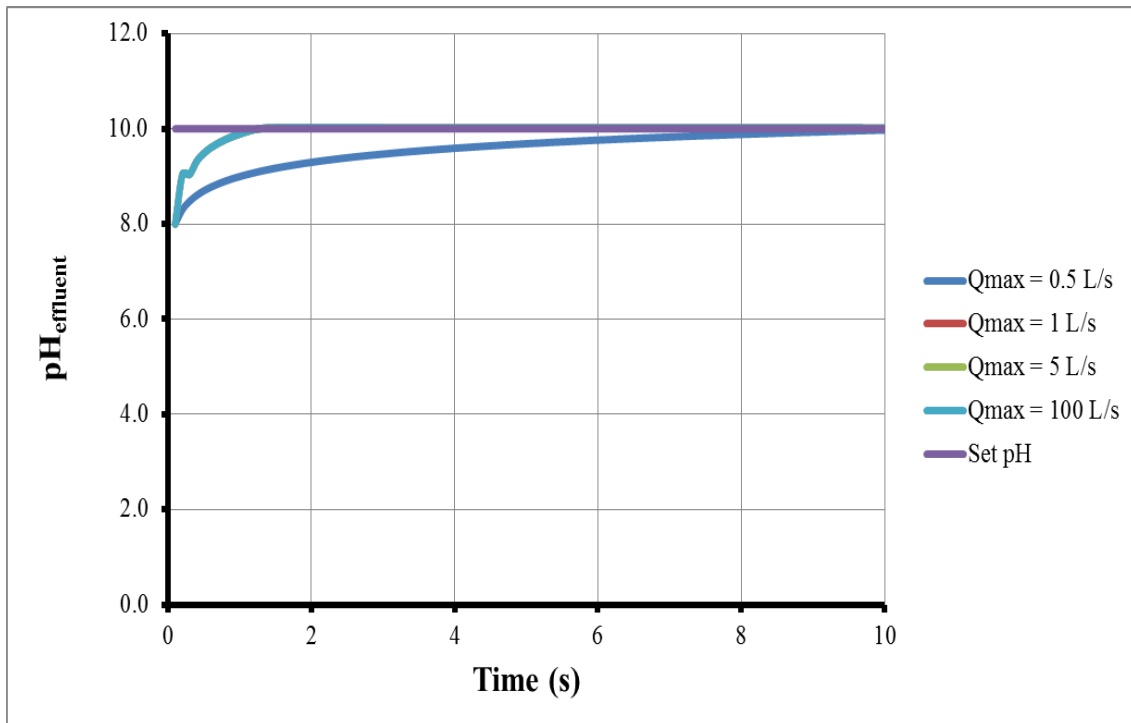


**Figure 57** pH as a function of time for a desired pH of 10.0 with a LA controller for the four different maximum reagent flow rates.

Table 6 provides a summary of the operating conditions and the optimal controller parameters obtained for the linear PID, the fractional  $PI^\lambda D^\mu$  and the LA controllers for the case study for which the pH set point was 10.0. Results of Table 6 show that all controllers lead to very fast response of the control system. The objective function obtained with the LA controller is the highest while the one for the fractional  $PI^\lambda D^\mu$  controller has the lowest sum of ITAE and ISDU. All controllers show short response time and low control performance metrics for reaching the desired pH of 10.0 when the maximum reagent flow rate  $Q_{\max}$  is 1.0 L/s.

**Table 6** Summary of simulation results for desired pH of 10.0 system for  $Q_{\max} = 1.0$  L/s.

<b>Operating Conditions</b>			
pH <sub>set</sub>	10		
pH <sub>in</sub>	8		
pH <sub>reagent</sub>	11		
Q <sub>min</sub> (L/s)	0.0001		
<b>Parameters</b>	<b>PID</b>	<b>PI<sup>λ</sup>D<sup>μ</sup></b>	<b>LA</b>
t <sub>response</sub> (s)	1.7	1.6	1.6
ITAE + ISDU	3.7	3.2	29.4
Q <sub>max</sub> (L/s)	1.0	1.0	1.0
K <sub>C</sub>	73.06	96.11	-
τ <sub>I</sub>	0.10	0.10	-
τ <sub>D</sub>	0.10	0.10	-
λ	-	1.00	-
μ	-	0.01	-
n <sub>1</sub>	-	-	60.00
n <sub>2</sub>	-	-	50.00

The derivative time parameter for the PID controller is at its minimum value, which suggests that the controller is in fact a PI controller. The derivative action did not appear as well in all the other PID controllers for all pH set point values.

The parameters obtained for the fractional  $PI^\lambda D^\mu$  controller, with an integration order of unity and a derivative order of zero, suggest that the controller is really an equivalent PI controller with the values of  $K_c$  and  $\tau_I$  of 105.7 and 0.11, respectively.

The parameters of  $n_1$  and  $n_2$  of the LA controller are relatively high values, equal to their upper bound limit. Like for other case studies, the third parameter  $\theta$  (Equation 3.16) was determined to be negligible.

Figure 58 displays the response of the effluent pH of the neutralization tank using PID, fractional  $PI^{\lambda}D^{\mu}$  and LA controllers for a series of disturbances in the influent pH with a desired pH of 10.0. The initial pH of the inlet stream was set to be 8.0 for the first 20 s. The pH was then changed to 3.0, 9.0 and 8.0 at, respectively, 20, 40 and 60 s. Results of Figure 58 show that PID, fractional  $PI^{\lambda}D^{\mu}$  and LA controllers are excellent for the control of the neutralization tank effluent pH at the desired pH of 10.0 in the presence of disturbances. Even though a large pH change was made at 20 s, the effect on the effluent pH is hardly noticeable on Figure 58. This is due to the relatively aggressive controllers that were obtained in this case study. The variation in the base solution flow rate (Figure 59) was very oscillatory for the PID and LA controllers to achieve this result (Figure 58). On the other hand, the manipulated variable associated with the fractional  $PI^{\lambda}D^{\mu}$  controller stabilized very rapidly compared to the other two controllers.

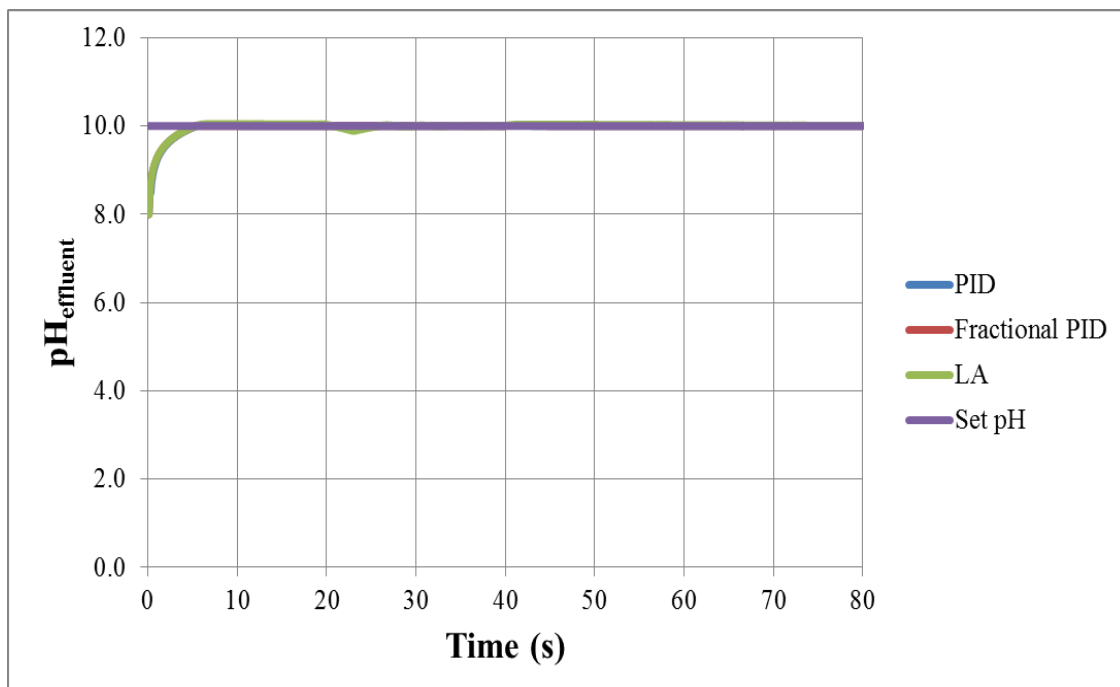


**Figure 58** Response of the effluent pH as a function of time for a series of disturbances in the influent pH for a desired pH of 10.0 for the three controllers.

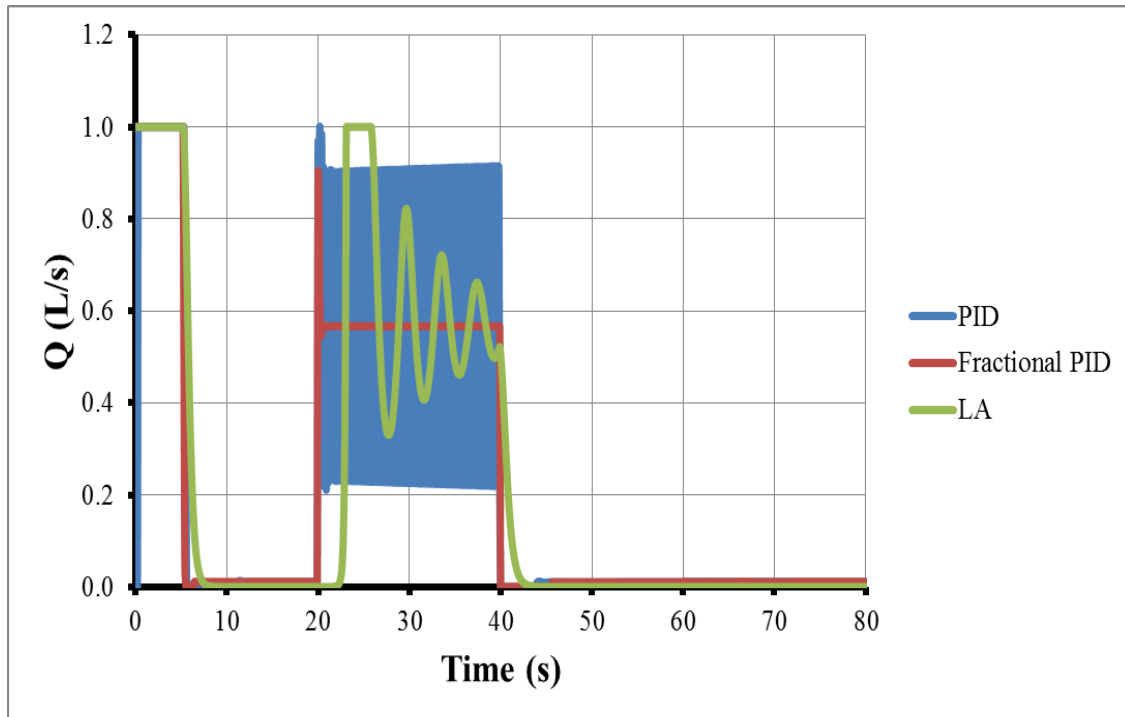


**Figure 59** Variation of the reagent flow rate as a function of time for a series of disturbances in the influent pH for a desired pH of 10.0 for the three controllers.

#### 4.2. Discussion on PID, $PI^{\lambda}D^{\mu}$ and LA Controllers for Controlling pH

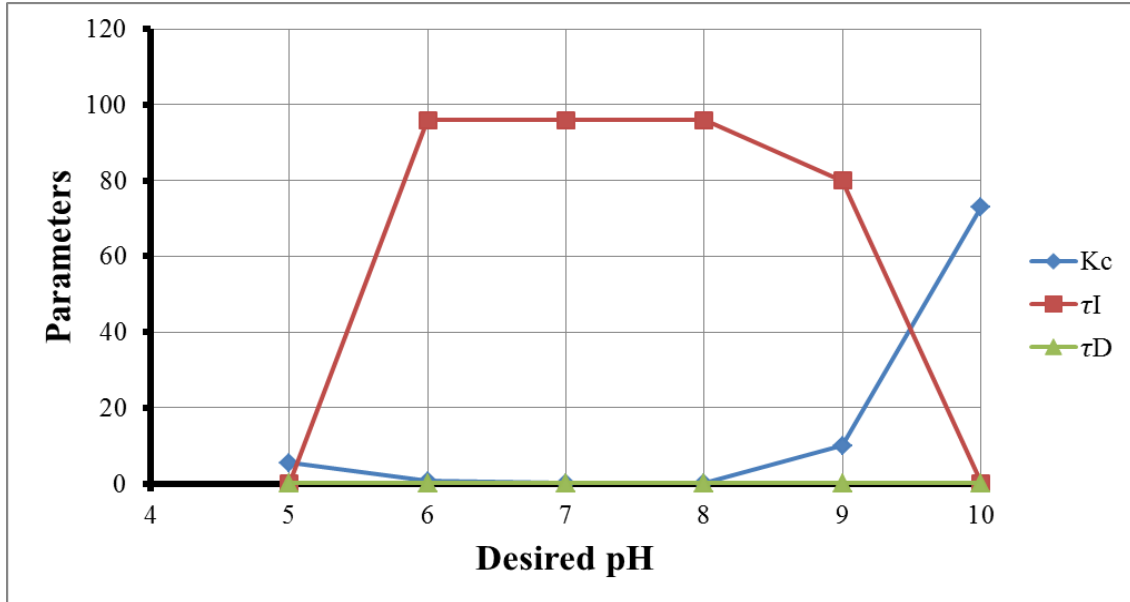
PID, fractional PID and LA controllers implemented in this research for the control of the neutralization tank effluent pH were found to be very good controllers for both set point changes and for disturbances. Because of the nonlinear nature of solution pH, the tuning of the three controllers was performed for each specific pH set point in the range of 5 to 10.

Table 7 presents a summary of the results obtained for the PID controller for all levels of pH. Results show that the response time for all levels of pH is very short in the case of a set point change. Table 7 also gives the value of the objective function (sum of ITAE and ISDU) for all levels of pH. The objective function for the control of pH at 5.0, 6.0 and 7.0 are relatively high compared to the objective function obtained at pH of 8.0, 9.0 and 10. The selected maximum reagent flow  $Q_{max}$  for proper control using a PID controller for set pH of 5, 6 and 7 and set pH of 8, 9 and 10 were 5 L/s and 1 L/s, respectively. The reagent flow has to be limited to these values to avoid excessive control action to be taken and potential pH overshoot. Since a one-directional pH control was used, it is important to

avoid important overshoot as the pH can only return to its set point via dilution. In all cases, the pH of the reagent stream was 11 and the minimum reagent flow  $Q_{\min}$  was 0.0001 L/s. Table 7 shows that all controllers were in fact PI controllers. The variation of the controller gain  $K_C$  is plotted on Figure 60 as a function of the desired pH in the range of 5 to 10. A higher value of the controller gain is required when the desired pH is further away from the neutralization point. At the neutralization point, the controller gain should be small to avoid excessive addition of the base solution to the neutralization tank and get smoother control. Similarly and for the same reason, the integration action should follow the trend of the controller gain, that is having higher values of the integration time. The parameters for the PID controller shown on Table 7 are the optimum parameters obtained by the steepest descent.

**Table 7** Summary of the results for the PID controller over the range of desired pH.

$\text{pH}_{\text{set}}$	<b>PID</b>					
	$t_{\text{response}}$ (s)	ITAE + ISDU	$Q_{\text{max}}$ (L/s)	$K_C$	$\tau_I$	$\tau_D$
5	6.9	36.2	5.0	5.73	3.89	0.01
6	4.9	69.8	5.0	0.65	96.00	0.10
7	2.4	30.6	5.0	0.14	96.00	0.10
8	0.6	8.1	1.0	0.11	96.00	0.10
9	2.0	3.2	1.0	9.94	80.00	0.10
10	1.7	3.7	1.0	73.06	0.10	0.10



**Figure 60** Trends of the parameters of the PID controller versus the desired pH.

Table 8 gives the summary of the results obtained using the fractional  $PI^\lambda D^\mu$  controller. The response times obtained with the fractional  $PI^\lambda D^\mu$  controller are small and shorter than the times obtained with the linear PID controller. In addition, fractional  $PI^\lambda D^\mu$  controllers for all levels of pH had in general smaller values of the objective function. The recommended maximum reagent flow  $Q_{max}$  for fractional  $PI^\lambda D^\mu$  controller is the same as for the linear PID controller. The variation of the controller gain  $K_C$  is plotted on Figure 61 as a function of the desired pH in the range of 5 to 10. The parameters obtained for the fractional  $PI^\lambda D^\mu$  controller are presented in Table 8 and were obtained via an optimization algorithm. All  $PI^\lambda D^\mu$  controllers could be reduced to PI or  $PI^\lambda$  controllers based on their values of integration order  $\lambda$  and derivation order  $\mu$ . The values of  $\lambda$  and  $\mu$  are plotted in Figure 62. The value of  $\lambda$  is minimum at the neutralization point whereas it tends to unity as the desired pH is moving away from the neutralization point. The derivation order  $\mu$  obtained via the optimization algorithm was found to be at its lowest value such that the derivative was always eliminated from the fractional  $PI^\lambda D^\mu$  controller.

**Table 8** Summary of the results for the  $PI^\lambda D^\mu$  controller over the range of desired pH.

$pH_{set}$	Fractional PID							
	$t_{response}$ (s)	ITAE + ISDU	$Q_{max}$ (L/s)	$K_C$	$\tau_I$	$\tau_D$	$\lambda$	$\mu$
5	7.5	44.0	5.0	0.10	0.12	50.00	1.01	0.01
6	2.0	4.0	5.0	0.12	24.54	13.46	0.85	0.01
7	1.4	2.3	5.0	0.21	27.98	0.11	0.40	0.01
8	0.2	0.2	1.0	0.30	36.51	0.12	0.36	0.01
9	0.4	0.8	1.0	98.54	0.10	0.10	1.00	0.01
10	1.6	3.2	1.0	96.11	0.10	0.10	1.00	0.01

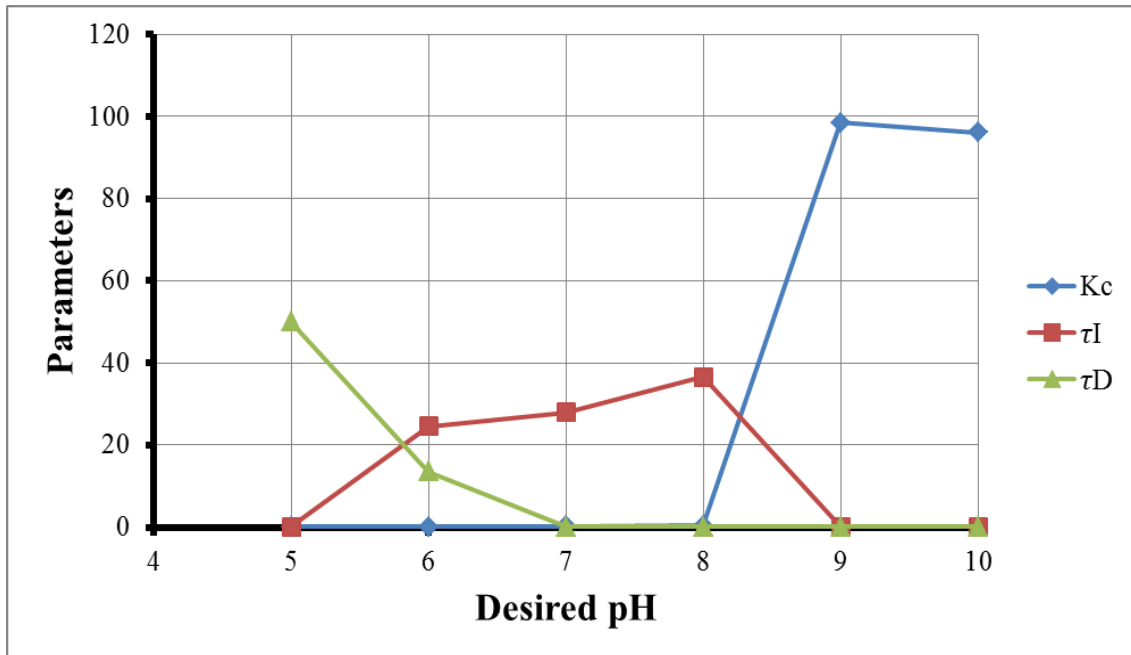


**Figure 61** Trends of the parameters of the fractional  $PI^\lambda D^\mu$  controller versus the desired pH

(1).

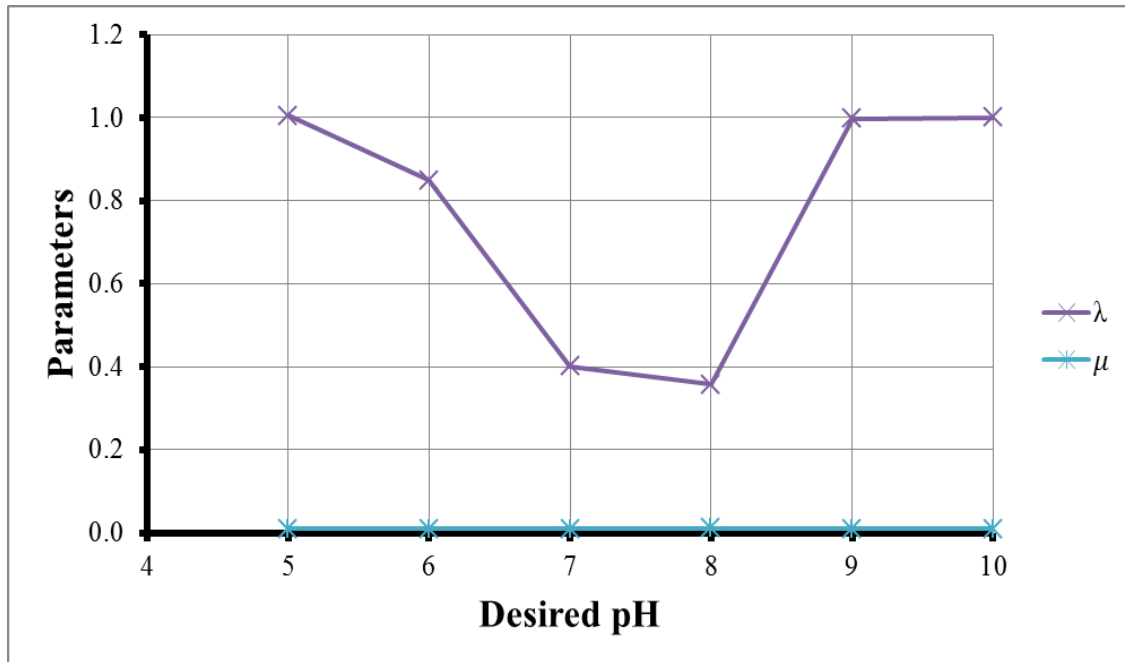


**Figure 62** Trends of the parameters of the fractional  $PI^\lambda D^\mu$  controller versus the desired pH (2).

Table 9 gives the summary of the results obtained using the LA controller. Like PID and fractional PID, LA is an excellent controller for pH control. Response time and the objective function for all desired pH are low to moderate. LA controller has two main parameters, the exponents of the ratios of process variables. A third parameter  $\theta$  (Equation 3.16) can be used to increase the sensitivity of the controller but was found to be negligible in this investigation. Relatively high values of  $n_1$  and  $n_2$  were obtained, often equal to the values of the upper limits. Higher values could be used but with the risk of having lower robustness.

**Table 9** Summary of the results for the LA controller over the range of desired pH.

pH <sub>set</sub>	LA				
	t <sub>response</sub> (s)	ITAE + ISDU	Q <sub>max</sub> (L/s)	n <sub>1</sub>	n <sub>2</sub>
5	7.0	35.1	5.0	20.35	51.25
6	1.1	4.7	5.0	28.85	47.10
7	2.1	5.7	5.0	5.45	60.00
8	0.2	2.3	1.0	60.00	50.00
9	0.5	5.0	1.0	50.00	60.00
10	1.6	29.4	1.0	60.00	50.00

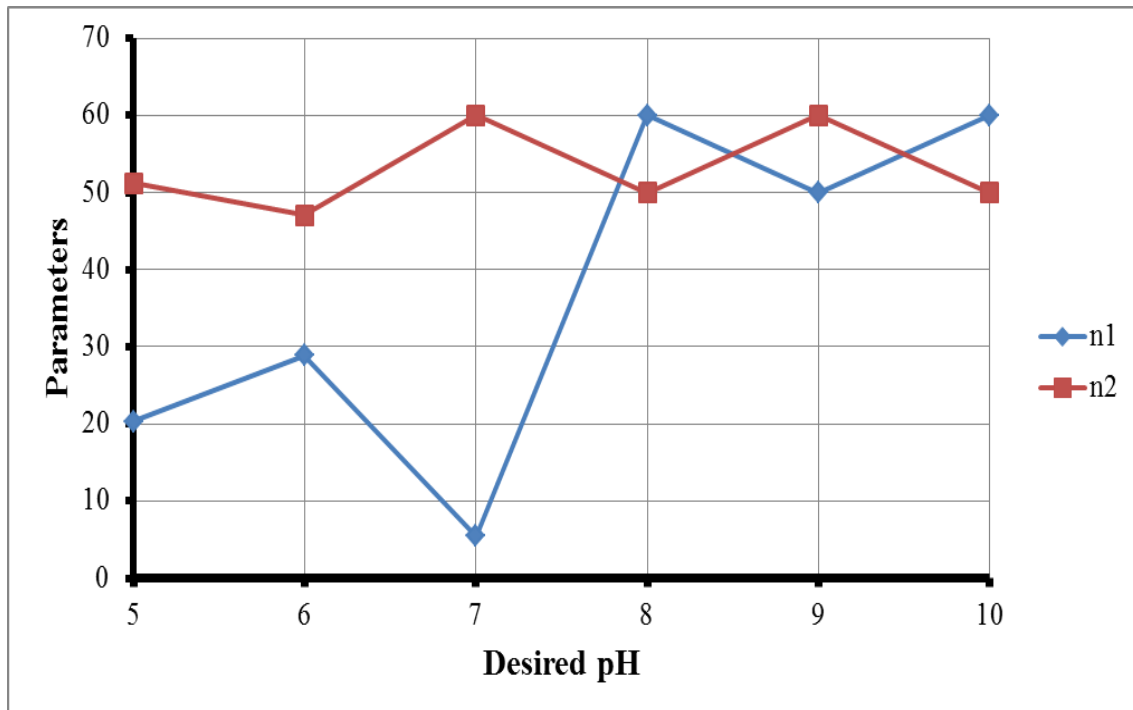


**Figure 63** Trends of the parameters of the LA controller versus the desired pH.

## Chapter 5

### Conclusion, Recommendations and Future Works

After assessing the performance of PID, fractional  $PI^\lambda D^\mu$  and LA controllers, it can be concluded that these three controllers are able to efficiently control and maintain pH of the effluent of a neutralization tank. The three controllers used to maintain the desired pH is very stable. The three controllers respond rapidly to bring the pH to its desired pH point. In addition, the three controllers, tuned for the set point change, performed well in the presence of disturbances. Given the higher complexity in terms of computation and coding of the fractional  $PI^\lambda D^\mu$  controller, it is recommended to use linear PID and LA controllers as they are simpler to implement and provide excellent control.

The actuator providing the maximum reagent flow rate is one of the important considerations in the design of a neutralization process and for a realistic pH control simulation besides reagent pH and optimal controller parameters. According to the simulation results, a maximum reagent flow selection was determined based on the objective criterion (sum of ITAE and ISDU) for each controller. Moreover, the determination of the maximum reagent flow rate aims to prevent an excessive overshoot that potentially leads to a large sum of ITAE and ISDU. In addition, the reagent pH is the other concern in bringing up pH from an initial set point to a desired pH point. The parameter optimization design is also important in determining optimum parameters to minimize the sum of objective criteria so that the controller can lead to smooth and rapid control and to maintain the pH at its desired value. In conclusion, it is recommended to choose the maximum reagent flow rate and reagent pH leading to no or acceptable overshoot, smooth response and good stability. Furthermore, the combination of the grid and gradient search method is recommended to determine the optimum parameters leading to a minimum sum of objective criteria. The small time increment which is about 0.1 to 0.5 second is also recommended to obtain accuracy in the acid-base reaction.

For future work, it is proposed to compare PID, fractional  $PI^\lambda D^\mu$  and LA as feedback controllers to neural network controller to determine if it could improve the quality of the

output by predicting the control action earlier so that errors can even be minimized earlier in the process.

It was assumed in this investigation that the dynamics of mixing and other components of the control loop (valve or pump, pH meter) have negligible time constants compared to dynamics of the whole system. Even though this may be valid in many cases, it would be interesting to evaluate their effect on the controller tuning and performance of each controller. It is expected that if there is significant mixing time and the time constant of the pH meter is non negligible, the controller would still offer appropriate control but the controllers would have to be detuned significantly.

The series of simulations were performed for a simple neutralization tank where it was assumed that only water was present. The next step could be to perform the same series of tests with solutions also containing weak acids such that more than one dissociation constant would prevail at different pH. In that case, the same mass balance would be performed for the neutralization tank except that it would be necessary to find the reaction rate that will satisfy simultaneously all dissociation constants.

It is recommended designing and building a simple experimental neutralization system to better assess the various types of controllers under real experimental limitations. This would allow evaluating controllers when the dynamics of the actuator, the measuring device and mixing would be taken into account along with measurement noise and potential dead time. This system could also serve for undergraduate students laboratories to perform control experiments with a wide variety of controllers.

## References

- [1] J. Spencer, "The Importance of pH in Food Quality and Production," *Sper Scientific*, 2015.
- [2] S. Wiman, "The Importance of pH Control," 2018.
- [3] J. Bell, S. Sanchez and T. Hazlett, "Liposomes in the Study of Phospholipase A2 Activity," *Methods in Enzymology*, vol. 372, pp. 19-48, 2003.
- [4] H. Azimi, F. Tezel and J. Thibault, "The impact of pH on VLE, pervaporation and adsorption of butyric acid in dilute solutions," *Can J Chem Eng*, vol. 17, pp. 1576-1584, 2017.
- [5] D. Michaud, "The Importance of pH in Flotation," 2015.
- [6] G. Alwan, "pH-Control Problems of Wastewater Treatment Plants," *Al-Khwarizmi Engineering Journal*, vol. 4, pp. 37-45, 2008.
- [7] G. Alwan, F. Mehdi and M. Murthada, "pH control of a wastewater treatment unit using Labview and genetic algorithm," *The Sixth Jordan International Chemical Engineering Conference*, pp. 1-10, 2012.
- [8] U. B. Singh and A. S. Ahluwalia, "Microalgae: a promising tool for carbon sequestration," *Mitig Adapt Strateg Glob Change*, vol. 18, p. 73-95, 2012.
- [9] M. Ghassoul, "PH Control Using MATLAB," *MATLAB – A Fundamental Tool for Scientific Computing and Engineering Applications*, vol. 1, pp. 243-268, 2012.
- [10] A. Johnson, "The control of fed-batch fermentation processes—A survey," *Automatica*, pp. 691-705, 1987.
- [11] A. Hermansson and S. Syafiie, "Model predictive control of pH neutralization

- processes: A review," *Control Engineering Practice*, vol. 45, pp. 98-109, 2015.
- [12] M. A. Henson and D. E. Seborg, "Adaptive Nonlinear Control of a pH Neutralization Process," *IEEE Transactions on Control Systems Technology*, vol. 2, pp. 169-182, 1994.
- [13] B. D. Kulkarni, S. S. Tambe, N. V. Shukla and P. B. Deshpande, "Nonlinear pH Control," *Chemical Engineering Science*, vol. 46, pp. 995-1003, 1991.
- [14] Z. Zhiyun, Y. Meng, W. Zhizhen, L. Xinghong, G. Yuqing, Z. Fengbo and G. Ning, "Nonlinear Model Algorithmic Control of a pH Neutralization Process," *Process Systems Engineering and Process Safety*, vol. 21, pp. 395-400, 2013.
- [15] M. Lawrynczuk, "Modelling and predictive control of a neutralisation reactor using sparse support vector machine Wiener models," *Neurocomputing*, pp. 311-328, 2016.
- [16] R. Wright, B. Smith and C. Kravaris, "Online identification and nonlinear control of pH processes," *Ind. Eng. Chem. Res.*, pp. 2446-2461, 1998.
- [17] S. S. Ram, D. D. Kumar and B. Meenakshipriya, "Designing of PID Controllers for pH Neutralization Process," *Indian Journal of Science and Technology*, pp. 1-5, 2016.
- [18] R. Aguiar, I. Franco, F. Leonardi and F. Lima, "Fractional PID Controller Applied to a Chemical Plant with Level and pH Control," *Chemical Product and Process Modeling*, pp. 1-12, 2018.
- [19] T. Johansen and B. Foss, "Nonlinear local model representation for adaptive systems," *In Proceedings of Singapore International Conference on intelligent control and instrumentation*, pp. 677-682, 1992.
- [20] E. G. Kumar and E. Gowthaman, "Cascade PID-Lead Compensator Controller for Non-overshoot Time Responses of unstable system," *1st International Conference*

- on *Power Engineering, Computing and Control*, vol. 117, pp. 708-715, 2017.
- [21] P. Shah and S. Agashe, "Review of fractional PID controller," *Mechatronics*, vol. 38, pp. 29-41, 2016.
- [22] C. Anil and R. P. Sree, "Tuning of PID controllers for integrating systems using direct synthesis method," *ISA Transactions*, vol. 57, pp. 211-219, 2015.
- [23] B. Khalifa and C. Abdelfateh, "Optimal tuning of fractional order  $PI\lambda D\mu A$  controller using Particle Swarm Optimization algorithm," *International Federation of Automatic Control*, Vols. 50-1, pp. 8084-8089, 2017.
- [24] K. Astrom and T. Hagglund, *PID Controllers: theory, design and tuning*, North Carolina, USA: Research Triangle Park, 1995.
- [25] X. Shen and J. Thibault, "Are Fractional  $PI\lambda D\mu$  Controllers Good for All Processes?," *The 4th International Conference of Control, Dynamic Systems, and Robotics*, pp. 1141-1146, 2017.
- [26] M. Lakrori, "Control Of A Continuous Bioprocess By Simple Algorithms of "P" And "L/A" Type," *IFAC Nonlinear Control Systems*, pp. 339-344, 1989.
- [27] J.-P. Ylén, "Measuring, modelling and controlling the pH value and the dynamic chemical state," Helsinki University of Technology, Helsinki, 2001.
- [28] P. Shah and S. Agashe, "Review of fractional PID controller," *Mechatronics*, vol. 38, pp. 29-41, 2016.
- [29] F. Shinskey, *Process Control System: Application, Design, and Tuning*, 4th ed., New York, USA: McGraw-Hill, 1996.
- [30] D. E. Seborg, T. F. Edgar, D. A. Mellichamp and F. J. Doyle III, *Process Dynamics and Control*, 3rd ed., Hoboken, New Jersey: John Wiley & Sons, 2011.

- [31] H. Chao, Y. Luo, L. Di and Y. Chen, "Roll-channel fractional order controller design for a small fixed-wing unmanned aerial vehicle," *Control Engineering Practice*, vol. 18, pp. 761-772, 2010.
- [32] C. A. Monje, B. M. Vinagre, V. Feliu and Y. Chen, "Tuning and auto-tuning of fractional order controllers for industry applications," *Control Engineering Practice*, vol. 16, pp. 798-812, 2008.
- [33] M. S. Tavazoei and M. Haeri, "A note on the stability of fractional order systems," *Mathematics and Computers in Simulation*, vol. 79, pp. 1566-1576, 2009.
- [34] S. Das, *Functional Fractional Calculus*, Mumbai: Springer, 2011.
- [35] C. Li and F. Zeng, *Numerical Methods for Fractional Calculus*, Boca Raton, Florida: CRC Press, 2015.
- [36] B. Khalifa and C. Abdelfateh, "Optimal tuning of fractional order PI $\lambda$ D $\mu$ A controller using Particle Swarm Optimization algorithm," *International Federation of Automatic Control*, vol. 50, pp. 8084-8089, 2017.
- [37] M. Lakrori, "Control of a continuous bioprocess by simple algorithms of "P" and L/A type," *Non Linear Control Systems*, pp. 339-344, 1989.
- [38] M. Lakrori and D. Rey, "On the use of "L/A" algorithms to control some chemical processes," *Dynamics and Control of Chemical Reactors*, pp. 283-290, 1989.
- [39] J. Thibault, *Process Control*, Ottawa, Ontario: University of Ottawa, 2015.
- [40] D. Lister and S. Uchida, "Determining water chemistry conditions in nuclear reactor coolants," *Journal of Nuclear Science and Technology*, vol. 52, pp. 451-466, 2015.
- [41] L. Wei and L. Jianfeng, "Analysis on Control Operating Conditions of Water Chemistry of Nuclear Power Unit," *Applied Mechanics and Materials*, Vols. 178-

- 181, pp. 553-556, 2012.
- [42] R. N. Gurram and T. J. Menkhaus, "Effects of pH, Slurry Composition, and Operating Conditions on Heat Transfer Fouling during Evaporation of a Lignocellulosic Biomass Process Stream," *Industrial & Engineering Chemistry Research*, vol. 52, pp. 22-31, 2013.
- [43] I. Podlubny, "Fractional-order systems and fractional-order controllers," *Inst Exp Phys Slovak Acad Sci*, pp. 4989-4990, 1994.
- [44] K. C. Timberlake and W. Timberlake, *Basic Chemistry*, 2nd ed., Upper Saddle River, New Jersey: Pearson Education, 2008, pp. 454-490.
- [45] R. Chang, *General Chemistry*, 5th ed., New York: McGraw Hill, 2008.
- [46] P. Flowers and K. Theopold, "Self-Ionization of Water and the pH Scale," Libretexts, 8 February 2016. [Online]. Available: [https://chem.libretexts.org/Textbook\\_Maps/General\\_Chemistry/Map%3A\\_General\\_Chemistry\\_\(Petrucci\\_et\\_al.\)/16%3A\\_Acids\\_and\\_Bases/16.3%3A\\_Self-Ionization\\_of\\_Water\\_and\\_the\\_pH\\_Scale](https://chem.libretexts.org/Textbook_Maps/General_Chemistry/Map%3A_General_Chemistry_(Petrucci_et_al.)/16%3A_Acids_and_Bases/16.3%3A_Self-Ionization_of_Water_and_the_pH_Scale). [Accessed 13 September 2018].
- [47] I. Podlubny, "Fractional-Order Systems and Fractional-Order Controllers," *Institute of Experimental Physics*, vol. 3, pp. 2-16, 1994.
- [48] S. Johnson, "Water Management: Policies, Guidelines, Provincial Water Quality Objectives," 2016.
- [49] S. Johnson, "Electronic Code of Federal Regulations," 2018.